International Journal of
Applied Sciences and Smart Technologies

Volume 03, Issue 02, December 2021

p-ISSN 2655-8564 & e-ISSN 2685-9432

International Journal of Applied Sciences and Smart Technologies

Volume 3, Issue 2, page i

p-ISSN 2655-8564, e-ISSN 2685-9432

CONTENTS

International Journal of Applied Sciences and Smart Technologies

Volume 3, Issue 2, page ii

p-ISSN 2655-8564, e-ISSN 2685-9432

EDITORIAL BOARD

Contact us
International Journal of Applied Sciences and Smart Technologies
Faculty of Science and Technology
Sanata Dharma University
Kampus III Paingan, Maguwoharjo, Depok, Sleman
Yogyakarta, 55282
Phone : +62 274883037 ext. 523110, 52320
Fax : +62 272886529
Email : editorial.ijasst@usd.ac.id
Website : http://e-journal.usd.ac.id/index.php/IJASST

IJASST is an open-access peer-reviewed journal that mediates the dissemination of research and studies conducted by academicians, researchers, and practitioners in science, engineering, and technology.

International Journal of Applied Sciences and Smart Technologies

Volume 3, Issue 2, pages iii-iv

p-ISSN 2655-8564, e-ISSN 2685-9432

PREFACE

Dear readers, we are delighted to serve you Volume 3, Issue 2 of *International Journal of Applied Sciences and Smart Technologies* (IJASST), which is managed and published by the Faculty of Science and Technology, Sanata Dharma University. IJASST is an open-access peer-reviewed journal that mediates the dissemination of research and studies conducted by academicians, researchers, and practitioners in science, engineering, and technology. Its scope also includes basic sciences which relate to technology, such as applied mathematics, physics, and chemistry.

In this edition, we have ten papers authored by researchers from Indonesia, India, and Nigeria. Submitted papers are reviewed fairly using the open journal system (OJS) of IJASST. After the review process, accepted papers of the journal are publicly available for free at the website of IJASST.

For future issues, we are looking forward to your contributions to IJASST.

Dr. I Made Wicaksana Ekaputra
Editor in Chief
IJASST

International Journal of Applied Sciences and Smart Technologies

Volume 3, Issue 2, pages iii-iv

p-ISSN 2655-8564, e-ISSN 2685-9432

This page intentionally left blank

International Journal of Applied Sciences and Smart Technologies

Volume 3, Issue 2, pages 145–152

p-ISSN 2655-8564, e-ISSN 2685-9432

Personal Assistant Robot

Ziany Alpholicy X.[1,*], Sagar S. Bhandari[1], Praveen P. Dsouza[1], Divanshu C. Raina[1]

[1]*Xavier Institute of Engineering, Opposite S.L. Raheja Hospital, Mahim (West), Mumbai 400037, Maharashtra, India*

[*]*Corresponding Author: ziaxavier@gmail.com*

(Received 02-08-2020; Revised 29-12-2021; Accepted 29-12-2021)

Abstract

Since the boom in science and technology, humans have been trying to invent machines that could reduce their efforts in day to day activities. In this paper, we develop a personal assistant robot that could pick up objects and return it to the user. The robot is controlled using an android application in mobile phones. The robot can listen to user's command and then respond in the best way possible. The user can command the robot to move to given location, capture images and pick objects. The robot is equipped with ultrasonic sensor and web camera that helps it to move to different location effectively. It is also equipped with sleds that play important role in object picking process. The robot uses a tiny YOLOv3 model which is rigorously trained on several images of the object. There are some possible improvements that can be achieved which could help this robot to be used in several other fields as well.

Keywords: actuators and sensors, TCP socket, object detection

Volume 3, Issue 2, pages 145–152
p-ISSN 2655-8564, e-ISSN 2685-9432

1 Introduction

In recent years, humans have been creating various machines to help the physically challenged people. As people age they tend to face challenges in their every-day life and hence they require assistance from others to carry out their routine work. They are challenged to move physically and if they need to pick up objects they may require someone's assistant. Also, there are workers in factories that might face difficulties while working as they might be surrounded with hazardous chemicals or dangerous machines. People working in hospitals might also be exposed to several diseases while handling the relocation of different medical equipment. In this paper, we develop a personal assistant robot that a user can operate without physically moving from their location. There exists many such robots that can carry out routine jobs automatically. Although many of them are still incapable of eradicating the above mentioned problem.

2 Research Methodology

A technical research paper in 2015, published by the students of Indian Institute of Information Technology, Chittoor, described the development of an assistant robot that can be operated using speech commands and that can be used in hospitals, homes, industries and educational institute. They developed a robot that can be controlled using human voice. The robot could move to different locations and relocate an object from one place to another. They implemented a robotic arm by calculating several parameters such as variation of angle and distance between the robotic hands with time, angular velocity of the robotic arm [1].

In 2005, another research paper was published by some students of National Chiao Tung University, which described the development of develop a personal assistant robot which should be able to assist the user physically with real movement and actions. They developed the robot that had its own intelligent sensors and actuators. They also implemented the face tracking function which was achieved by radial basis function type neural network (RBFNN). They implemented several features like home care, remote monitoring, security, etc [2].

Volume 3, Issue 2, pages 145–152
p-ISSN 2655-8564, e-ISSN 2685-9432

Recently, in 2018, another research paper was published where an interactive personal assistant robot was developed using the Raspberry Pi computing engine. The robot that they developed was self-balancing which was implemented with the help of principle of dynamic balancing. They used Google Text To Speech (GTTS) to convert the voice commands into texts which can be recognized by the computing engine. They used bluetooth services to maintain connection between the robot and the mobile application. They also implemented multiple face recognition system so that they could replace the robot with the security guard [3]. More information can be found in the literature [4], [5], [6].

3 Results and Discussion

The object detection model used here is YOLO V3. The raspberry pi, due to its limited computing power, cannot be used to implement the original YOLO model. Hence, we use YOLO Tiny, a tiny and yet efficient version of YOLO. For the datasets we used Google's open images dataset V6. To train the model, we have to set the number of batches for the datasets so as to determine the iteration of training the model. The ideal number of iterations should be 2000 batches per number of objects. In our case we are dealing with 7 objects so the batches should be 14,000. While the model is training the prime objective of the algorithm is to decrease the average loss. We started with average loss of 4.5 and reached to an average loss of 1.08. Figure 1 shows the graph depicting the decrease in average loss as the number of iteration increases.

The robot and android are connected through TCP socket connection. The Raspberry Pi is cond to work as a standalone network and whenever booted up starts its hotspot. The android application is required to connect to the pi hotspot. A server socket is created by raspberry pi upon boot up which waits for the client to connect to the server. As soon as the android application is connected to pi hotspot through Wi-Fi network, the user can create a client socket and connect to the server listening on pi. The client-server socket connection then can be used to transfer data between the robot and the android application.

In order to execute the movement of robot from its starting place to the desired location, the paths need to be set within robot. The robot uses this pre-defined path to

Volume 3, Issue 2, pages 145–152
p-ISSN 2655-8564, e-ISSN 2685-9432

reach to a particular location. There can be several paths for different location within an area. To set a path, the user is supposed to move the robot from its home location to that particular spot. While the robot is moving it records the command given to it by the user and save it in the dynamic python list. When the user completes the moving job, the robot saves the path from the list in the form of text file and saves it into its path directory. The robot also computes the returning path just by reversing the commands given it by the user. So, two files are saved as one complete path and these files are used to execute the movement of robot from home location to path and vice versa.

When the user commands the robot to pick an object, the robot uses the path text files saved within the path directory to reach to the desired location. As soon as the robot reaches the location, it uses its webcam to capture the images and then uses those images to search for the object which user has decided to pick. It uses YOLO algorithm to detect the object in the captured image. As soon as the object is detected, the robot uses the ultrasonic sensor to measure the distance between itself and the object. According to the readings of sensor, it then relocates itself as much close to the object such that it can pick it up. After picking the object it then gets back to its home location using the path files. Figure 2 and Figure 3 show the object detection result on two different objects. Figure 4 shows the robot with sled opened while Figure 5 shows the robot with sled closed.

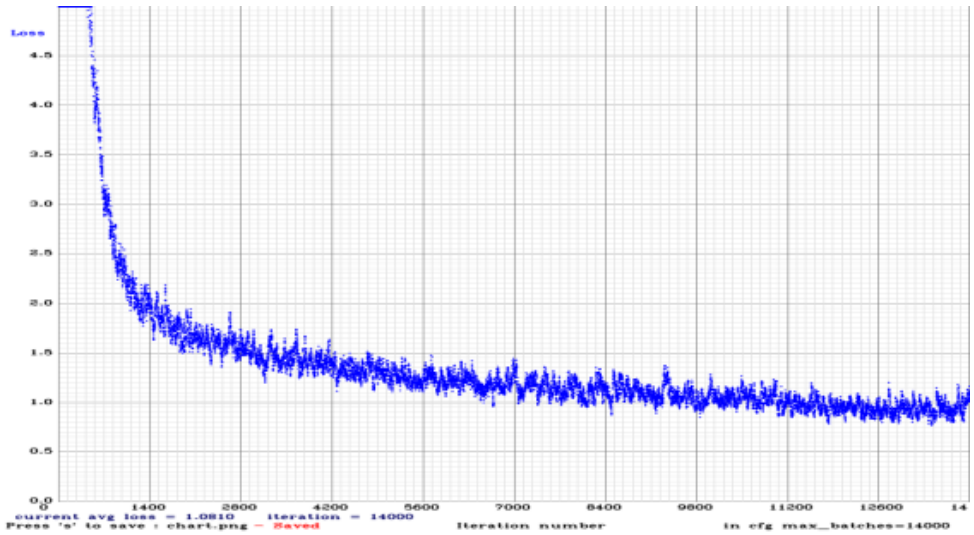

Figure 1. Graph depicting the decrease in average loss as the number of iteration increases

International Journal of Applied Sciences and Smart Technologies

Volume 3, Issue 2, pages 145–152

p-ISSN 2655-8564, e-ISSN 2685-9432

Figure 2. The object detection result on two different objects

Figure 3. The object detection result on two different objects

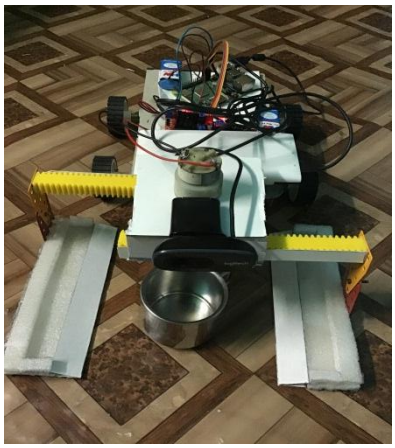

Figure 4. The robot with sled opened

International Journal of Applied Sciences and Smart Technologies

Volume 3, Issue 2, pages 145–152

p-ISSN 2655-8564, e-ISSN 2685-9432

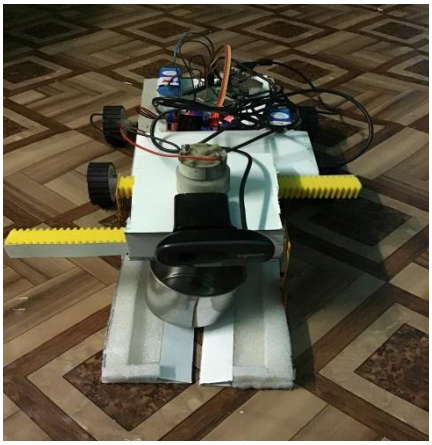

Figure 5. The robot with sled closed

4 Conclusion

The robot developed can be used in different scenario ranging from normal home use to hospital or chemical industries. It is equipped with intelligent features that can be used for efficiently picking several objects. The path storing and object detection via ultrasonic sensor helps the robot to precisely locate from one place to another. The robot can be equipped with voice recognition feature enabling its usage effectively and directly to physically challenged people. The robot can also be equipped with speakers which can speak out information regarding the position of the robot relative to the path saved in its memory. It can also speak out list of object available, paths set within its memory. The robot can also be equipped with Google Coral in order to increase its speed and allow the user to get live stream video from robot's webcam. It will also increase its speed in detecting object. The number of ultrasonic sensor can also be doubled so as to prevent the repeated checking of object by turning left. There's an alternate solution to this solution i.e. using stepper motor to use one ultrasonic sensor for both the direction. The robot sled can also be converted to robotic hands or design inspired from claw to increase its capabilities of picking objects.

Volume 3, Issue 2, pages 145–152

p-ISSN 2655-8564, e-ISSN 2685-9432

References

[1] A. Mishra, P. Makula, A. Kumar, K. Karan and V. K. Mittal, "A Voice-Controlled Personal Assistant Robot." *International Conference on Industrial Instrumentation and Control (ICIC)*, 2015.

[2] I.H. Shanavas, P.B. Reddy and M.C. Doddegowda, "A Personal Assistant Robot Using Raspberry Pi." *International Conference on Design Innovations for 3Cs Compute Communicate Contro*, 2018.

[3] C.H. Lin, H. Andrian, Y.Q. Wang, and K.T. Song, "Personal Assistant Robot." *Proceedings of the 2005 IEEE International Conference on Mcchafronics*, 2005.

[4] Real-time object detection with deep learning and OpenCV, https://www.pyimagesearch.com/2017/09/18/real-time-object-detection-with-deep-learning-and-opencv/

[5] Train your own tiny YOLO v3 on Google colaboratory with the custom dataset, https://medium.com/@today.rafi/train-your-own-tiny-yolo-v3-on-google-colaboratory-withthe-custom-dataset-2e35db02bf8f

[6] The AI Guy. (2020, January 28). YOLOv3 in the CLOUD: Install and Train Custom Object Detector (FREE GPU) [Video file]. Retrieved from https://www.youtube.com/watch?v=10joRJt39Ns&t=1440s

International Journal of Applied Sciences and Smart Technologies

Volume 3, Issue 2, pages 145–152

p-ISSN 2655-8564, e-ISSN 2685-9432

This page intetntionally left blank

International Journal of Applied Sciences and Smart Technologies

Volume 3, Issue 2, pages 153–160

p-ISSN 2655-8564, e-ISSN 2685-9432

Text Classification on Tamil

Omprakash Yadav[1], Alcina Judy[1], Praveen D'souza[1], Calvin Galbaw[1,*], Hinal Rane[1]

[1]*Department of Computer, Xavier Institute of Engineering, Mahim, Mumbai 400016, India*

[*]*Corresponding Author: calving2012@gmail.com*

(Received 01-09-2020; Revised 29-12-2021; Accepted 29-12-2021)

Abstract

By and large, we don't know to talk and read the territorial dialects that are spoken in our nation. So we have accepted Tamil language as it is our territorial and numerous doesn't get it. In our task, the content in Tamil language is stacked from Wikipedia. It is then sifted through and extraordinary characters are evacuated it is then characterized by the titles like id, title, URL, etc. It is then used to prepare the model utilizing CNN calculation and the dataset is created. Along these lines, you would now be able to test utilizing an irregular Wikipedia page and the content is grouped by the titles and anticipated.

Keywords: tamil text classification, feature classification, vocabulary set or bag-of-words, text mining, natural language processing

1 Introduction

For the most part, we don't comprehend huge numbers of the local dialects in our nation. So at whatever point an individual of various state language is spoken or composed, we were unable to get it. In this task, we characterize the content dependent on the sort like name, nation, id, and so on. Here, we use CNN to arrange the content

Volume 3, Issue 2, pages 153–160
p-ISSN 2655-8564, e-ISSN 2685-9432

and train the dataset. It is useful for individuals to order the sort and in any event, get a thought of what the content looks like.

It will be simple for the individual to know and recognize the various segments present in the information. The sort of information is helpful for various logical purposes for getting it.

2 Literature Survey

We refer to references [1], [2], [3], [4], [5]. In deep learning, a convolutional neural system (CNN or ConvNet) is a class of deep neural systems, most usually applied to investigating visual features. These utilize the spatial loads of channels to extricate highlights from the picture. They have applications in picture and video acknowledgment, recommender frameworks, picture arrangement, clinical picture examination, regular language handling, and money related time arrangement. Convolutional neural systems use convolutional layers as building squares to gain from the dataset. Alongside these, pooling layers and completely associated layers are utilized.

A convolution is the basic use of a channel to an info that outcomes in an activation. These channels slide over width and tallness to convolve the information and use actuation capacity to make a highlighted map. This guide can be passed to another convolutional layer to make an increasingly itemized map.

These component maps can be unfurled to take care of into a completely associated layer to get the explicit prescient displaying issue, for example, picture arrangement. Since information like pictures, recordings, and other multi-dimensional information have a quadratic number of highlights, an ordinary neural system needs to process a huge measure of straight capacities and enactments which takes a quadratic measure of time. Be that as it may, convolutional organize registers each weight in a straight time utilizing channels.

Volume 3, Issue 2, pages 153–160
p-ISSN 2655-8564, e-ISSN 2685-9432

he outcome is profoundly explicit highlights that can be distinguished anyplace on input images [3].

1. Convolutional neural systems apply a channel to a contribution to make a component map that sums up the nearness of recognized highlights in the input [3].
2. Filters can be high quality, for example, line finders, yet the advancement of convolutional neural systems is to get familiar with the channels during preparing with regards to a particular forecast problem [3].
3. How to figure the component map for one-and two-dimensional convolutional layers in a convolutional neural system [3].

For regular language handling tasks, counterfeit neural systems, for example, intermittent neural systems (RNN) and long transient memory systems (LSTM) are favored because they go off past initiation or yield as a contribution to the following concealed states. This aids in recalling the word/character figured which helping I processing the following ward word. That is the reason these models are utilized most often in language models.

Since the attempted assignment is of order, convolutional neural systems are utilized which changes in input. Instead of contributing a picture, word installing can be utilized as the info. Word installing is made utilizing different models, for example, Word2Vec. Since the forecast will be made on Wikipedia information, we have made an installation on Wikipedia pages.

Input Layers: It's the layer where we contribute to our model. The quantity of neurons in this layer is equivalent to add up to estimate of the word implanting.

Hidden Layer: For grouping utilizing word implanting, for the most part, a single layer of completely associated layers are utilized to shape the concealed layer. Additionally, a single layer of convolutional layer followed by a completely associated layer can be utilized.

Volume 3, Issue 2, pages 153–160
p-ISSN 2655-8564, e-ISSN 2685-9432

Output Layer: Since there are n number of words, the yield from the concealed layer is then taken care of into a calculated capacity of the softmax layer which changes over the yield of each word into the likelihood score of each class.

The information is then taken care of into the model and yield from each layer is acquired this progression is called feedforward, we at that point figure the blunder utilizing a mistake work, some normal mistake capacities are cross-entropy, square misfortune blunder and so forth. From that point forward, we back engender into the model by figuring the subsidiaries. This progression is called Backpropagation which fundamentally is utilized to limit the misfortune.

3 Existing System

Natural language processing represents computational techniques used for processing human language. The language can either be represented in terms of text or speech. NLP in the context of deep learning has become very popular because of its ability to handle text which is far from being grammatically correct. The ability to learn from the data has made the machine learning system powerful enough to process any type of unstructured text. Machine learning approaches have been used to achieve state of the art results on NLP tasks like text classification, machine translation, question answering, text summarization, text ranking, relation classification, and others. The focus of our work is text classification of Tamil language. Text classification is the most widely used NLP task. It finds application in sentiment analysis, spam detection, email classification, and document classification to name a few. It is an integral component of conversational systems for intent detection. There have been very few text classification works in literature focusing on the resource-constrained Tamil language. While the most important reason for this is the unavailability of large training data; another reason is the generalizability of deep learning architectures to different languages. However, Tamil is a morphologically rich and relatively free word order language so we investigate the performance of different models on the Tamil text classification task. Moreover, there has been a substantial rise in Tamil language digital content in recent years. Service providers, e-commerce industries are now targeting local languages to improve their

Volume 3, Issue 2, pages 153–160
p-ISSN 2655-8564, e-ISSN 2685-9432

visibility. An increase in the robustness of translation and transliteration systems has also contributed to the rise of NLP systems for Tamil text. This work will help in the selection of the right models and provide a suitable benchmark for further research in Tamil text classification tasks.

4 Proposed Methodology

The proposed methodology is as follows.

Step 1: Obtain the text from Wikipedia for Tamil pages

Go to https://ta.wikipedia.org/wiki/முதற்_பக்கம் from this extract the text and convert it into csv file this file is then taken for further processing.

Step 2: Filtering and removal of special characters:

The special characters and the ambiguity present in the text are removed such as comma, semicolon, asterisk mark, brackets and so on. This will help the text to be simplified for further processing of data.

Step 3: Classify using titles

The text is classified according to the titles such as id, name, title, url, recursive words etc.

Step 4: Train the dataset using CNN

The dataset is trained using Convolutional Neural Networks (CNN) is one kind of feed forward neural network. CNN is an efficient recognition algorithm which is widely used in pattern recognition and image processing. It has many features such as simple structure, less training parameters and adaptability.

Step 5: Test using random Wikipedia page

Now we are able to test any random Wikipedia page and the text is classified according to the titles and predicts the results.

International Journal of Applied Sciences and Smart Technologies

Volume 3, Issue 2, pages 153–160

p-ISSN 2655-8564, e-ISSN 2685-9432

5 Implementation

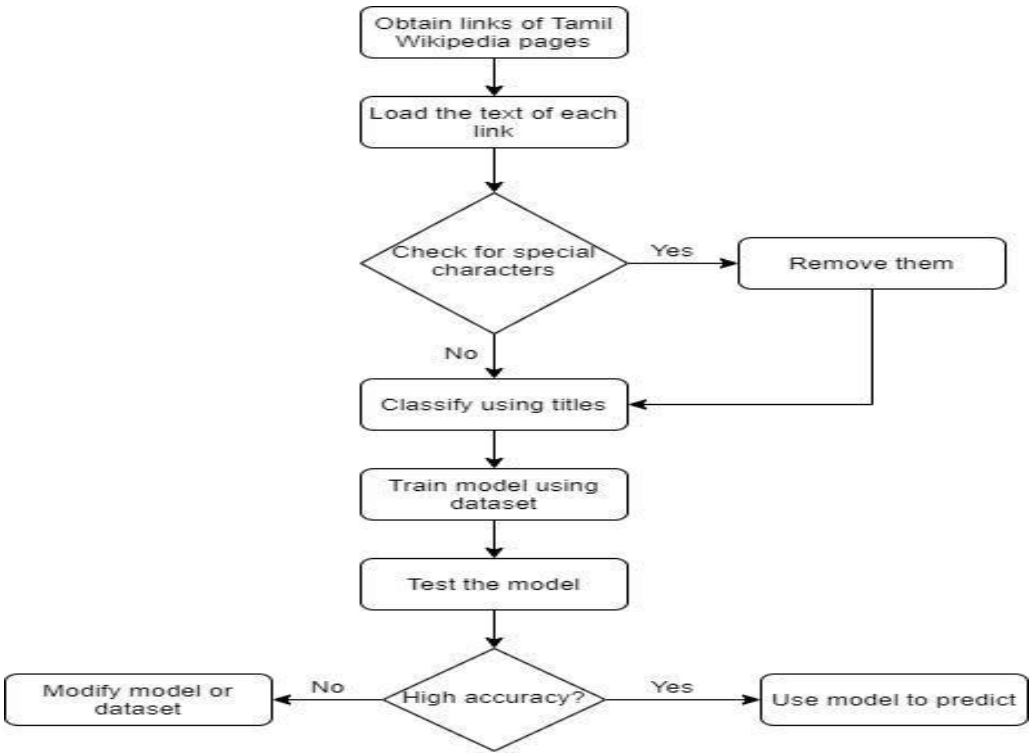

Figure 1. Flowchart.

The above Figure 1 is the Flowchart of our system. The working of our system is as follows:

1. The text from Tamil Wikipedia pages are extracted and checked for special characters.
2. Such characters create problem while classifying that is these special characters are not important to be classified.
3. The text is classified according to the title, tags, key words, and what the text is about.
4. This is used as the dataset for the model to be trained on.
5. Once we achieve high accuracy on the model, the user can use this model to get the details of an unknown Tamil text such as titles, etc.

Volume 3, Issue 2, pages 153–160

p-ISSN 2655-8564, e-ISSN 2685-9432

6 Conclusion

In this report, we have introduced a Tamil language text arrangement that encourages the client to distinguish the sort of text and create a dataset by expelling all the ambiguities in the content and preparing the dataset which will be useful to test any irregular Wikipedia page.

References

[1] E. Annamalai and S. B. Steever. Modern Tamil in Dravidian languages. *Newyork: Routledge Publication*, 1999.

[2] R. K. Belew, "Adaptive information retrieval." *In Proceedings of the 12th annual international ACM/SIGIR conference on research and development in information retrieval*, NY, 11–20, 1989.

[3] L. Chanunya and R. Peachavanish, "Automatic Thai language essay scoring using neural network and latent semantic analysis." *In Proceedings of the first Asia international conference on modeling and simulation*, 2007.

[4] C.H. Li and S.C. Park, "Text categorization based on artificial neural networks." *In ICONIP*, **4234**, LNCS 302–311, 2006.

[5] C.H. Li and S.C. Park, "Neural network for text classification based on singular value decomposition." *In Seventh international conference on computer and information technology*, 47–52, 2007.

International Journal of Applied Sciences and Smart Technologies

Volume 3, Issue 2, pages 153–160

p-ISSN 2655-8564, e-ISSN 2685-9432

This page intetntionally left blank

International Journal of Applied Sciences and Smart Technologies

Volume 3, Issue 2, pages 161–170

p-ISSN 2655-8564, e-ISSN 2685-9432

Study of Nickel Extraction Process from Spent Catalysts with Hydrochloric Acid Solution: Effect of Temperature and Kinetics Study

Kevin Cleary Wanta[1,*], Ivanna Crecentia Narulita Simanungkalit[1], Elsha Pamida Bahri[1], Ratna Frida Susanti[1], Gelar Panji Gemilar[2], Widi Astuti[3], Himawan Tri Bayu Murti Petrus[4]

[1]*Department of Chemical Engineering, Parahyangan Catholic University, Jl. Ciumbuleuit 94, Bandung 40141, Indonesia*
[2]*PT Petrokimia Gresik, Jl. Jenderal Ahmad Yani, Gresik 61119, Indonesia*
[3]*Research Unit for Mineral Technology, Indonesian Institute of Sciences (LIPI), Jl. Ir. Sutami Km. 15, Tanjung Bintang 35361, Indonesia*
[4]*Department of Chemical Engineering, Universitas Gadjah Mada, Jl. Grafika 2, Kampus UGM, Yogyakarta, 55281, Indonesia*
[*]*Corresponding Author: kcwanta@unpar.ac.id*

(Received 20-08-2021; Revised 19-09-2021; Accepted 20-09-2021)

Abstract

As one of the hazardous and toxic solid wastes, spent catalysts need to be treated before the waste is discharged into the environment. One of the substances that need to be removed from the spent catalysts is the heavy metal ions and/or compounds contained therein. The method that can be applied is the extraction method using an acid solvent. In this study, the extraction process was carried out on spent catalysts samples from PT. Petrokimia Gresik. The focus of the study is on nickel extraction by varying the temperature in the range of 30–85 ^{o}C. A 1 M hydrochloric acid (HCl) solution was used as a solvent while the extraction process was 120 minutes. The experimental results show that the maximum nickel recovery of 14.70%

can be achieved at a temperature of 85 ^{o}C. Kinetic studies were carried out using two kinetic models. The results of both models evaluation on the research data show that the lump model gives better results than the shrinking core model. The average error percentage of the lump model is smaller than the shrinking core model. It indicates that the extraction process was controlled by the diffusion step through the ash layer in the solid and chemical reactions simultaneously.

Keywords: Extraction, lump model, nickel, shrinking core model

1 Introduction

Various chemical industries, such as the oil, fertilizer, and petrochemical industries require catalysts to increase the rate of chemical reactions. The catalysts used can be solid catalysts containing different metal contents, such as nickel (Ni), iron (Fe), cobalt (Co), vanadium (V), molybdenum (Mo), and various other heavy metals [1]. The use of catalysts in the long term will make the catalyst saturated and no longer adequate for use. Thus, these catalysts will be replaced and disposed of as a used catalyst or what is usually called spent catalysts. Spent catalysts can not be disposed of directly into the environment because these catalysts are classified as hazardous solid waste. Therefore, this waste needs to be treated first with the aim of taking hazardous compounds, such as heavy metals contained in it.

One of the spent catalysts solid waste treatment that can be done is extracting ions or compounds contained in the catalysts. This method is usually referred to as the leaching method. This method is a commonly used method and has been done by several researchers before. This extraction process requires a solvent to react and dissolve the metal ions and/or compounds. The solvents usually used are acidic solvents, both strong acids and weak acids [1], [2], [3], [4].

In this study, the extraction process was carried out using a hydrochloric acid solution. Furthermore, this research also studies parameters that have a significant impact on the extraction process, such as temperature. Temperature is an important parameter in the extraction process because temperature affects the rate of molecular

diffusion and the rate of chemical reactions. Furthermore, by studying the effect of temperature in the extraction process, the kinetic study of this process can be investigated by utilizing the existing kinetic models, such as the shrinking core model and the lump model. By studying the kinetics of the extraction process, a proper extractor can be designed. A proper extractor design must follow the applicable mechanism of the extraction process. Thus, the results of this study are expected to provide the appropriate information for the extractor design process.

2 Research Methodology

Materials. The main raw material of this research is the spent catalyst from PT. Petrokimia Gresik. These catalysts have a nickel content of 16.7% wt, where the largest nickel phase in these catalysts is nickel elements (metals) and nickel oxide compounds (NiO). In addition, another main material used is a 1 M hydrochloric acid (HCl) solution. This HCl solution acts as a solvent in this extraction process.

Equipment. The main equipment used for the extraction process is a series of equipment consisting of a three–neck flask (as an extractor), stirrer and motor, condenser, water bath and thermostat (to maintain a constant operating temperature), and a thermometer. As a sample analysis instrument, the instrument used is Atomic Absorption Spectroscopy (AAS).

Research procedure. 180 mL of 1 M hydrochloric acid solution was put into a three–neck flask. After the equipments were assembled, the solution was heated to the desired temperature. In this study, the operating temperature was varied at 30, 60, and 85^{o} C. After the temperature was reached, 36 grams of the spent catalyst solids (<74 microns) were put into the extractor. This solids intake will be counted as t = 0. The extraction process lasted for 120 minutes where during the operation time, the sampling was carried out periodically at 5, 10, 15, 30, 60, and 120 minutes. The samples that had been taken would be separated first between the solid and the liquid phase. This separation process was carried out using a centrifuge which was operated at 1,000 rpm for 10

Volume 3, Issue 2, pages 161–170
p-ISSN 2655-8564, e-ISSN 2685-9432

minutes. The supernatant formed was then analyzed for the nickel content in the solution using Atomic Absorption Spectroscopy (AAS) instruments.

Data analysis. The data obtained from the analysis using the AAS instrument is processed to obtain the result in the form of nickel recovery percentage where the equation used to calculate the value is:

$$x = \frac{C_{Ni}}{C_{Ni,tot}} \; x\,100\% \tag{1}$$

where x is the percentage of nickel recovery, CNi is the concentration of nickel extracted during the extraction process in ppm, CNi,tot is the total nickel concentration extracted from raw materials in ppm.

Furthermore, the nickel recovery data will be used to study the kinetics of the extraction process. There are two kinetic models applied in this study, namely the shrinking core model and the lump model. For the shrinking core model, the equations used are [5], [6], [7]:

Diffusion in liquid film layer controlling : $x' = k_f.t$ (2)

Diffusion in ash layer controlling : $1 - 3(1-x')^{0,67} + 2\,(1-x') = k_d.t$ (3)

Chemical reaction controlling : $1 - (1-x')^{0,33} = kr.t$ (4)

where x' is the nickel recovery fraction, kf, kd, and kr are the rate constants for the extraction process, and t is the operating time. For the lump model, the equations used are [8]:

$$\frac{dx}{dt} = \left[\alpha.\frac{1}{(1-x')} + \beta.\frac{\left\{(1-x')^{1/3} - 1\right\}}{(1-x')^{1/3}}\right]^{-1} \tag{5}$$

where α is a constant related to the rate at the chemical reaction step while β is a constant related to the rate at the diffusion step in the ash layer.

Determination of the suitable mathematical model is done by calculating the percentage error of research data and simulation data. The equation used is as follows:

$$\%E = \left|\frac{(x'_{data} - x'_{sim})}{x'_{data}}\right| \; x\,100\% \tag{6}$$

International Journal of Applied Sciences and Smart Technologies
Volume 3, Issue 2, pages 161–170
p-ISSN 2655-8564, e-ISSN 2685-9432

where %E is the percentage of error, x'_{data} is the percentage of nickel recovery from experimental data, and x'_{sim} is the percentage of nickel recovery from the simulation results of mathematical models.

3 Results and Discussion

Effect of temperature on nickel recovery. Temperature is a very important parameter and has a significant influence on determining the rate of the extraction process. In this study, the temperature used is in the range of 30–85 ^{o}C. The experimental results are presented in Figure 1.

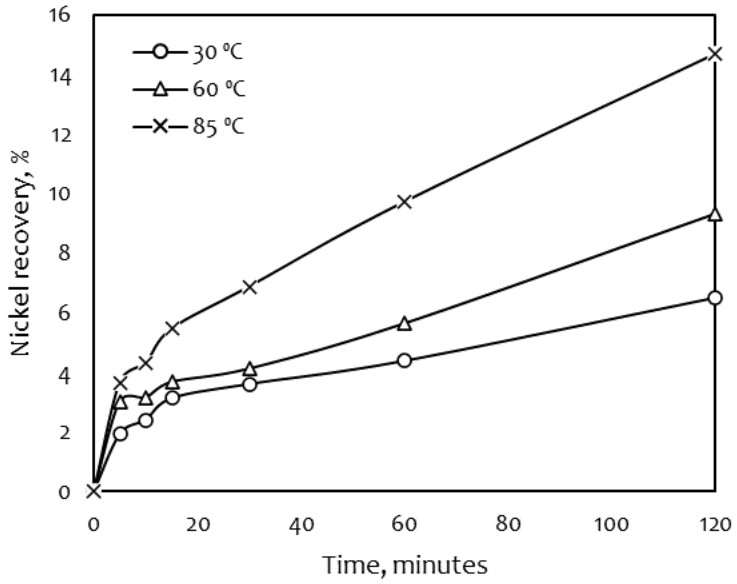

Figure 1. Effect of temperature on nickel recovery

Figure 1 shows that the higher the temperature used, the more nickel can be obtained. In this study, the highest nickel recovery was obtained during the process at a temperature of 85 ^{o}C for 120 minutes, where the percentage of nickel recovery was 14.70%. In general, the nickel recovery that occurs during the process can reach 1.44 (for a temperature of 60 ^{o}C) and 2.25 times (for a temperature of 85 ^{o}C) compared to nickel recovery at a temperature of 30 ^{o}C. This phenomenon can occur because an

Volume 3, Issue 2, pages 161–170
p-ISSN 2655-8564, e-ISSN 2685-9432

increase in temperature will enhance the kinetic energy of each molecule in the system. Consequently, each molecule will collide more often so that chemical reactions will also take place more quickly. In addition, an increase in temperature will also enhance the rate of diffusion, both molecular diffusion in the liquid film layer and diffusion in the ash layer in the solid.

Kinetics study using the shrinking core model. The first kinetic model to be evaluated against the experimental data above is the shrinking core model. This model is the model most widely used by previous researchers in the hydrometallurgy or metal extraction process. The evaluation of this model is carried out using mathematical equations (2–4) and the evaluation results obtained are presented in Figure 2.

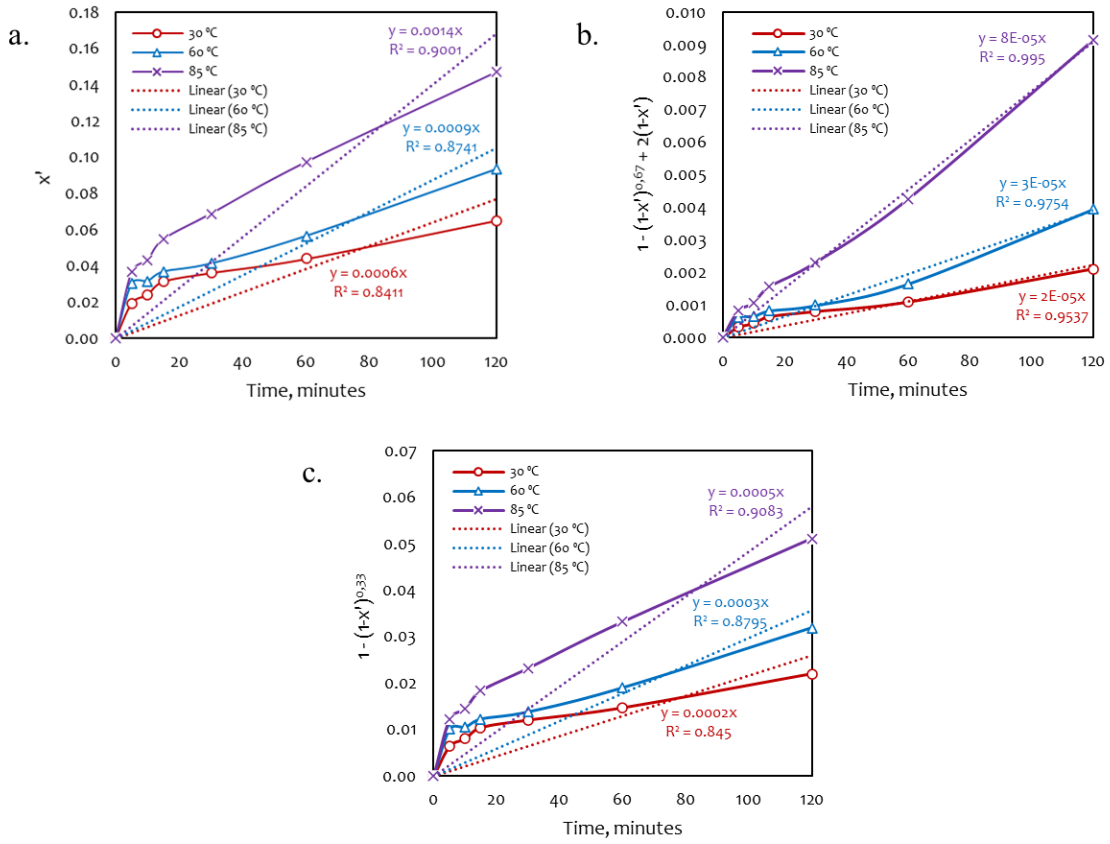

Figure 2. Simulation results of the shrinking core model when (a) diffusion in the liquid film layer controlling; (b) diffusion in the ash layer controlling; (c) chemical reactions controlling

Volume 3, Issue 2, pages 161–170
p-ISSN 2655-8564, e-ISSN 2685-9432

Figure 2 shows the simulation results of the experimental data. The simulation results show that the shrinking core model in which the diffusion step in the ash layer controlling is the best model to illustrate the overall mechanism during the extraction process. This can be concluded because the R^2 value obtained in this model is better than the other two models (diffusion step in the film layer and chemical reactions that control the process). A good R^2 value is an R^2 value that is close to 1.

The evaluation results obtained indicate that the diffusion step through the ash layer in the solid is the step with the slowest rate. In solids, there are pathways used for each molecule (both reactant and product molecules) to diffuse. This pathway has a small size so that the reactant molecules that diffuse from the surface of the liquid to the unreacted surface in the solid will interfere with each other with the product molecules that diffuse from the surface that has reacted in the solid to the liquid body. It causes diffusion through the ash layer in the solid to be the step that controls the extraction process. Thus, the total rate of nickel extraction from the spent catalyst is determined by the rate of diffusion in the solid (the slowest rate).

Another parameter commonly used to evaluate the kinetics of a process is the activation energy. Activation energy is the minimum energy required for a reaction to occur. The value of this parameter can be found using the Arrhenius equation as follows [9]:

$$k = A \exp\left(-\frac{Ea}{RT}\right) \tag{7}$$

$$\ln k = \ln A - \frac{Ea}{RT} \tag{8}$$

where A is the collision frequency, E_a is the activation energy, R is the gas constant, and T is the absolute temperature. In this extraction process, the value of the collision frequency (A) obtained is 0.1384, while the activation energy value is 22.65 kJ/mol. According to Havlík, if the activation energy value is in the range of 20–35 kJ/mol, the extraction process is controlled by the diffusion and chemical reactions simultaneously [10]. Therefore, this kinetic study will be continued by using the lump model, which combines the two stages to prepare the mathematical model.

International Journal of Applied Sciences and Smart Technologies

Volume 3, Issue 2, pages 161–170

p-ISSN 2655-8564, e-ISSN 2685-9432

Kinetics study using the lump model. One of the weaknesses of the shrinking core model is that mathematical problem compiled in the model only assume one step that controls the extraction process; other steps are ignored because those steps are considered to have a very fast rate. In fact, in the solid–liquid extraction process, there are five steps involved in the system. For some cases, the use of assumptions as mentioned above does not represent the actual mechanism that occurs during the extraction process. As a result, the designed extractor will not be suitable for this process. Therefore, in this study, to complete the kinetic study, the lump kinetic model is evaluated against the experimental data where the equation used for the simulation process follows equation (5). The simulation results of the lump model are then compared with the evaluation results of the shrinking core model, where the diffusion step in the ash layer controls the extraction process. The comparison of the two kinetic models is presented in Table 1.

Table 1. Comparison of the simulation results of the shrinking core model (diffusion step in the ash layer) with the lump model

Time, minutes	Nickel Recovery – Experimental, %			Nickel Recovery - SCM*, %			Nickel Recovery – Lump Model, %			Error - SCM*, %			Error – *Lump, %*		
	30^{o}C	**60^{o}C**	**85^{o}C**	**30^{o}C**	**60^{o}C**	**85^{o}C**	**30^{o}C**	**60^{o}C**	**85^{o}C**	**30^{o}C**	**60^{o}C**	**85^{o}C**	**30^{o}C**	**60^{o}C**	**85^{o}C**
0	0.00	0.00	0.00	0.00	0.00	0.00	0.00	0.00	0.00	0.00	0.00	0.00	0.00	0.00	0.00
5	1.92	3.02	3.66	0.74	1.17	2.35	1.41	1.89	3.04	61.35	61.28	35.67	26.56	37.42	16.94
10	2.41	3.16	4.32	1.29	1.96	3.49	1.99	2.67	4.28	46.36	37.90	19.23	17.43	15.51	0.93
15	3.13	3.68	5.46	1.75	2.60	4.51	2.43	3.27	5.23	44.07	29.27	17.44	22.36	11.14	4.21
30	3.61	4.13	6.88	2.84	4.09	6.83	3.43	4.60	7.34	21.32	0.91	0.78	4.99	11.38	6.69
60	4.39	5.65	9.73	4.44	6.24	10.10	4.83	6.46	10.27	1.08	10.36	3.80	10.02	14.34	5.55
120	6.51	9.34	14.70	6.73	9.27	14.67	6.78	9.05	14.30	3.33	0.76	0.23	4.15	3.10	2.72
						The average error percentage per temperature:				**25.36**	**20.07**	**11.02**	**12.22**	**13.27**	**5.29**
						The average error percentage per kinetics model:					**18.82**			**10.26**	

*SCM: the shrinking core model with a diffusion step in the ash layer controls the process.

Based on Table 1, the lump kinetics model provides better evaluation results than the shrinking core model. This can be concluded from the average error percentage for both

models, namely 10.26% for the lump model and 18.82% for the shrinking core model. These results further corroborate the previous information that the spent catalyst extraction process using 1 M hydrochloric acid solution is controlled by the diffusion step through the ash layer and chemical reactions simultaneously.

4 Conclusion

Based on the experimental dan simulation results, temperature significantly affects the nickel extraction process from spent catalysts with hydrochloric acid as solvent. At a temperature of 85 oC, the nickel recovery can reach 14.70% after the process lasts for 120 minutes. From the research data, the mechanism of the extraction process was studied and it was found that the rate of the extraction process was determined by the diffusion step through the ash layer in the solid and the chemical reaction step. Both of these stages occur simultaneously. The use of the lump model proves the conclusions obtained. Based on the average error percentage, the model gives a smaller error value than the shrinking core model. The average error percentage for the lump model is 10.26%.

Acknowledgements

The authors thank the Institute for Research and Community Service of Parahyangan Catholic University, which has supported this research financially. In addition, the authors also thank PT. Petrokimia Gresik, which has provided the main raw materials for this research.

References

[1] M. Marafi dan A. Stanislaus, "Waste Catalyst Utilization: Extraction of Valuable Metals from Spent Hydroprocessing Catalysts by Ultrasonic–Assisted Leaching with Acids." *Industrial & Engineering Chemistry Research*, **50,** 9495–9501, 2011.

[2] P.K. Parhi, K.H. Park, G. Senanayake, "A kinetic study on hydrochloric acid leaching of nickel from Ni–Al2O3 spent catalyst." *Journal of Industrial and Engineering Chemistry*, **19,** 589–594, 2013.

Volume 3, Issue 2, pages 161–170

p-ISSN 2655-8564, e-ISSN 2685-9432

[3] J. Ramos–Cano, G. González–Zamarripa, F.E. Carrillo–Pedroza, M. de J.Soria–Aguilar, A. Hurtado–Marcías, A. Cano–Vielma, "Kinetics and statistical analysis of nickel leaching from spent catalyst in nitric acid solution." *International Journal of Mineral Processing*, **148,** 41–47, 2016.

[4] W. Mulak, B. Miazga, A. Szymczycha, "Kinetics of nickel leaching from spent catalyst in sulphuric acid solution." *Int. J. Miner. Process*, **77,** 231–235 2005.

[5] O. Levenspiel, Chemical Reaction Engineering. 3rd Edition, New York: John Wiley & Sons, Inc., 1999.

[6] O.S. Ayanda, F.A. Adekola, A.A. Baba, O.S. Fatoki, B.J. Ximba, "Comparative Study of the Kinetics of Dissolution of Laterite in some Acidic Media." *Journal of Minerals & Materials Characterization & Engineering*, **10** (15), 1457–1472, 2011.

[7] K.C. Wanta, F.H. Tanujaya, R.F. Susanti, H.T.B.M. Petrus, I. Perdana, W. Astuti, "Studi Kinetika Proses Atmospheric Pressure Acid Leaching Bijih Laterit Limonit Menggunakan Larutan Asam Nitrat Konsentrasi Rendah." *Jurnal Rekayasa Proses* **12** (2), 77–84, 2018.

[8] K.C. Wanta., W. Astuti, I. Perdana, H.T.B.M. Petrus, "Kinetic Study in Atmospheric Pressure Organic Acid Leaching: Shrinking Core Model versus Lump Model." *Minerals*, **10**, 1–10, 2020.

[9] H.S. Fogler, Element of Chemical Reaction Engineering. 4th Edition, New Jersey: Prentice Education, Inc., 2006.

[10] T. Havlík, Hydrometallurgy. Cambridge: Woodhead Publishing Limited, 2006.

International Journal of Applied Sciences and Smart Technologies

Volume 3, Issue 2, pages 171–184

p-ISSN 2655-8564, e-ISSN 2685-9432

Alarm System and Emergency Message from Wheelchair User Emergency Condition

Yavez E. Loho[1], Diana Lestariningsih[1,*], Peter R. Angka[1]

[1]*Department of Electrical Engineering, Faculty of Engineering, Surabaya Widya Mandala Catholic University, Indonesia*

[*]*Corresponding Author: diana@ukwms.ac.id*

(Received 12-09-2021; Revised 31-12-2021; Accepted 31-12-2021)

Abstract

When someone uses a wheelchair, there is still the possibility of an accident to the user, such as when the user suddenly falls down from the wheelchair or the user falls down along with the wheelchair. For notification of emergency conditions for wheelchair users, an alarm system is designed that can send messages to the intended mobile number. The system is designed using Wemos D1 mini, Ultrasonic, MPU-6050 and Proximity E18-D80NK sensors. The conclusion from the measurement and test results are: the value read by the MPU-6050 sensor is taken one axis for each direction when the wheelchair was falling down, $Y \leq 180°$ for left falling down, $X \leq 50°$ for right falling down, $Z \leq 65°$ for forward falling and $Z \geq 140°$ for backwards falling down. The Ultrasonic sensor works well for detecting the presence of user's legs and the E18-D80NK proximity sensor works well for detecting the position of the user who is sitting in a wheelchair. Receiving notifications through the BLYNK server works well, not affected by distance provided there is an internet connection connected to the device.

Keywords: Wheelchair, MPU-6050 sensor, ultrasonic sensor, emergency conditions, Wemos D1 mini

International Journal of Applied Sciences and Smart Technologies
Volume 3, Issue 2, pages 171–184
p-ISSN 2655-8564, e-ISSN 2685-9432

1 Introduction

The use of wheelchairs in society is widely used to help people who have difficulty walking on their feet, either due to injury or disability. This tool is not only available in hospitals but is also sold in general at health outlets in every area. So it is relatively easy for people who have difficulty walking to buy a wheelchair. There are various types of wheelchairs, manual, electric, and sport. However, the most often found in the general public is the manual type because the price is affordable and its use is practical for ordinary people. The manual type wheelchair is moved by being pushed another person or by the user's own hand. In its use, it is often found that the safety of wheelchairs is not perfect. There are still many emergency conditions that occur in wheelchair users, such as when the user falls down from the wheelchair or the user falls along with the wheelchair. The cause of these emergency conditions can occur because the user moves excessively or it can also be due to the condition of the user being tired or weak and the lack of supervision of the user. For notification of the emergency condition of the wheelchair user, a warning device or notification is needed to other people when the wheelchair user at the emergency condition and so they can immediately provide assistance.

Several literature reviews that have been carried out relating to wheelchair safety systems are smart wheelchairs that can avoid obstacles by using 8 proximity sensors and cameras (Yeounggwang Ji, 2013). Electric wheelchair to avoid obstacles using the HC-SR04 sensor where the wheelchair can detect obstacles less than 2m (Taizo Miyachi et al, 2016). The electric wheelchair safety system from impact uses 6 proximity sensors to detect obstacles (Darul, Muslimin, 2017). Automatic wheelchair with intelligent control mode and Wi – Fi placement system. A wheelchair specifically for users who have low-level visual impairment, by scanning the position of the wheelchair and controlling the direction of the wheelchair remotely (Manjunath, Gurukiran, 2018). From the reference review, what is being done is to maintain safety while using a wheelchair, whereas in the event of an emergency, a wheelchair user has not planned to report the emergency condition. Therefore, the purpose of this study is to design an alarm system for

Volume 3, Issue 2, pages 171–184
p-ISSN 2655-8564, e-ISSN 2685-9432

notification of emergency conditions for wheelchair users and send messages to telephone numbers that have been stored in advance.

The goal to be achieved is to produce a wheelchair alarm system that can provide notifications automatically when wheelchair user at emergency condition. The emergency condition is that the wheelchair user falls along with the wheelchair or the wheelchair user falls down without a wheelchair. So, further action can be taken from the notification recipient or the people around who hear the alarm sound. Note that readers are referred to published work [1], [2], [3], [4], [5], [6], [7], [8], and [9].

2 Research Methodology

This section provides research methodology that we use in this work.

2.1 Block Diagram

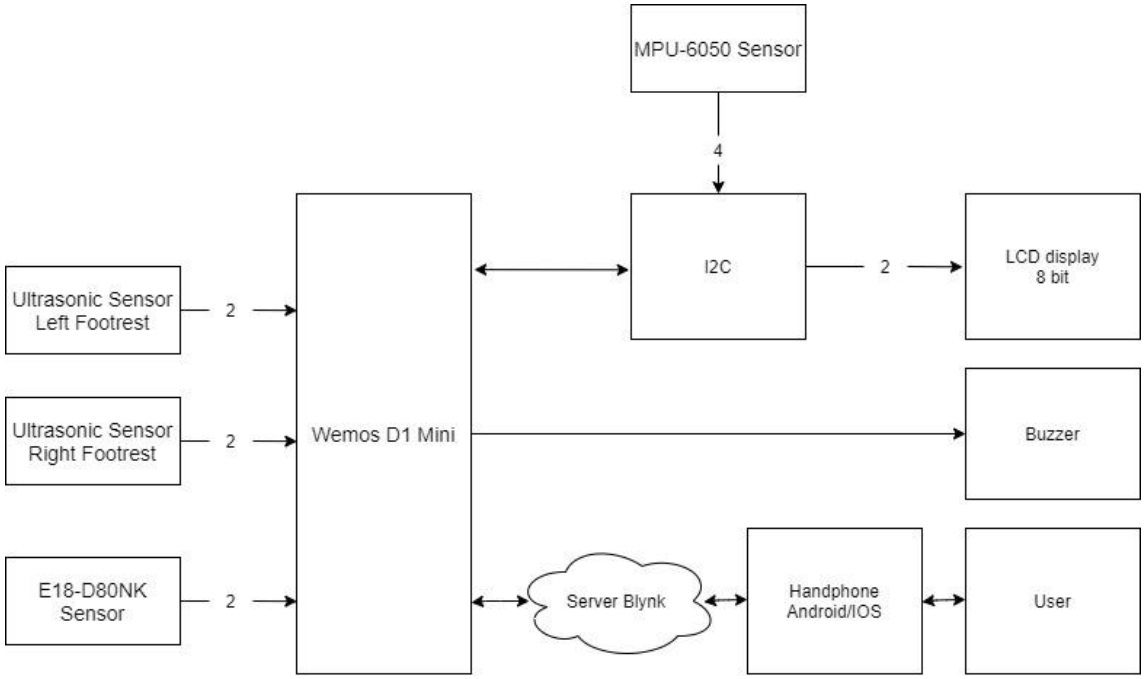

Figure 1. Block Diagram

Figure 1 shows a block diagram of the designed system. The overall working principle of the tool system is governed by the Wemos D1 mini as the main microcontroller. In the design of the tool there are 2 pairs of Ultrasonic Sensors which are placed on the pipe on the right and left side of the wheelchair footrest retainer and

Volume 3, Issue 2, pages 171–184
p-ISSN 2655-8564, e-ISSN 2685-9432

the Proximity E18-D80NK sensor on the right side of wheelchair seat and the MPU-6050 sensor on the back side of the wheelchair.

Ultrasonic and proximity E18-D80NK sensor serves to detect the presence of users sitting in wheelchairs. Ultrasonic sensors on the right and left side pipes of the footrest supports are used to detect the user's legs with the soles of the feet in the wheelchair footrest position. When the user is about to get out of the wheelchair, the footrest is automatically opened and the ultrasonic sensor will detect the open footing and the Proximity E18-D80NK sensor on the right side of the wheelchair seat will detect there is no wheelchair user. This proves that the user left the wheelchair.

The MPU-6050 sensor on the wheelchair functions as a detector of a certain slope value to determine if the wheelchair is in a normal position or falling down. If the user falls along with the wheelchair, the MPU-6050 sensor will detect a change in the predetermined value indicating that the user is in an emergency condition and the Wemos D1 mini wifi module will send an emergency message in the form of a notification on BLYNK server to the target person's cellphone where the cellphone number is previously saved. Under certain conditions, wheelchair users may fall forward without a wheelchair. In this case, the ultrasonic sensor will detect that there is no user in a wheelchair so that the Wemos D1 mini Wifi Module will send an emergency notification to the target phone via BLYNK server.

The explanation of the system block diagram is as follows:

1. Wemos D1 mini is the main controller that functions to process all data and becomes communication from the device to BLYNK server to send notifications.
2. The MPU-6050 sensor is used to detect the tilt of the wheelchair when the user on the wheelchair at an emergency condition.
3. Ultrasonic sensors on the left and right side of the footrest supports are used to detect the user's legs with the soles of the feet in the wheelchair footrest position
4. The E18-D80NK Proximity Sensor functions to detect the presence of the user while sitting in a wheelchair.
5. Eight-bit LCD Display functions to display characters in the form of information on the position of wheelchair users and who can be contacted when wheelchair users are in an emergency condition.

Volume 3, Issue 2, pages 171–184
p-ISSN 2655-8564, e-ISSN 2685-9432

6. BLYNK server is used as an application to receive notifications from wheelchair users at emergency conditions.

2.2 Hardware Design

Figure 2 shows the placement of the black box at the back side of the wheelchair. The black box has dimensions of 18 x 11 x 6 cm containing the MPU-6050 sensor, Wemos D1 mini, and LCD Display. The MPU-6050 sensor is placed in a box that aims to keep at the stable position.

Figure 2. Black Box Placement at the back side of Wheelchair

Wemos D1 mini as a microcontroller functions to process data received from each sensor used. Wemos D1 mini is placed in a box with the aim of preventing circuit damage due to external factors such as accidental collisions. Figure 3 shows the position of the component placement.

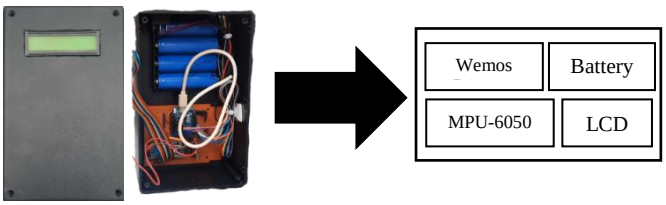

Figure 3. Components Position in Black Box

Volume 3, Issue 2, pages 171–184
p-ISSN 2655-8564, e-ISSN 2685-9432

Figure 4. Placement Position of Ultrasonic Sensor on Footrest Pipe

Figure 4 shows the position of ultrasonic sensor on the right and left side pipes of the footrest holder. Ultrasound sensors are placed not facing each other to avoid confusing for the expected data reading. Figure 5 shows the placement of the E18-D80NK Proximity sensor. The sensor is placed on the right side of the wheelchair which is used to detect the presence of the user while sitting in a wheelchair.

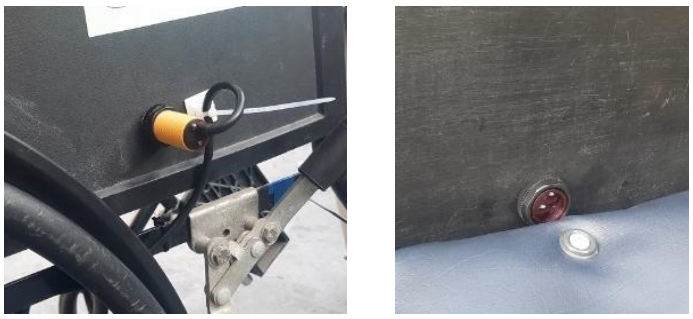

Figure 5. Proximity Sensor E18-D80NK

Table 1. shows the relationship between the Wemos D1 mini pins and the components used.

International Journal of Applied Sciences and Smart Technologies
Volume 3, Issue 2, pages 171–184
p-ISSN 2655-8564, e-ISSN 2685-9432

Table 1. Pins on Wenos D1 mini and Components

Wemos D1 mini Pin	Components	**Pin I/0** Components
A0	Proximity E18-D80NK Sensor	In
D0	*infrared* Sensor	VCC : *Infrared* Sensor
D1	LCD, MPU-6050	SCL
D2	LCD, MPU-6050	SDA
D3	Buzzer	Out
D5	Ultrasonik Sensor	In
D6	Ultrasonik Sensor	In
D7	Ultrasonik Sensor	In
D8	Ultrasonik Sensor	In
GND	LCD, *infrared* Sensor, *buzzer*	GND : LCD, *infrared* Sensor, *buzzer*
5V	LCD	VCC

2.3 Flowchart

The flow chart used to detect the falling down position of wheelchair users with or without wheelchairs can be seen in Figure 6.

International Journal of Applied Sciences and Smart Technologies

Volume 3, Issue 2, pages 171–184

p-ISSN 2655-8564, e-ISSN 2685-9432

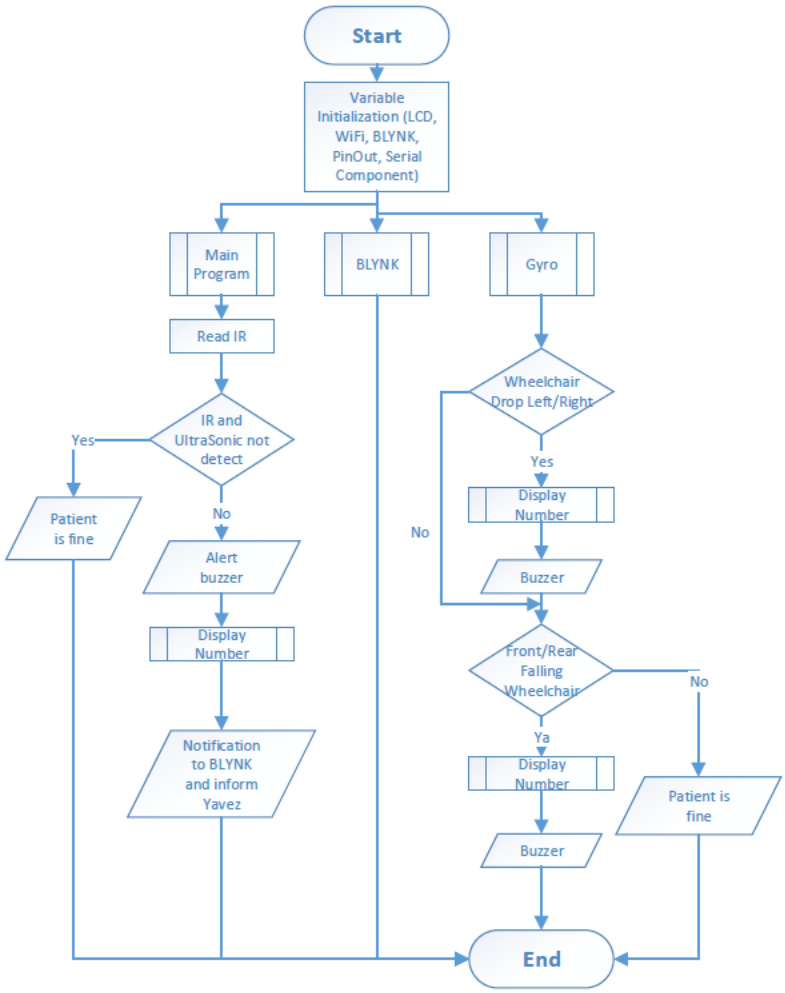

Figure 6. Flowchart

Figure 6. Flowchart starts with initializing variables, LCD, Wifi, BLYNK, Pinout and serial components. The next process is to run the BLYNK, Main Program and Gyro functions. The Main Program is executed to read the E18-D80NK IR or Proximity sensor. If the IR and Ultrasonic Sensors detect a wheelchair user, the LCD will display the words “Patient is fine”. Furthermore, if the IR sensor does not detect a sitting user and the ultrasonic does not detect the user's legs, then the buzzer will sound and perform the display number function. The display number function is to send a notification to the BLYNK server as an emergency condition which will display information telephone numbers that can be contacted on the LCD.

Volume 3, Issue 2, pages 171–184

p-ISSN 2655-8564, e-ISSN 2685-9432

When the gyro function is run, it will detect the position of the wheelchair when it falls down to the left side, right side, forward side or backward side. If the wheelchair is dropped, the display number function will be executed and the buzzer will sound as a warning sign of an emergency wheelchair user and vice versa if it does not detect the falling down position, the LCD will display that the user is fine.

3 Results and Discussions

3.1 MPU-6050 Sensor Test Results For Falling Down Conditions With Wheelchairs

The test is carried out to get a value that can be used as a reference when the wheelchair is in a fallen condition and it is necessary to send a notification alert to BLYNK. The sensor has an X, Y, and Z axis that will read the degree value obtained when the wheelchair is dropped. The degree value obtained is recorded and used as a reference for the direction of falling the wheelchair. Please see Figure 7.

(a) (b)

(c) (d)

Figure 7. Testing the MPU-6050 Sensor on a wheelchair (a) Dropped to the left, (b) Dropped to the right, (c) Dropped forward, (d) Dropped backwards

Volume 3, Issue 2, pages 171–184

p-ISSN 2655-8564, e-ISSN 2685-9432

Table 2. Reading of the MPU-6050 Axis Value on a wheelchair

Position	X-axis value	Y-axis value	Z-axis value
Upright	100^o	216^o	97^o
Fall left	135^o	181^o	91^o
Fall right	53^o	1^o	89^o
Fall forward	106^o	255^o	148^o
Fall backward	115^o	103^o	26^o

From the results of Table 2 it can be seen that the MPU-6050 sensor is very sensitive with the readable axis values changing easily. The sensor axis value can be change when the wheelchair moves quickly or there is a shock that affects the sensor. In determining the angle value used as a reference when the wheelchair is in a falling down position, it is taken only one of the axis values with the largest change in each falling down position. That only one axis value is taken as a reference because if you take all the three axes as a reference, there is a possibility that one of the value of the axes will have the same value which will cause confusion in determining the direction of the wheelchair's fall. The axes taken in each falling down condition can be seen in Table 3.

Table 3. Reference Axis for Falling Down Conditions

Fall Condition	Axis
Left	$Y \leq 180°$
Right	$X \leq 50°$
Foward	$Z \leq 65°$
Backward	$Z \geq 140°$

In accordance with Table 3 if the value of the axes is more than or less than the predetermined value, the wheelchair is considered to have fallen and wemos sends an emergency warning.

3.2 The Test Results of Ultrasonic and Proximity E18-D80NK Sensors for Falling Down Conditions without the Wheelchair

The test was carried out with a user sitting in a wheelchair and performing an emergency fall without a wheelchair. Two Ultrasonic sensors on the right and left sides of the footrest and Proximity E18-D80NK on the right side of the wheelchair will detect

Volume 3, Issue 2, pages 171–184
p-ISSN 2655-8564, e-ISSN 2685-9432

the presence or absence of a wheelchair user. The test starts from a wheelchair where there is no one at first time, then the footrest is open and both sensors detect it as a normal condition.

Both sensors will send an unsafe signal when the ultrasonic sensor detects no user's foot or foot object and the Proximity E18-D80NK sensor on the right side also detects no thigh object from the user. The test results can be seen in Table 4.

Table 4. The Test Results of Ultrasonic and Proximity E18-D80NK sensors to detect the presence of wheelchair users

Sensor	Detect or Not detect	Object	Wheelchair users condition(*)
Ultrasonik Proximity E18-D80NK	Detect Not detect	Footrest -	No wheelchair users
Ultrasonik Proximity E18-D80NK	Detect Detect	Legs Upper thigh	Wheelchair user detected
Ultrasonik Proximity E18-D80NK	Not detect Not detect	- -	The wheelchair user in a falling down position
Ultrasonik Proximity E18-D80NK	Not detect Detect	- Upper thigh	Wheelchair user detected in fine condition

(a) (b) (c)

Figure 8. Testing of Ultrasonic and Proximity E18-D80NK Sensors (a) The sensor detects the presence of the user, (b) The user falls down in front of the wheelchair then the sensor can't detect the user, (c) Wemos sends emergency message

Figure 8 shows several positions when the sensor detects and does not detect the presence of a wheelchair user. Figure 8(a) shows an active ultrasonic sensor blocked by the legs of a wheelchair user and an active proximity sensor blocked by a seated user. Figure 8(b) shows the user falling towards the front of the wheelchair and the wheelchair position does not change. In moments later the ultrasonic sensor detects that

Volume 3, Issue 2, pages 171–184
p-ISSN 2655-8564, e-ISSN 2685-9432

the wheelchair user's legs are not blocked and the Proximity E18-D80NK sensor is not blocked by the wheelchair user's thigh. Figure 8(d) shows the system detects the user's emergency situation and sends a message to the previously saved mobile number. From the test results above, it can be concluded that the ultrasonic sensor and Proximity E18-D80NK sensors function properly when detecting or not detecting the presence of wheelchair users.

3.3 Notification Delivery Test Results

The test aims to find out how far the recipient of the emergency warning can receive notification of an emergency message from the location of the wheelchair user. Notifications are sent by the Wemos D1 mini Wifi Module and utilize the BLYNK application platform as a recipient of emergency warnings for wheelchair users. Testing is done by turning on BLYNK to receive notifications.

To test the mileage for sending notifications, it is carried out as follows: the device that receives the notification of an emergency is placed in a predetermined location, then a test of receiving the notification of an emergency is carried out. The wheelchair was placed on the Kalijudan campus of Widya Mandala Catholic University Surabaya, which is located in Tambaksari District in the East Surabaya area. The results of sending and receiving notifications can be seen in Table 5.

Table 5. Testing the Mileage of Notification Delivery

No	Distance from wheelchair location (km)	District or Location	Area	**Message Sent or not sent**
1.	8,5 km	Sukolilo	East Surabaya	Sent
2.	10 km	Pabean Cantian	North Surabaya	Sent
3.	13 km	Gayungan	South Surabaya	Sent
4.	19 km	Lakarsantri	Surabaya Barat	Sent
5.	26,1 km	Kota	Gresik	Sent
6.	28 km	Icon Mall Gresik	Gresik	Sent
7.	32 km	Plaza Sidoarjo	Sidoarjo City	Sent
8.	34,8 km	Sidoarjo Fishing	Sidoarjo	Sent
9.	37 km	Rest area at Toll Road Mojokerto	Mojokerto	Sent
10.	48 km	Tjiwi Kimia Paper Mills Tol Road Mojokerto	Mojokerto	Sent

Volume 3, Issue 2, pages 171–184
p-ISSN 2655-8564, e-ISSN 2685-9432

From the above test, it can be concluded that the user can receive emergency notifications in all places with the condition that the device must be connected to the BLYNK server and connected to the internet.

4 Conclusion

The conclusion from the measurement and testing results are as follows:

a. The value read by the MPU-6050 sensor is taken one axis for each direction when the wheelchair was falling down, $Y \leq 180^o$ for left falling down, $X \leq 50^o$ for right falling down, $Z \leq 65^o$ for forward falling down and $Z \geq 140^o$ for backwards falling down.
b. The Ultrasonic sensor works well for detecting the presence of user's legs and the E18-D80NK proximity sensor works well for detecting the position of the user who is sitting in a wheelchair.
c. Receiving notifications through the BLYNK server works well, not affected by distance provided there is an internet connection connected to the device.

References

[1] D. M. Putri, "Mengenal Wemos D1 Mini Dalam Dunia IoT," *Ilmu Teknologi dan Informasi*, **1**, 2–4, 2017.

[2] Baktikominfo, Pengertian, fungsi dan kelebihan accelerometer yang tak banyak orang ketahui, https://www.baktikominfo.id/id/informasi/pengetahuan/pengertian_fungsi_dan_kelebihan_accelerometer_yang_tak_banyak_orang_ketahui-785 (Accessed: 22/11/2020).

[3] R. T. Asnada dan Sulistyono, "Pengaruh Inertial Measurement Unit (IMU) MPU-6050 3-Axis Gyro dan 3-Axis Accelerometer pada Sistem Penstabil Kamera (Gimbal) Untuk Aplikasi Videografi." **11** (1), 48–55, 2020.

[4] F. N. Riyadi, "Perancangan Pendeteksi Banjir menggunakan Sensor Water Level berbasis PLC Schneider TM221CE16R dan SMS Gateaway." 26–27, 2018.

[5] Nyebarilmu, Mengenal aplikasi blynk untuk fungsi IOT, https://www.nyebarilmu.com/mengenal-aplikasi-blynk-untuk-fungsi-iot/ (Accessed: 10/11/2020)

Volume 3, Issue 2, pages 171–184

p-ISSN 2655-8564, e-ISSN 2685-9432

[6] S. M. Sari, "Aplikasi Sensor Ultrasonik Srf04 Dan Sensor Proximity Pada Level Pengisian Tangki Air Berbasis Atmega8535," 25–26, 2015.

[7] Muslimin dan Darul, "Sistem Pengaman Kursi Roda Elektrik dari Benturan Melalui Evaluasi Sensor Jarak." https://repository.its.ac.id/id/eprint/46208, 2017.

[8] Y. Ji, J. Hwang, and E. Y. Kim, "An intelligent wheelchair using situation awareness and obstacle detection," *Procedia, Social and Behavioral Sciences*, 97, 620–628, 2013.

[9] Miachi, "A study of Aware Wheelchair with sensor networks for avoiding Two Meters Danger." *Procedia*, 1004–1010, 2016.

International Journal of Applied Sciences and Smart Technologies

Volume 3, Issue 2, pages 185–202

p-ISSN 2655-8564, e-ISSN 2685-9432

The Simulation of Traffic Signal Preemption using GPS and Dijkstra Algorithm for Emergency Fire Handling at Makassar City Fire Service

M. Friaswanto[1], E. A. Lisangan[1,*], S. C. Sumarta[1]

[1]*Department of Information Technology, Atma Jaya University of Makassar, Indonesia*

[*]*Corresponding Author: erick_lisangan@lecturer.uajm.ac.id*

(Received 04-11-2021; Revised 28-12-2021; Accepted 28-12-2021)

Abstract

The Makassar City Fire Department often faces obstacles in handling fires. Problems that often hinder such as congestion at crossroads, panic residents, and others. The result of this research is a system that can assist firefighters when handling fire cases in terms of accelerating the firefighting team to the location of the fire. Dijkstra's algorithm will be used to find the shortest path to the fire location and the travel time. Then the traffic signal preemption simulation adjusts the color of the lights when the GPS vehicle approaches the traffic lights on the path to be traversed. The simulation results show that the use of traffic signal preemption in collaboration with Dijkstra's algorithm and GPS can help the performance of the Makassar City Fire Department, especially for handling fires that require fast time.

Keywords: Fire service, traffic signal preemption, GPS simulation, Dijkstra algorithm

International Journal of Applied Sciences and Smart Technologies

Volume 3, Issue 2, pages 185–202

p-ISSN 2655-8564, e-ISSN 2685-9432

1 Introduction

Based on report data obtained from the Makassar City Fire Service, in the Makassar city area in 2018 there were 209 incidents spread across 14 sub-districts. Where from 209 fire cases that occurred throughout 2018 in the city of Makassar there were losses estimated at around Rp. 22,040,000,000 and 10 people died due to fire and 7 people were injured. Realizing the dangers of fire, a Fire Department has been established in every region of Indonesia, including Makassar city, in order to prevent and overcome fires that can occur at any time. When a fire occurs, firefighters must always be ready to handle and extinguish the fire. But usually to deal with fires before the firefighters arrive, the community usually works together to extinguish the fire manually while helping the victim. But obviously very difficult if the fire has grown and the wind is strong. Therefore the presence of a fire extinguisher is very necessary.

Based on the results of the author's interview with one of the Makassar City Fire Department officers, there are several problems that can interfere with or hinder the performance of officers. The problems commonly faced by the Makassar City Fire Department when dealing with fires are road congestion and also at traffic light intersections, the fastest route to the fire location, information that is slow to receive, residents and journalists covering which hinder the work of officers, citizens who are always willing use extinguishing equipment to help but do not even know the function of the tool, and so on. These problems can certainly cause harm to the victim. This makes every minute very valuable in fire fighting.

The problem of congestion and traffic lights are also things that can interfere with the performance of the Makassar City Fire Department. Whereas based on the Regulation of the Minister of Public Works No. 20 of 2009, the emergency response time for fires in Indonesia should not be more than 15 minutes after receiving notification of a fire in a location 7.5 km from the nearest fire station. For the Makassar City area, there are 7 fire stations scattered in several places in the Makassar city area. The problem of congestion and traffic conditions at crossroads with traffic lights were also complained of by firefighters interviewed by researchers. When the fire engine is on a road that is in a traffic jam, the fire engine is forced to reduce the speed of the vehicle and make the

Volume 3, Issue 2, pages 185–202
p-ISSN 2655-8564, e-ISSN 2685-9432

firefighters late to the fire location, resulting in delays in handling fires and can result in more losses. Even though they have the right to break through traffic lights or take the opposite lane, firefighters are also often hampered at intersections if the traffic light is still red and cannot move to the opposite lane.

For the problem of finding a route for fire trucks to get to the fire location so far at the Makassar City Fire Department, it is still based on the knowledge of the team leader and other officers in charge of extinguishing the fire, and when there is an obstacle on the road, the team leader must be able to find alternative routes for his team to fire location. One of the algorithms that can be used to find the shortest route is Dijkstra's algorithm. Dijkstra's algorithm is an algorithm invented by Edsger W. Dijkstra and published in 1959. This algorithm is used to solve the shortest path problem for a directed graph. This algorithm finds the shortest path from the starting point to the end point based on the smallest weight from one point to another. The way the Dijkstra algorithm works uses a greedy strategy, where at each step the side with the smallest weight is selected that connects a node that has been selected with another node that has not been selected [1], [2]. The results of the Dijkstra's algorithm will be used as directions for Makassar city firefighters when heading to the fire location. To find the shortest path to the fire location, the Dijkstra algorithm method is used where the weight values to be used are the distance of each node and the value of traffic density.

Several previous studies have examined the search for the shortest route as in [3], [4], [5], [6]. Ratnasari et al (2013) concluded that Dijkstra's algorithm can produce a simulation of the shortest path along with alternative paths and the travel time required for a vehicle to reach a certain location. Iswanjono and Wijaya (2015) designed an automatic system to regulate traffic lights at crossroads. This automatic system works after a vehicle that has a special priority to go through a red light sends GPS coordinates via radio waves which will later be captured by a receiver mounted on a traffic light. Aquarizky et al (2017) concluded that the Floyd-Warshall Algorithm can be used to find the shortest route for firefighters, but it has not been integrated with congestion data and red light settings in real time. In addition, this algorithm is also not appropriate to be used in a wide area because the suggested results are not optimal. Septifany et al (2017) compared finding the optimum route with the Dijkstra's algorithm method and the A*

Volume 3, Issue 2, pages 185–202
p-ISSN 2655-8564, e-ISSN 2685-9432

algorithm. The results of this comparison state that there is no significant difference between the two. In addition, the suitability of the route obtained from the routing process using PostgreSQL, is still less accurate than the route generated by Google Maps. Due to incomplete road shape file data such as those owned by Google Maps and PostgreSQL, it is not equipped with weighting for traffic directions. As a result, there are routes that cannot be used due to inappropriate road taking. In this study, the determination of the shortest route is only based on the distance between nodes and no weight is given to traffic conditions that will be traversed by firefighters.

Several developed countries have implemented Traffic Signal Preemption / Traffic Signal Priorization to regulate traffic lights so that vehicles that have priority to pass through the road will be given a road. If the vehicle that has priority will pass then the light will be green and the surroundings will be red. This can be used to allow vehicles handling emergency vehicles to pass through the road by turning the light green. This light change can help emergency vehicles to arrive at the location faster and increase safety when heading to the fire location [7]. One method that can be used to implement traffic signal preemption is to use the Global Positioning System or GPS [8]. The Global Positioning System (GPS) is a radio navigation system using 24 satellites orbiting the earth in 6 circular orbits. Where all units can transmit signals to earth and later will be captured by the signal receiver. This GPS system was originally developed by the US Department of Defense in the early 80s [9].

Meanwhile, to design Traffic Signal Preemption / Traffic Signal Priorization, it is simply made using Wemos D1. In this simulation, the GPS simulation is set using JavaScript to coordinate the vehicle that will go to the location of the fire. And when the fire department vehicle starts to go to the fire location, the simulation of the GPS coordinates of the fire squad vehicle will start to be compared with the coordinates of the nearest traffic light on the path that the fire fighting vehicle will take when heading to the fire location. The nearest traffic light will turn green on the path to be traversed in order to give priority to firefighter vehicles so that every vehicle on the path to be passed by the firefighters will run so that there is no accumulation of vehicles on the path that will be traversed by fire vehicles to the location of the fire. When the traffic

Volume 3, Issue 2, pages 185–202
p-ISSN 2655-8564, e-ISSN 2685-9432

light has been passed, the traffic light will return to its normal status, while the next nearest traffic light will be a priority until the fire engine passes.

2 Research Methodology

Research design

The design method used is the Waterfall method (Figure 1) which consists of analysis, design, writing, testing, and implementation and maintenance. The data collection method used by the author in this research is to use literature studies and interviews. The literature study used in the study to collect data on traffic signal preemption, Wemos and the Ddijkstra algorithm obtained from various reference sources, books, offline and online journals. Interviews were used to obtain information by asking questions directly to the resource persons, namely the Makassar City Fire Department.

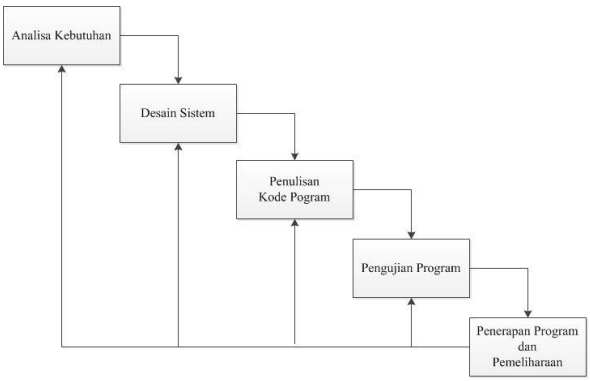

Figure 1. Waterfall's method [10]

The author has conducted an interview process with the Makassar city fire department to find out the problems faced by firefighters when carrying out their duties to extinguish fires. From the interviewer, it was concluded that the Makassar City Fire Department currently requires a system that is able to display the path to the location of the fire from the Pemadam Headquarters, as well as a traffic light control system to assist fire trucks to the location of the fire.

International Journal of Applied Sciences and Smart Technologies

Volume 3, Issue 2, pages 185–202

p-ISSN 2655-8564, e-ISSN 2685-9432

Traffic Light Simulation Circuit

The traffic signal preemption simulation requires a digital traffic light circuit. The traffic light simulation circuit can be seen in Figure 2. In Figure 2 it can be seen that the circuit consists of several components, namely Wemos, traffic light module, and I2C LCD. The Wemos board is used as a microcontroller whose job is to control the lights that will be turned on at traffic lights based on the information received from the server. Communication between Wemos and the server uses the internet which is connected via the ESP8266 Wifi module on Wemos. In addition, the I2C LCD is an information display on the traffic light to provide information to motorists that the fire engine will pass through the area around the traffic light so that the driver can pull over to make room for the fire engine.

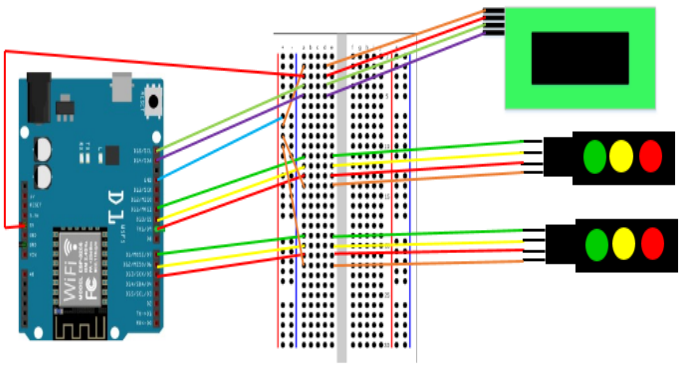

Figure 2. Traffic light simulation circuit

3 Results and Discussion

Traffic Signal Preemption Algorithm Design

In the calculation of the Dijkstra algorithm, it is necessary to have a weight for each related node, in this study the weight is taken from the distance of each node in meters and the value of traffic density where the value is randomly generated assuming a value range of 0 to 100. The limit value is 100. selected with the assumption that a road segment can accommodate a maximum of 100 vehicles at one time, so that when the density value is above 75 it will be categorized as a moderately dense vehicle. The distance of each node along with the value of traffic density will be summed and will be

Volume 3, Issue 2, pages 185–202

p-ISSN 2655-8564, e-ISSN 2685-9432

the main weight used in Dijkstra's algorithm.

The results of the algorithm in the form of path, distance, and time of the vehicle will be displayed on the map. Based on the distance obtained, the travel time will also be calculated with a standard speed of 40 km/hour or 666.67 meters/minute. For traffic light settings, the coordinates of the vehicle will be calculated the distance to the traffic light on the path to be traversed. The traffic light that will be traversed and closest to the vehicle will turn green, and when the vehicle has passed the traffic light, the light will return to normal. Then if the fire has been handled, a fire case report will be included. The flowchart of the traffic signal preemption system simulation can be seen in Figure 3.

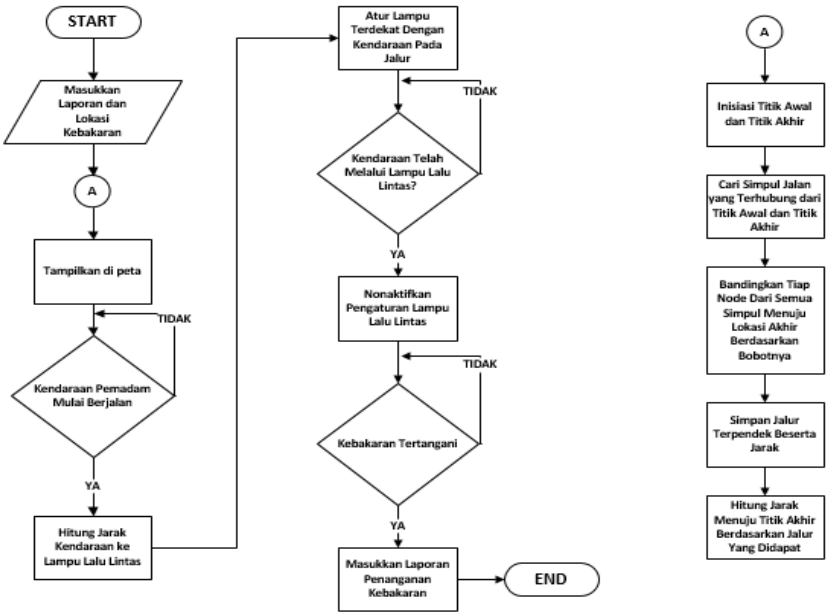

Figure 3. Flowchart of Traffic Signal Preemption system simulation

System Workflow

Figure 4 illustrates the workflow of the system mechanism for the fire brigade. Fire location information in the form of distance and travel time to the location will be received by the fire brigade. Furthermore, when the firefighters will leave for the location of the fire, the leader of the firefighting team will press the "Depart" button when the vehicle will go to the location of the fire. And when the vehicle moves, the coordinates will be sent to the system to calculate the distance from the vehicle to the nearest traffic light on a predetermined path. When a nearby light is found it will be set to green to give priority to the fire department. When the firefighters

International Journal of Applied Sciences and Smart Technologies

Volume 3, Issue 2, pages 185–202

p-ISSN 2655-8564, e-ISSN 2685-9432

have arrived at the location, the team leader can turn off the map and when the fire is finished, the fire team leader can send information that the fire has been handled.

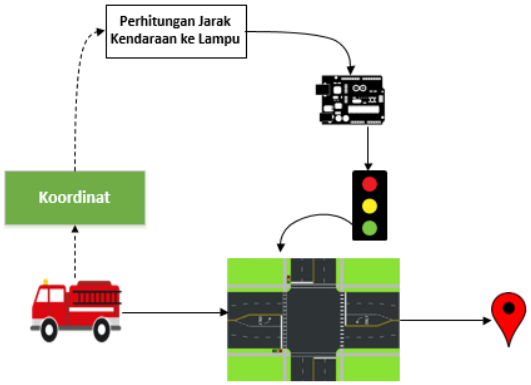

Figure 4. Fire Squad System Workflow

Graph Representation

To form a graph of a real road, the latitude and longitude coordinates of each road is needed along with the distance of each road. To form a graph from geolocation data, the nodes/points of each location must first be determined. After that the nodes will be connected. A node can be connected to several nodes at once, it will form a node which will later form a graph. In this study, researchers used 103 nodes to connect 45 road points in the Makassar city area adjacent to the fire station on Jalan Ratulangi with a total of 190 nodes (Figure 5).

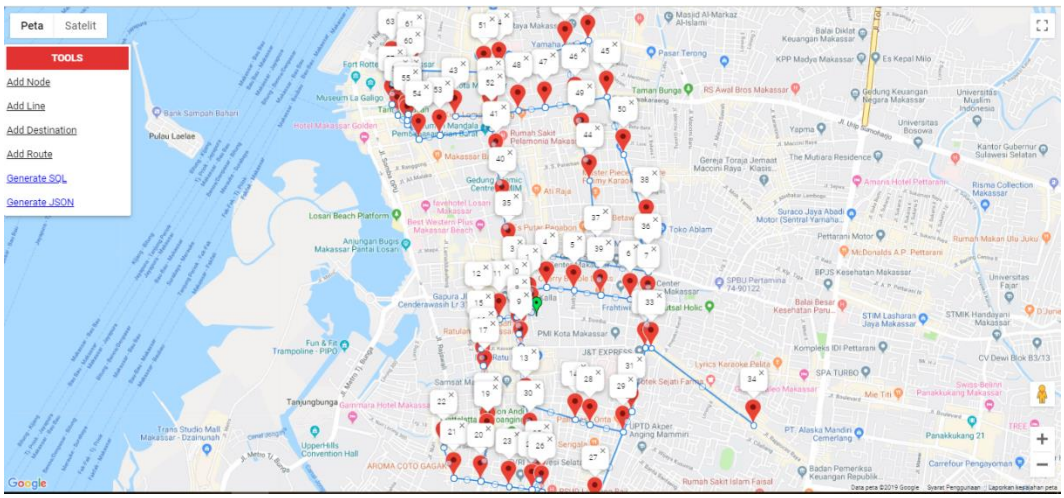

Figure 5. Graph representation of several Makassar city roads

Volume 3, Issue 2, pages 185–202
p-ISSN 2655-8564, e-ISSN 2685-9432

The Implementation of Dijkstra's Algorithm

The process of Dijkstra's algorithm in the system is carried out by determining the starting point and ending point to be processed. The starting point/departure point used is the Makassar city fire station, namely at coordinates -5.149009661835451, 119.4167173586253 or at the Fire Department on Ratulangi road, while the end point is the coordinates of the road where a fire will occur. For the weight on a road is obtained from the length or distance of each interconnected node and from the value of traffic density where the value ranges from 0 to 100 where this value is assumed to be the number of vehicles at a road point.

For selected waypoints to be given a certain weight at 16:00-16:30. Meanwhile, at times other than these hours, the value of traffic density will be randomly generated at each road point so that it can generate several possible paths. When the value of traffic density on a road is higher, this value will affect the process of finding the shortest path. From the departure point, each neighbor point that has not been passed will be considered and then the weight will be calculated. For example, suppose the distance from point A to point B is smaller than the distance from point A to C then the data A to B will be stored. If then there is a smaller distance then the old data will be deleted and replaced with new data. Each node/point that has been passed will not be calculated again for that point. Then the point that has not been traversed with the smallest distance (from the departure node) will be set as a new departure node.

Determination of the shortest path calculated using the Dijkstra algorithm will produce the shortest path along with the travel time that can be traversed by fire fighting vehicles when heading to the fire location. Then for the traffic lights in the city of Makassar, most of them are still analog or manual where at the traffic lights a timer is installed to change the color of the lights in under 1 minute. The lights are unresponsive and cannot adapt to crossing conditions.

The use of a microcontroller can be used to change the status of the lights when the vehicle is on the vehicle path to be traversed. For the change of lights, when the firefighters enter the map display page, the GPS simulation will start running and will start sending the coordinates of the traffic lights on the path that has been obtained in the results of the Dijkstra algorithm which will be a priority for the firefighters who will

International Journal of Applied Sciences and Smart Technologies
Volume 3, Issue 2, pages 185–202
p-ISSN 2655-8564, e-ISSN 2685-9432

be tasked with extinguishing the fire. . Then when the fire engine has passed the traffic light coordinates, the lights will automatically return to normal status.

In this simulation, the search for the shortest path and traffic light settings is carried out when the fire engine is heading to the location of the fire. The location point that will be used is on Jalan Panampu, where in the results of the interview there is information that there has been a delay in getting to the location of the fire. The delay limit used by the author is based on the Regulation of the Minister of Public Works No. 20 of 2009, where the emergency response time for fires in Indonesia should not be more than 15 minutes after receiving notification of a fire in a location 7.5 km from the nearest fire station.

To search for the shortest path, there are two simulations, namely simulations around 16:00-16:30 and outside these times (Figure 6). In the hours outside 16:00-16:30 there are several possible paths that can be passed. However, a route with the shortest distance will be sought from the Pemadam Headquarters to Jalan Panampu along with the travel time to the location of the fire at a standard speed of 40 km/hour or 666.67 meters/minute.

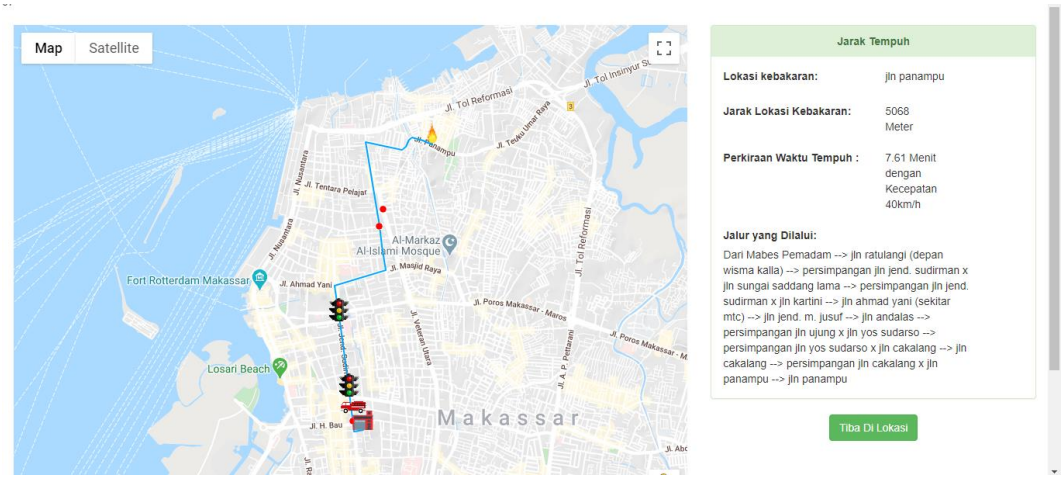

Figure 6. Route search results at 16:00-16:30

From the results of the path search by the Dijkstra algorithm at 16:00-16:30, the distance to the fire location on Jalan Panampu is 5068 meters with an estimated path and travel time of 7 minutes to get to the location of the fire on Jalan Panampu and

Volume 3, Issue 2, pages 185–202

p-ISSN 2655-8564, e-ISSN 2685-9432

depart from Ratulangi Street Fire Department Headquarters. The path found by Dijkstra's algorithm is as follows:

Mabes Pemadam → jln ratulangi (depan wisma kalla) → persimpangan jln jend. sudirman x jln sungai saddang lama → persimpangan jln jend. sudirman x jln kartini → jln ahmad yani (sekitar mtc) → jln jend. m. jusuf → jln andalas → persimpangan jln ujung x jln yos sudarso → persimpangan jln yos sudarso x jln cakalang → jln cakalang → persimpangan jln cakalang x jln panampu → jln panampu.

From the results of the path search by the Dijkstra algorithm, it was found that there were two possible distance paths to the location of the fire on Jalan Panampu, the first was as far as 5068 meters with an estimated path and travel time of 7 minutes to get to the location of the fire which was on Jalan Panampu and departed from the Road Fire Department Headquarters. Ratulangi (Figure 7). The path found by Dijkstra's algorithm is as follows:

Mabes Pemadam → jln ratulangi (depan wisma kalla) → persimpangan jln jend. sudirman x jln sungai saddang lama → persimpangan jln jend. sudirman x jln kartini → jln ahmad yani (sekitar mtc) → jln jend. m. jusuf → jln andalas → persimpangan jln ujung x jln yos sudarso → persimpangan jln yos sudarso x jln cakalang → jln cakalang → persimpangan jln cakalang x jln panampu → jln panampu.

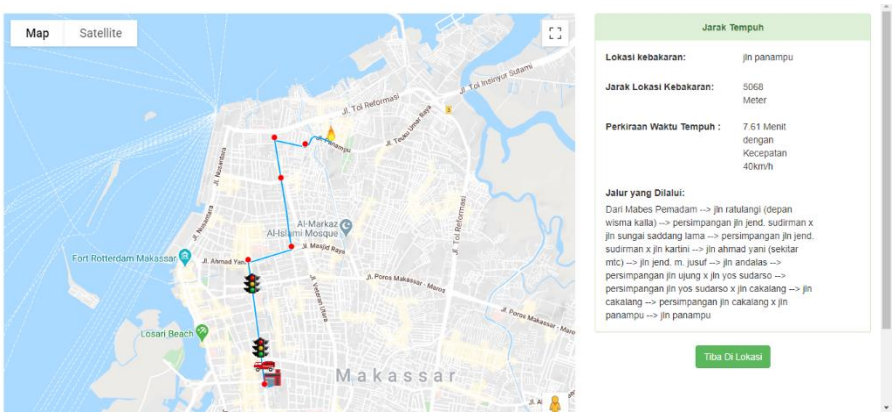

Figure 7. Search results for the first path to Jalan Panampu

The second route is 5287 meters with an estimated route and travel time of 7.94 minutes to get to the fire location on Jalan Panampu and depart from the Fire Department Headquarters Jalan Ratulangi (Figure 8). The path found by Dijkstra's algorithm is as follows:

International Journal of Applied Sciences and Smart Technologies

Volume 3, Issue 2, pages 185–202

p-ISSN 2655-8564, e-ISSN 2685-9432

Mabes Pemadam → jln ratulangi (depan wisma kalla) → persimpangan jln jend. sudirman x jln sungai saddang lama → persimpangan jln jend. sudirman x jln kartini → jln ahmad yani (sekitar mtc) → jln jend. m. jusuf → persimpangan jln jend. m. jusuf x jln veteran utara → jln bandang → persimpangan jln bandang x jln ujung → persimpangan jln ujung x jln yos sudarso → persimpangan jln yos sudarso x jln cakalang → jln cakalang → persimpangan jln cakalang x jln panampu → jln panampu

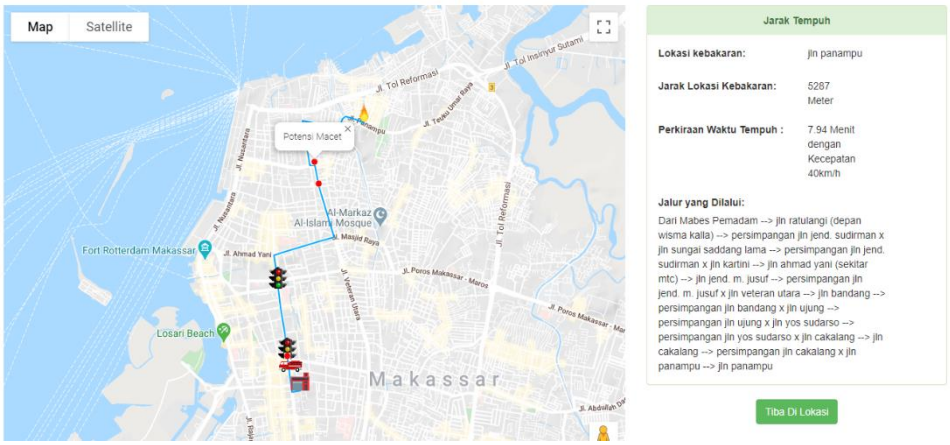

Figure 8. Search results for the second path to Jalan Panampu

The difference in the results of this path search is due to the different weights obtained in each lane that allows fire vehicles to pass when heading to the location of the fire on Jalan Panampu. The weight in question is the distance of each connected node from the starting point, namely the Pemadam Headquarters to the location of the fire on Jalan Panampu and also the value of traffic density which is assumed to be in the range 0-100. So that when there is a determination of a different path then on another path there is a higher traffic density value than the other lane or it can be said that on another path there is congestion so the dijkstra algorithm will choose a path with a low density value with a low distance also.

User Interface

The user interface for the firefighters can be seen in Figure 9. If there is a fire report there will be a warning. To enter the system, the fire squad leader can directly enter to view the map and the path that has been calculated by the Dijkstra algorithm along with the travel time. In addition, when the firefighters enter the map page, the status of the nearest traffic light on the vehicle on the path to be traversed will be changed to green. When the firefighters get a fire report and start leaving for the fire location, the

Volume 3, Issue 2, pages 185–202

p-ISSN 2655-8564, e-ISSN 2685-9432

firefighters leader can press the "GO" button to start the process of calculating the estimated travel time needed for vehicles to pass traffic lights that are on the path to be traversed. In addition, the path display on the map will be displayed based on the calculation results of the Dijkstra algorithm. For lighting settings, the vehicle coordinates in this study use coordinate simulation in Javascript. In this study, traffic lights are located at two points, namely point A which is at the intersection of Jend. Sudirman with Saddang Lama River road or at coordinates -5.14528510434342, 119.41523463271892. And point B which is at the intersection of Jend. Sudirman by Amampanga Street or at coordinates -5.13698889347666, 119.41410191337218.

When the firefighter's vehicle starts walking towards the location of the fire, the GPS simulation of the vehicle will begin to be sent and the vehicle's coordinates will begin to be calculated the distance to the traffic light that is in the path that will be passed by the firefighter's vehicle to the location of the fire. When the coordinates of the vehicle have passed the coordinates of the nearest light, the light will return to its normal status and the next closest light will turn green to give priority to the fire engine when it comes to the fire location. When the fire department vehicle has arrived at the fire location, the team leader can press the Arrive at Location button to indicate that the firefighters have arrived at the fire scene. When the firefighters have finished extinguishing the fire, the team leader can press the Handled button to notify the system that the fire has been controlled and the fire status in the database is Handled.

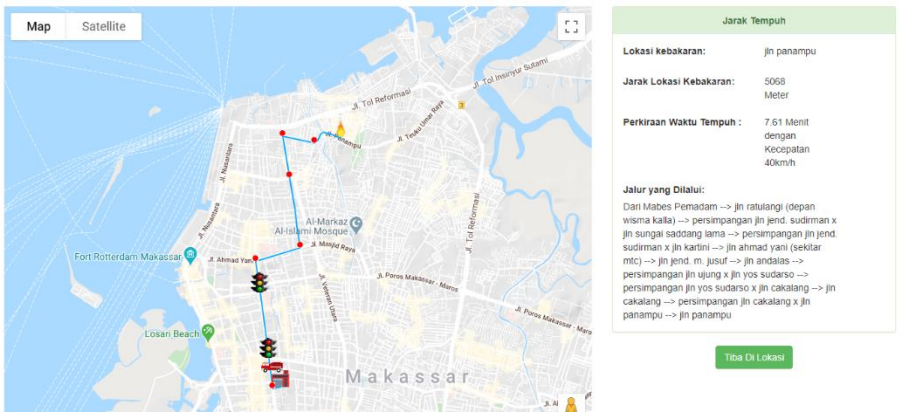

Figure 9. User Interface for Firefighters Squad

International Journal of Applied Sciences and Smart Technologies

Volume 3, Issue 2, pages 185–202

p-ISSN 2655-8564, e-ISSN 2685-9432

Simulation Testing

In the results of the Traffic Signal Preemption simulation design, the system is made to adjust the color of the traffic lights that will be passed by fire vehicles. Traffic Signal Preemption Simulation using Wemos will capture the results of calculations between vehicle GPS simulation data and traffic light point data on the path that will be traversed by the fire to the location of the fire. Each Wemos will be given coordinates according to the coordinates of the traffic lights, which in this case the traffic lights are located at two points, namely point A which is at the Jend. Sudirman with Saddang Lama River road or at coordinates -5.14528510434342, 119.41523463271892. And point B which is at the intersection of Jend. Sudirman by Amampanga Street or at coordinates -5.13698889347666, 119.41410191337218.

Wemos which will connect to the server will read the led.json file sent by the GPS simulation file and contain the coordinates of the lights which will be changed to the priority of the fire department. Next Wemos will read a json file containing the coordinates of the traffic lights that will be prioritized. The coordination of the lights in the data sent to Wemos is the same as certain Wemos coordinates, then Wemos with the coordinates sent will change the lights from a normal state to a priority for firefighting vehicles so that vehicles on the path to be traversed by fire vehicles will be able to run well. there are vehicles on the path that will be traversed by firefighters. See Figure 10.

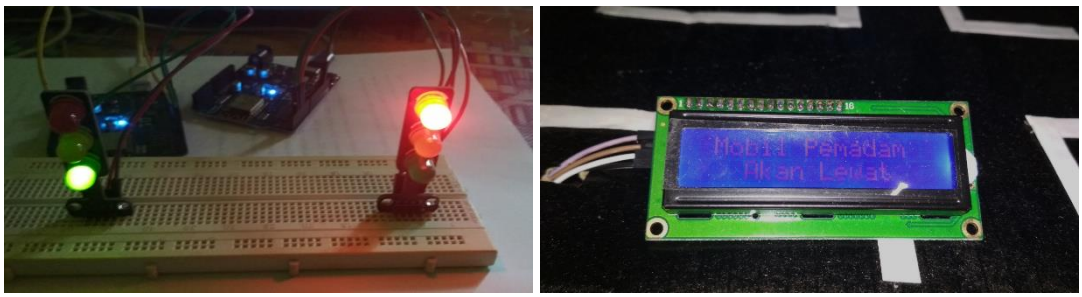

Figure 10. Lamp and LCD on Priority Condition

When the light status changes to priority, Wemos D1 takes a fraction of a second to read the led.json file until it changes the color of the lane 1 light to green and the lane 2

Volume 3, Issue 2, pages 185–202
p-ISSN 2655-8564, e-ISSN 2685-9432

light to red at the traffic lights at points A and B. In addition, the I2C LCD also displays the words notice that a fire engine is about to pass. When the coordinates of the nearest traffic light have been traversed by the fire vehicle heading to the location of the fire, the next light closest to the coordinates of the fire engine will be the priority and the previous light will return to its normal situation. And when the fire brigade has arrived at the scene of the fire, the last light will also return to its normal status.

From the light change test, it can be seen that the traffic lights A and B can run well in manual mode, where the red, yellow and green lights run alternately. The traffic lights at points A and B can only change automatically when the vehicle simulation starts. At points A and B there are 2 lights each, each of which will change color where the first light at point A will turn green while light 2 will turn red, as well as the two lights at point B. When the vehicle approaches the nearest light, the lights will turn red. becomes a priority, for example, if the vehicle simulation approaches the point A light, one light will turn green while the second light will turn red. The light that turns green is the path that will be traversed by the fire fighting vehicle, when the GPS simulation of the vehicle has passed the coordinates of the lights at point A, the lights at point A will return to their normal status. Then the next closest light, namely the light at point B, will turn green on the path to be traversed and on the other side of the road the lights will turn red until the vehicle has passed the coordinates of the red light at point B. changes quickly because Wemos depends on the speed of the connected internet to read json files on the server.

Implementation Testing

The author has carried out implementation tests carried out with program demonstration activities and also used the interview method to the Head of the Operational Section of the Makassar City Fire Department. The results of interviews and demonstration activities carried out with resource persons indicate that:

1. The functions in the application for fire admins have been running well according to needs, but it is hoped that there will be development so that it does not only include

Volume 3, Issue 2, pages 185–202
p-ISSN 2655-8564, e-ISSN 2685-9432

fire reports but several other types of reports such as animal disturbance reports, rescue of people or animals, and others.

2. The simulated Traffic Signal Preemption simulation is considered to be very good and is considered to be able to help the firefighters because there is a path to get to the fire location and for traffic lights it can help because it can make fire engines run without interference at crossroads where there are traffic lights. and minimize the possibility of crossing accidents when trying to break through traffic lights.
3. If it is to be implemented, collaboration with several relevant agencies in the Makassar city area is needed, namely the Makassar City Communications and Information Service Office, the Makassar City Transportation Service and South Sulawesi Province, and the Makassar City Health Office.

The conclusion that can be drawn from this implementation test is that the system created has been able to run well and is said to be able to help the performance of the Makassar City Fire Department, especially for handling fires that require handling speed. In addition, it is hoped that there will be development of applications for input from the admin side so that they can not only input fire reports but several other types of reports. In addition, collaboration with several agencies will be needed so that it can be implemented properly.

4 Conclusion

Traffic Signal Preemption simulation using GPS and Dijkstra's algorithm for emergency response to fire handling at the Makassar City Fire Service which is designed to help the performance of the firefighters. Where the Traffic Signal Preemption simulation has been able to adjust the color of the traffic lights when the GPS simulation of the fire vehicle approaches the traffic light coordinates and gives priority to the fire vehicle. Meanwhile, the fire emergency application to find the shortest path to the fire location along with the estimated travel time using the Dijsktra algorithm has been able to find the shortest path to the fire location.

Volume 3, Issue 2, pages 185–202

p-ISSN 2655-8564, e-ISSN 2685-9432

In this study, testing has not been carried out on the condition of changing lanes in real time. Future research is expected to accommodate changes in real time paths and also use a more optimal route determination algorithm.

References

[1] Ferdiansyah dan A. Rizal, "Penerapan Algoritma Dijkstra untuk Menentukan Rute Terpendek Pembacaan Water Meter Induk PDAM Tirta Kerta Raharja Kabupaten Tangerang". *Jurnal TICOM*, **2** (1), 51–57, 2013.

[2] A. S. Girsang, "Algoritma Dijkstra." (Online) (https://mti.binus.ac.id/2017/11/28/algoritma-dijkstra/, diakses 10 November 2018).

[3] A. Ratnasari, F. Ardiani, dan F. Nurvita, "Penentuan Jarak Terpendek dan Jarak Terpendek Alternatif Menggunakan Algoritma Dijkstra Serta Estimasi Waktu Tempuh." *Seminar Nasional Teknologi Informasi dan Komunikasi Terapan*, 29-34, 2013.

[4] Iswanjono dan G. I. Wijaya, "Automatization Of Traffic Light For imergency Vehicles." *Jurnal Ilmiah Widya Teknik*. **14** (2), 49–56, 2015.

[5] A. G. J. W. Aquarizky, B. Irawan, dan C. Setianingsih, " Perancangan Dan Implementasi Aplikasi Pencarian Rute Optimal Untuk Pemadam Kebakaran Berbasis Android Menggunakan Algoritma Floyd-Warshall." *e-Proceeding of Engineering*, **4** (3), 3993–4000, 2017.

[6] D. S. Septifany, A. Laila, dan M. Awaluddin, "Analisis Optimalisasi Rute Pemadam Kebakaran Berdasarkan Area Cakupan Pipa Hidran Di Kota Semarang." *Jurnal Geodesi Undip*, **6** (3), 28–36, 2016.

[7] H. R. Al-Zoubi, B. A. Mohammad, S. Z. Shatnawi, dan A. I. Kalaf, "A Simple and Efficient Traffic Light Preemption by Emergency Vehicles using Cellular Phone Wireless Control." *Mathematical Methods and Techniques in Engineering and Environmental Science*, 167–170, 2011.

[8] J. F. Paniati, "Traffic Signal Preemption For Emergency Vehicles Traffic Signal Preemption For Emergency Vehicles A Cross-Cutting Study A Cross-Cutting Study," *First Edition. ITS Joint Program Office*, 2006.

Volume 3, Issue 2, pages 185–202

p-ISSN 2655-8564, e-ISSN 2685-9432

[9] Y. Yuniati, M. Ulvan, and M. Azzarah, ”Implementasi Modul Global Positioning System (GPS) Pada Sistem Tracking Bus Rapid Transit (BRT) Lampung Menuju Smart Transportation.” *Jurnal Sains, Teknologi dan Industri*, **14** (2), 150–156, 2017.

[10] Kadir. A., “Pengenalan Sistem Informasi,” Penerbit ANDI, Yogyakarta, 2003.

International Journal of Applied Sciences and Smart Technologies

Volume 3, Issue 2, pages 203–214

p-ISSN 2655-8564, e-ISSN 2685-9432

The Effect of Water Impact on the Refrigerant Pipeline between Compressor and Condensor on COP and Efficiency of Cooling Machine

Wibowo Kusbandono[1,*]

[1]*Department of Mechanical Engineering, Faculty of Science and Technology, Sanata Dharma University, Yogyakarta, Indonesia*
[*]*Corresponding Author: bowo@usd.ac.id*

(Received 04-11-2021; Revised 10-11-2021; Accepted 10-11-2021)

Abstract

The purpose of this research is (a) to design and assemble a steam compression cycle cooling machine using the main components on the market (b) to obtain the characteristics of the cooling engine, which includes the Coefficient of Performance (COP) and the efficiency of the cooling engine. The research was conducted experimentally in the laboratory. The refrigeration machine works by using a steam compression cycle, with the main components: a compressor, an evaporator, a capillary tube and a condenser. The compressor power is 1/6 PK, while the other main components are adjusted to the size of the compressor power. The refrigerant used is R134a. Variations of the research were carried out on the condition of the refrigerant pipe located between the compressor and condenser: (a) without being submerged in water (b) submerged in 0.50 liters of water and (c) submerged in 0.75 liters of water. The results of the study provide information that the water immersion in the refrigerant pipe which is located between the compressor and condenser affects the COP value and the efficiency of the refrigeration machine. Consecutively (1)

International Journal of Applied Sciences and Smart Technologies
Volume 3, Issue 2, pages 203–214
p-ISSN 2655-8564, e-ISSN 2685-9432

without being submerged in water, the COP value is 2.45 and the efficiency is 0.64 (2) submerged in liter of water, the COP value is 2.41 and the efficiency is 0.62 (3) submerged in liter of water, the value COP is 2.34 and efficiency is 0.60.

Keywords: COP, efficiency, cooling engine, steam compression cycle, submerged in water

1 Introduction

A two-door refrigerator is one example of a cooling machine commonly used by housewives. A two-door refrigerator is a cooling machine that can be used to cool a variety of foodstuffs and various kinds of beverages and can be used to freeze food and water. The working temperature of the two-door refrigerator cooling machine is generally below $0°C$. The working temperature of the evaporator ranges from $-15°C$ until $-28°C$. In a two-door refrigerator, there are 2 rooms that have different functions, one room has a very low temperature, which functions to freeze food ingredients (freezer room), and the other room serves to cool or lower the temperature of various foodstuffs and beverages, without freezing.

In a two-door refrigerator, the process of freezing and cooling food ingredients is carried out by cold air circulated by a fan, passing through every food ingredient in the refrigerator. The circulated air is of very low temperature, which is obtained when air is passed through the evaporator. This air temperature is close to the working temperature of the evaporator. After passing through the evaporator, the air is flowed into the freezer chamber and then only flown into the cooling chamber. From the cooling chamber the air is recirculated through the evaporator and sent to the freezer again. Thus the air circulation takes place continuously. When the air passes through the evaporator, the water content in the air will be frozen and will become ice flowers that will stick to the evaporator. The air can contain moisture, because the refrigerator door is often opened. As time goes by, the ice in the evaporator is getting more and more or thicker so that it will interfere with the performance of the two-door refrigerator cooling machine.

Volume 3, Issue 2, pages 203–214
p-ISSN 2655-8564, e-ISSN 2685-9432

Therefore, these frosts must be removed, and immediately removed from the evaporator so that the performance of the refrigeration machine remains high.

In general, frost is removed by heating. After a certain period of time (about 7 hours), the electric heater attached to the evaporator will work and melt the ice flowers attached to the evaporator pipes into water. The water produced will fall and fall into the water reservoir, which is located at the bottom of the cooling machine. As time goes by, over time there will be more and more water in the reservoir and it will fill the water reservoir. This water reservoir is useless, and the water must be discarded, otherwise it will spill.

For some of the newer two-door refrigerators, the water stored in the water reservoir is removed in a way that does not bother the user. You do this by evaporating water in a water reservoir with heat energy. One way is, the water in the water reservoir is immersed in the high-temperature refrigerant pipeline, which is part of the cooling machine. The part that is immersed in the water is the refrigerant pipe which is located between the compressor and the condenser. With this method, the stored water can evaporate completely, so that refrigerator users are not bothered to dispose of stored water. Another way is, the water reservoir is heated by touching the surface of the compressor casing. The heat received by the reservoir is then used to estimate the water.

How to estimate the water in this reservoir is very interesting for the author to find out how the effect of the volume of soaking water on the characteristics of the refrigeration machine, when the refrigerant pipeline located between the compressor and the condenser is submerged in water. How is the effect of the immersion water on the COP and efficiency of the cooling machine? In this research, we refer to the references [1], [2], [3], [4], and [5].

2 Research Methodology

Researched object

The object under study is a refrigeration machine that works with a vapor compression cycle, with a hermetic compressor power of 1/6 hp, other main components such as: finned tube evaporator, pipe condenser with reinforcing radius and

Volume 3, Issue 2, pages 203–214
p-ISSN 2655-8564, e-ISSN 2685-9432

capillary tube, the size of which adjusts to the magnitude of the compressor power. All components are standard components obtained in the market. A schematic drawing of the tested cooling engine is presented in Figure 1.

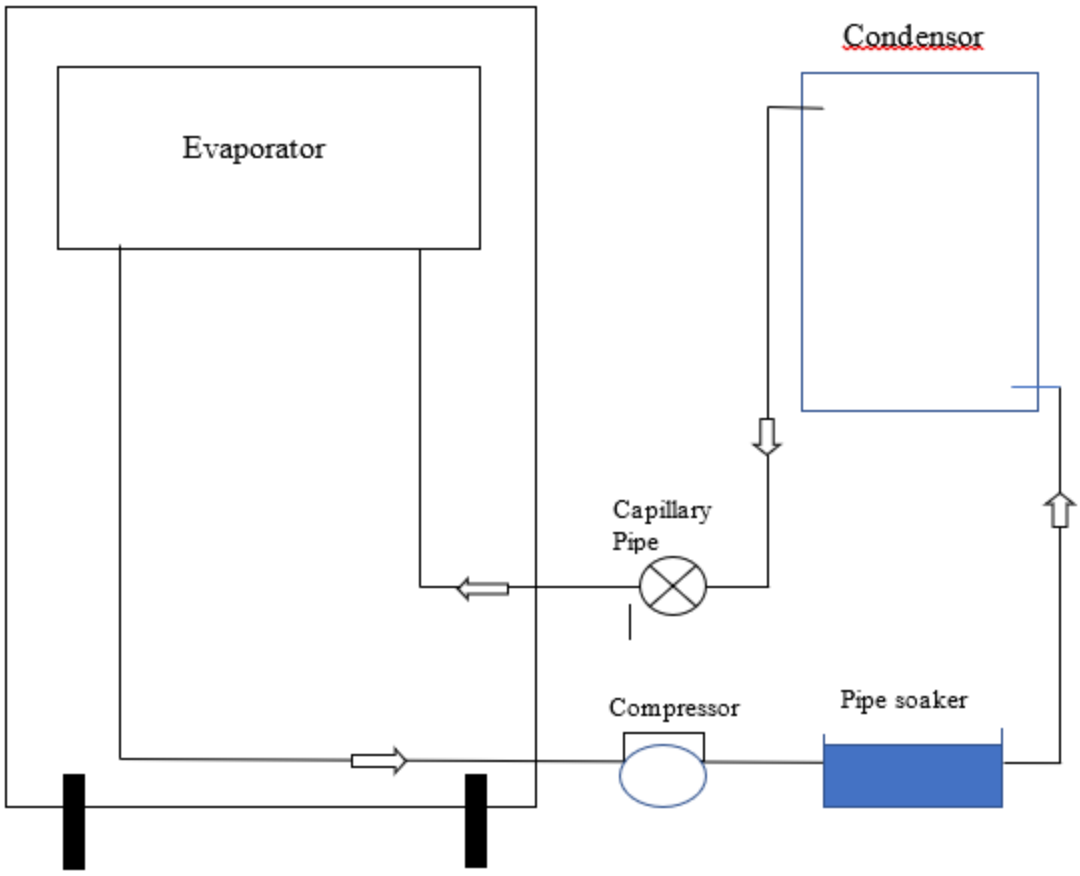

Figure 1. Schematic of the cooling machine under study.

International Journal of Applied Sciences and Smart Technologies
Volume 3, Issue 2, pages 203–214
p-ISSN 2655-8564, e-ISSN 2685-9432

Research Flow

The research was conducted experimentally. The research flow is presented in Figure 2.

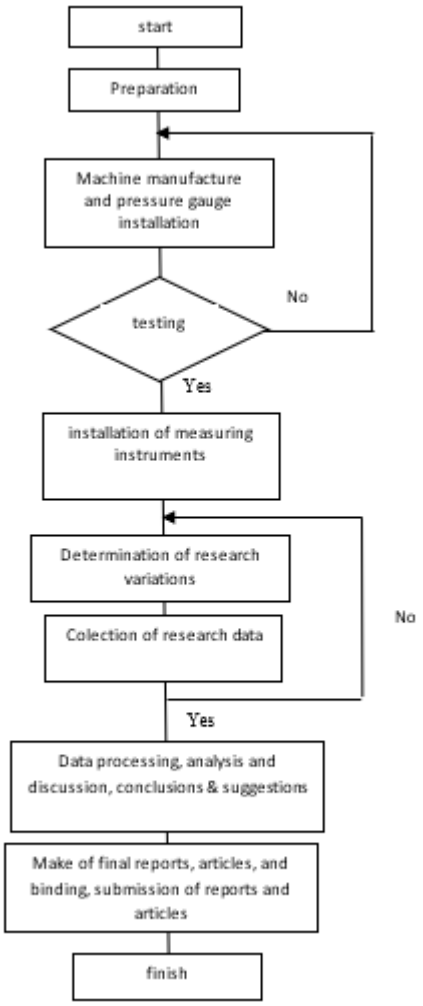

Figure 2. Research flow chart

Research Variation

The research was conducted by varying the volume of water used to immerse the refrigerant pipe located between the compressor and condenser (a) volume of water: 0 ml or without immersion (b) volume of water: 0.5 liters and (c) volume of water 0.75 liters. Variations are made to see the COP_{actual} and efficiency of the cooling machine.

International Journal of Applied Sciences and Smart Technologies
Volume 3, Issue 2, pages 203–214
p-ISSN 2655-8564, e-ISSN 2685-9432

3 Results and Discussion

The results of the research and the results of data processing required to determine the characteristics of the cooling machine are presented in Table 1 to Table 3. The data presented is the result of recording data at 180 minutes, after the cooling machine is turned on/run. With the reason, that at that minute, the work of the machine can be considered "calm".

In the discussion of the results of this study, to facilitate data processing, the process of further cooling and further heating on the compression cycle is ignored. This is due to the difficulty of obtaining refrigerant properties such as the entropy and enthalpy of the refrigerant at high heat conditions. It is actually possible in other ways to obtain data on hot conditions (hot gas conditions) and further cold based on the P-h R134a diagram, but researchers have difficulty getting accurate and definite data that can be accounted for, because it is only based on estimates.

From the research that has been done, the cooling machine that is designed and assembled is able to work well as desired. Able to work continuously without jamming / dead machines or overheating. From the research data, the machine is able to provide a relatively very low working temperature of the evaporator, below $-23°C$. Likewise with the working temperature of the condenser, it can work at temperatures above the surrounding ambient temperature (above $37°C$).

Table 1. Working pressure and temperature of the evaporator and condenser

Condition of the pipe between compressor and condenser	Evaporator working pressure		Condenser working pressure		Evaporator working temperature		Condenser working temperature	
	P_1 (psia)	P_1 (kPa)	P_2 (psia)	P_2 (kPa)	T_{evap} (^0C)	T_{evap} (K)	T_{cond} (^0C)	T_{cond} (K)
Not submerged in water	16,83	116	155,52	1072	-23	250	42	315
Submerged in water ½ $liter$	14,65	101	143,57	989,6	-26	247	39	312
Submerged in	13,63	94	135,97	937,2	-27,5	245,5	37,2	310,2

International Journal of Applied Sciences and Smart Technologies

Volume 3, Issue 2, pages 203–214

p-ISSN 2655-8564, e-ISSN 2685-9432

water $\frac{3}{4}$ $liter$				

Table 2. Enthalpy values in the vapor compression cycle for each study variation

Condition of the pipe between compressor and condenser	P_1 (kPa)	P_2 (kPa)	h_1 (kJ/kg)	h_2 (kJ/kg)	h_3 (kJ/kg)	h_4 (kJ/kg)
Not submerged in water	116	1072	384	437,3	259,4	259,4
Submerged in water ½ $liter$	101	989,6	382,82	436,0	254,9	254,9
Submerged in water ¾ $liter$	94	937,2	381,90	435,1	251,9	251,9

Table 3. Calculation results of cooling engine characteristics

Condition of the pipe between compressor and condenser	$Q_{in} = h_1 - h_4$ (kJ/kg)	$Q_{out} = h_2 - h_3$ (kJ/kg)	$W_{in} = h_2 - h_1$ (kJ/kg)	$COP_{actual} = Q_{in}/Q_{out}$
Not submerged in water	124,60	177,90	53,30	2,34
Submerged in water ½ liter	127,92	181,10	53,18	2,41
Submerged in water ¾ liter	130,00	183,10	53,10	2,45

Condition of the pipe between compressor and condenser	$COP_{ideal} = T_e/(T_c - T_e)$	$Efficiency = \frac{COP_{actual}}{COP_{ideal}}$	refrigerant mass flow rate (kg/s)
Not submerged in water	3,91	0,60	0,002807
Submerged in water ½ liter	3,86	0,62	0,002813
Submerged in water ¾ liter	3,85	0,64	0,002817

The research data in Table 1 shows that the condition of the pipe (which is located between the compressor and the condenser) is immersed in water, providing different

Volume 3, Issue 2, pages 203–214
p-ISSN 2655-8564, e-ISSN 2685-9432

research data than if the pipe is not immersed in water. This means that the water immersion in the pipe affects the working conditions of the cooling machine or in other words affects the characteristics of the cooling machine. It also appears that the volume of water used to submerge the pipe also affects the research data, this also means that the volume of water affects the characteristics of the cooling machine.

If the pipe is not immersed in water, the working temperature of the condenser gives the highest value compared to other conditions (Table 1 and Table 2). If the pipe is immersed in water, the working temperature of the condenser decreases. When the volume of the immersion water is increased or increased in amount, the working temperature of the condenser decreases. This means that the working temperature of the condenser is influenced by the type of fluid and the amount of fluid around the condenser. When the fluid is replaced, the working temperature of the condenser changes and adapts to the new environment, until a new working temperature of the condenser is obtained. For the liquid fluid environment (in this case water) it provides a lower working temperature of the condenser compared to the gas (air) environment. This may be due to: (a) The specific heat of water is greater than the specific heat of air. The greater the specific heat of the fluid around the condenser, the more difficult it is to change the temperature of the fluid around the condenser. The nature of this fluid seems to make the working temperature of the condenser more attracted to the fluid temperature (b) the value of the convection heat transfer coefficient when the heat transfer process takes place between the condenser and water is greater than when it is with air. The greater the value of the convection heat transfer coefficient, the lower the working temperature of the condenser.

The results show that the heat released by the cooling engine (Q_{out}) tends to be more when the condenser's working temperature is lower. This is probably because the value of the heat transfer coefficient of water is greater than that of air. The greater the value of the convection heat transfer coefficient, the greater the heat released by the cooling engine to the water. The existence of a pipe that is immersed in water causes the ability of the cooling machine to release heat to be greater. The largest amount of heat released by the cooling engine is when the pipe is submerged in ¾ liter of water (Table 3).

Volume 3, Issue 2, pages 203–214
p-ISSN 2655-8564, e-ISSN 2685-9432

The results showed that when the pipe was immersed in water, the working temperature of the evaporator changed (Table 1). Move towards lower temperatures. As it is known that the working temperature of the condenser is directly proportional to the working pressure of the condenser. When the working temperature of the condenser decreases, the working pressure of the condenser also decreases. For the same refrigeration machine, the compressor's ability to suppress refrigerant is certainly not much different. Both when pressing refrigerant from the evaporator to the condenser and when from the condenser to the evaporator when passing through the capillary tube. So when the working pressure of the condenser drops, the pressure of the evaporator also tends to fall. Because the pressure difference between the condenser pressure and the evaporator pressure tends to be constant. So it is understandable if the decrease in working pressure in the condenser causes the working pressure of the evaporator to also decrease. The decreasing working pressure of the evaporator causes the working temperature of the evaporator to decrease as well.

The results showed that when the pipe leading to the condenser was immersed in water, the heat absorbed by the evaporator increased (Table 3). This is understandable because the working temperature of the evaporator is lower. The lower working temperature of the evaporator will cause the ability of the evaporator to absorb heat to be greater because the temperature difference between the working temperature of the evaporator and the temperature of the fluid around it is getting bigger. The largest heat can be absorbed by the evaporator, when the immersed pipe goes to the condenser with a volume of ¾ liter of water.

The decrease in the working pressure and temperature of the evaporator, in fact has an impact on the work of the compressor in flowing refrigerant (Table 3). The results showed that the work done by the compressor to move refrigerant per unit mass tends to decrease. This provides information that the compressor work tends to "feel" lighter when the working pressure of the evaporator decreases. Compressor work is most “feeling” light when it is located between the compressor and condenser immersed with a volume of liter of water.

Thus, the important information obtained from this research is, when the pipe between the compressor and the condenser is immersed in water, the pressure and

Volume 3, Issue 2, pages 203–214
p-ISSN 2655-8564, e-ISSN 2685-9432

working temperature of the condenser decrease. The decreasing pressure and temperature of the condenser also has an impact on the decrease of working pressure and working temperature of the evaporator. The working pressure decreases in the evaporator, causing the compressor work to tend to be lighter. When the pipe leading to the condenser is immersed in water, the working conditions change, with a new equilibrium condition which is the simultaneous result of the work of each component of the refrigeration engine that works with the vapor compression cycle.

The calculation of the actual COP_{actual} value is based on the comparison between the calculation of the heat absorbed by the evaporator (Q_{in}) and the compressor power used in the cooling machine (W_{in}). If the Q_{in} value tends to increase while (W_{in}) tends to decrease, then the resulting COP value tends to increase. Table 3 shows the (COP_{actual}) values for each variation. The highest actual CO value is when the pipe is immersed in water with a volume of liter, of 2.45, followed by the condition of the pipe being immersed in water with a volume of liter and without being immersed in water. The order of this COP_{actual} values is the opposite of the COP_{ideal}value. If the order of COP_{actual} values is increasing, then the order of COP_{ideal}values tends to decrease.

The value of the cooling engine efficiency is based on the comparison between the COP_{actual} value and the COP_{ideal} value. The results of this study show that the COP_{actual} value tends to increase while the COP_{ideal} value tends to decrease. Because efficiency is a comparison between COP_{actual} and COP_{ideal}, the efficiency value will tend to increase. The highest efficiency value of the cooling machine is 0.64, produced when the pipe is immersed in water with a volume of liter. The lowest efficiency value when the pipe is not immersed in water.

4 Conclusions

The results of the study provide the following results:

a. The designed cooling machine can work well and smoothly as desired. The working temperature of the evaporator is able to reach temperatures below $-23°C$, and the working temperature of the condenser is able to reach temperatures above the temperature of the fluid in its environment, above $37°C$.

Volume 3, Issue 2, pages 203–214
p-ISSN 2655-8564, e-ISSN 2685-9432

b. The COP_{actual} value of the refrigeration machine from the largest to the lowest, respectively, is owned when the pipe located between the compressor and condenser is immersed with full volume of water, full volume of water immersed, and without water immersion, of 2.45, 2. 41 and 2.34.
c. The efficiency values of the refrigeration engine from the largest to the lowest are respectively owned when the pipe located between the compressor and the condenser is immersed with full volume of water, full volume of water immersed, and without water immersion, of 0.64, 0.62 and 0.60.

References

[1] K. Anwar, E. Arif, dan W. H. Piarah, "Effects of Capillary Pipe Temperature on Cooling Engine Performance." *Mechanical Journal*, **1** (Januari 1), 30 – 3, 2010.

[2] Matheus M Dwinanto, Hari Rarindo and Jonri Lomi Ga, "The effect of the dimensions of the capillary tube and the mass of the refrigerant used on the performance of a double evaporator refrigeration machine for fish preservation," *Proceedings of the Annual National Seminar on Mechanical Engineering & Thermofluid IV*, **1** (1), 2012.

[3] Said H. I., Abbas, Lita A.Latif, "Experimental study of cooling engine performance in the Mechanical Engineering laboratory, Khairun University, Ternate," *Proceedings Annual National Seminar on Mechanical Engineering & Thermofluid IV*, **1** (1), 2012.

[4] Soegeng Witjahjo, "Performance Test of Refrigeration Machines Using LPG Refrigerant," *Austenite Journal*, **1** (2), 2009.

[5] Wibowo Kusbandono, P.K. Purwadi, "The Effect of the Existence of Fan in the Wood Drying Room on the Drying Time and the Performance of the Electric Energy Wood Dryer," *International Journal of Applied Sciences and Smart Technologies (IJASST)*, **3** (1), 2021.

International Journal of Applied Sciences and Smart Technologies

Volume 3, Issue 2, pages 203–214

p-ISSN 2655-8564, e-ISSN 2685-9432

This page intentionally left blank

International Journal of Applied Sciences and Smart Technologies

Volume 3, Issue 2, pages 215–224

p-ISSN 2655-8564, e-ISSN 2685-9432

Heat Transfer Characteristic on Wing Pairs Vortex Generator using 3D Simulation of Computational Fluid Dynamic

Petrus Setyo Prabowo[1], Stefan Mardikus[2,*],

Ewaldus Credo Eukharisto[2]

[1]*Department of Electrical Engineering, Sanata Dharma University, Paingan, Maguwoharjo, Depok, Sleman, Yogyakarta 55282, Indonesia*
[2]*Department of Mechanical Engineering, Sanata Dharma University, Paingan, Maguwoharjo, Depok, Sleman, Yogyakarta 55282, Indonesia*
[*]*Corresponding Author: stefan@usd.ac.id*

(Received 08-11-2021; Revised 07-12-2021; Accepted 07-12-2021)

Abstract

Vortex generators are addition surface that can increase heat transfer area and change the fluid flow characteristics of the working fluid to increase heat transfer coefficient. The use of vortex generators produces longitudinal vortices that can increase the heat transfer performance because of the low pressure behind vortex generators. This investigation used delta winglet vortex generator that was combined with rectangular vortex generator to Reynold numbers ranging 6.000 to 10.000. The parameters of Nusselt number, friction factor, velocity vector and temperature distribution will be evaluated.

Keywords: Parallelogram winglet vortex generator, heat exchanger, heat transfer performance

International Journal of Applied Sciences and Smart Technologies
Volume 3, Issue 2, pages 215–224
p-ISSN 2655-8564, e-ISSN 2685-9432

1 Introduction

Heat exchanger is one of various important components in the industries. Chemical industry, power plants, food factories hospitals, and super computers are using heat exchanger for their daily operation. Heat exchanger is used to transfer heat such as cooling system in super computers, boilers in power plants, evaporators to dry food at food factories, hot and cold piping system in hospitals and separator in chemical industries. One type of heat exchangers that is used most in the operation of those industries is circular tube heat exchanger.

Circular tube heat exchanger performance is affected by some parameters. Heat transfer area and fluid flow characteristics are two parameters that have great effect on heat exchanger performance. The wider the heat transfer area, the higher the heat transfer rate of heat exchanger. The addition of heat transfer area can make some adjustments to the flow characteristics of the working fluid based on the method. The method that can increase heat transfer area and change the fluid flow characteristics is the use of vortex generators.

Vortex generators are added surface that can increase heat transfer area and change the fluid flow characteristics of the working fluid to increase heat transfer performance. The use of vortex generators produces longitudinal vortices that can increase the heat transfer performance. Longitudinal vortices shapes because of the low pressure behind vortex generators. Low pressure region makes the working fluid in the middle of the flow changes its course to the side and from the side to the middle. Previous researches show that the use of vortex generators can increase heat transfer performance [1].

Deshmukh and Vedula, 2014 shows that circular tube heat exchanger using curved delta winglet vortex generator in the inner side has higher heat transfer performance compared with plain circular tube. Using the variations of Reynolds number ranging from 10.000 to 45.000, the use of curved delta winglet vortex generator can increase Nusselt number from 1.3 to 5.0 [2]. Islam and Kharoua, 2018 studied thermal performance and flow behaviour of winglet vortex generators in circular tube using experimental method. Attack angle of 0°, 15°, 30°, 45°, blockage ratio of 0.1, 0.2, 0.3, row values of 4, 8, 12, and relative pitch ratios of 4.8, 2.4, 1.6 were investigated using

Volume 3, Issue 2, pages 215–224
p-ISSN 2655-8564, e-ISSN 2685-9432

Reynolds number of 6.000 to 33.000. The result shows the decrease of Nusselt number with pitch row but increase with attack angle and blockage ratio [3]. Liu et al., 2018 numerically and experimentally studied heat transfer performance on circular tube heat exchanger enhanced with rectangular winglet vortex generators [4]. Reynolds number ranging from 5.000 to 17.000 was used to investigate the effect of rectangular winglet vortex generators in circular tube heat exchanger using slant angle variations of 10°, 20°, 30°, and 35°. The result shows the increase of Nussselt number from 1.15 to 2.49 and friction factor from 2.09 to 12.32. Modhi and Rathod, 2019 compared the use of sinusoidal wavy and elliptical curved rectangular winglet vortex generators using 2D numerical method. Reynolds number of 400 to 1000 was used to study heat transfer enhancement and pressure drop varying in wavy-up, wavy-down, curved-up, and curved-down with plain rectangular winglet vortex generators as the baseline. The result shows the increase of heat transfer performance with moderate pressure drop [5]. Zhai et al., 2019 did a research of heat transfer augmentation on circular tube using delta winglet pairs vortex generator. Reynold number ranging from 5.000 to 25.000 was used to study heat transfer enhancement characteristics using the variations angle of attack 10°, 20°, 30°, 40°, height 5 mm, 7.5 mm, 10 mm, and space 10 mm, 15 mm, 20 mm. Experiment result shows the application of delta winglet pairs vortex generators can increase Nusselt number up to 75% compare with plain circular tube [6]. Sun et al., 2020 studied the effect of rectangular winglet vortex generators in circular tube heat exchanger using some parameter variations. Those variations are the amount of vortex generator deployed 4, 6, 8, height ratio 0.05, 0.1, 0.2, and pitch ratio 1.57, 3.14, 4.71. The result shows the increase of Nusselt number by 1.15 to 2.23 while the friction factor 1.46 to 11.63 [7]. Pourhedajat et al., 2020 numerically studied the use of triangular winglet vortex generators in circular tube. Longitudinal and latitudinal variations were used in that study. The result shows the smaller the longitudinal pitch the higher the heat transfer rate. The application of latitudinal pitch variations from 0 mm to 40 mm shows 20 mm latitudinal pitch resulting in the highest heat transfer enhancement [8]. Zang et al., 2020 investigated heat transfer performance of rectangular winglet vortex generators applied in circular tube heat exchanger. Parallel and v-shaped configuration was used in that study with the variations of attack angle and length ratio. The use of parallel

Volume 3, Issue 2, pages 215–224
p-ISSN 2655-8564, e-ISSN 2685-9432

configuration results in the increase of heat transfer rate by 54% to 188% and flow resistance by 152% to 568%. The use of v-shaped configuration results in the increase of heat transfer rate by 60% to 118% and flow resistance by 141% to 644% [9].

Based on those previous studies that are reviewed above, there are still many improvements that can be done by researchers. This study focus on heat transfer enhancement using a novel type of vortex generators, parallelogram winglet vortex generator. Parallelogram winglet vortex generator is a new type of vortex generators that is inspired by combining the characteristics of delta winglet vortex generator and rectangular winglet vortex generator.

Parallelogram winglet vortex generator has the shape of delta winglet vortex generator that is combined with rectangular vortex generator. Heat transfer enhancement of circular tube heat exchanger using parallelogram winglet vortex generators was studied numerically with plain circular tube heat exchanger as the baseline. Reynolds number ranging from 6.000 to 10.000 was used in this study to identify the heat transfer performance with the variations of parallelogram vortex generators lean following the flow and lean against the flow configuration. Nusselt number, friction factor, velocity vector and temperature distribution were used in this research as evaluation parameters.

2 Research Methods

Three dimensional numerical method was carried out in this study to investigate heat transfer performance of circular tube heat exchanger embedded with parallelogram winglet vortex generators.

2.1. Model Description

The simulation was carried out in two different parallelogram winglet vortex generators configurations that are lean following the flow as can be seen at Figure 1, and against the flow as can be seen at Figure 2. The length of the pipe is 700 mm with vortex generators embedded inside the circular tube. As can be seen at Figure 3, the diameter of the tube is 50.8 mm with the thickness of 3 mm. Six pairs parallelogram

Volume 3, Issue 2, pages 215–224

p-ISSN 2655-8564, e-ISSN 2685-9432

winglet vortex generators with the pitch of 100 mm. Each pair composed of 4 vortex generators that was arranged at 0°, 90°, 180°, 270° of the cross section area. The attack angle of 0° was applied to the parallelogram winglet vortex generators to investigate the most basic effect of it used in circular tube heat exchanger. The geometry of parallelogram winglet vortex generator is shown in Figure 4. The parallelogram winglet vortex generator has the short diagonal of 15 mm and long diagonal 30 mm.

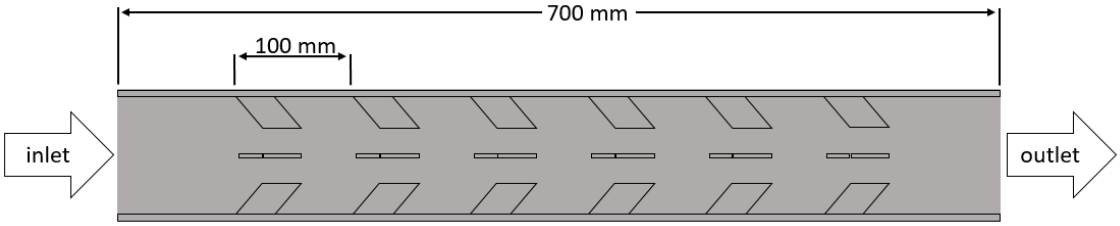

Figure 1. Lean following of the flow configuration.

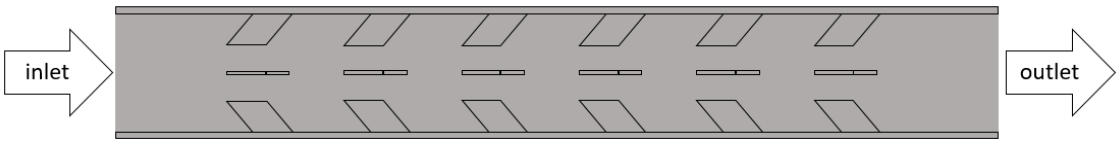

Figure 2. Lean against of the flow configuration.

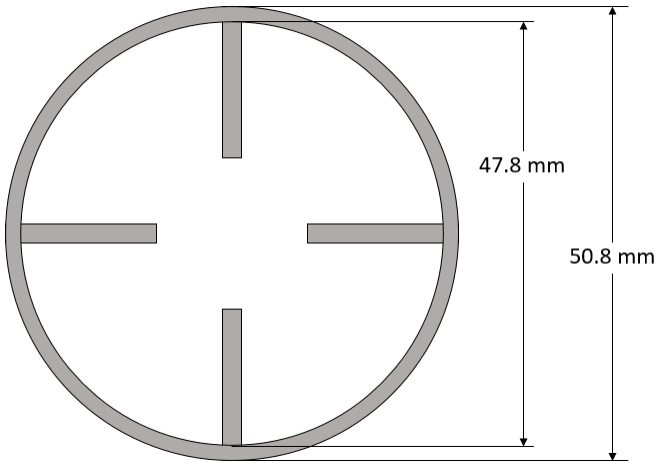

Figure 3. Cross section of the physical model.

International Journal of Applied Sciences and Smart Technologies

Volume 3, Issue 2, pages 215–224

p-ISSN 2655-8564, e-ISSN 2685-9432

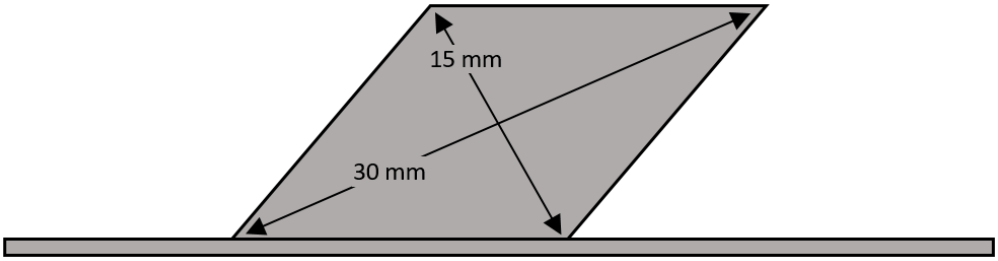

Figure 4. Cross section of the physical model of parallelogram winglet vortex generator

2.2. Boundary Condition

Three dimensional numerical method was carried out using Reynolds number ranging from 6.000 to 10.000. The working fluid was assumed to be steady turbulent flow. Inlet temperature of the working fluid was 322.2 K. The wall and the vortex generator assumed to have the same temperature of 300 K. The working fluid used in this study was ammonia. Coupled pressure and velocity in governing equation in this study was solved using the SIMPLE algorithm. The thermal convection and the velocity was discretized by second order upwind. The residual criteria less than 10-6 was used for the energy equation and 10-4 for the other variables.

3 Results and Discussion

Heat transfer performance of the cases studied was evaluated using Nusselt number and thermal gradient. Figure 5 shows the Nusselt number increases with Reynolds number that is similar in the tendency of the study by Liu et al [4]. This study has overall Nusselt number higher than Liu et al [4] study due to the use of ammonia as the working fluid that is lower in thermal conductivity than water used by Liu et al study.

The Nusselt numbers in Figure 5 increase with Reynolds numbers in all cases studied. In the case of the plain circular tube the increase of Nusselt number from 6.000 to 7.000, 8.000, 9.000, and 10.000 are 12.86%, 25.54%, 37.18%, and 47.38%. In the case of vortex generators leaned following the flow configuration the increase of Nusselt numbers are 11.34% 22.55% 33.71% and 44.79%. In the case of vortex generators lean against the flow configuration the increase of Nusselt numbers are 10.72%, 21.61%, 32.44%, and 43.00%. Based on the data showed in this study the plain

Volume 3, Issue 2, pages 215–224
p-ISSN 2655-8564, e-ISSN 2685-9432

tube has the highest increase in Nusselt number with the increase of Reynolds number. It is followed by the use of vortex generators leaned following the flow and the lowest Nusselt number increase is by the used of vortex generators leaned against the flow.

Based on the use of vortex generators compare with the plain case, the vortex generators leaned following the flow configuration has the average increase of Nusselt number 5.38% with the lowest value 4.39% in the Reynolds number 9000 and the highest 7.1 % in Reynolds number 6000 and the vortex generators leaned against the flow configuration has the average increase of Nusselt number 22,49% with the lowest value 21.04% in the Reynolds number 9000 and the highest 25.36% in the Reynolds number 6000. The use of vortex generators leaned against the flow configuration has the higher increase of Nusselt number compare with vortex generators leaned following the flow configuration with the lowest and highest value in the same Reynolds number variations. The highest increase in Nusselt number value occurred in the use of Reynolds number 6000 was caused by the contact time between the working fluid and the heat transfer surface area of the tube and the vortex generators applied [10].

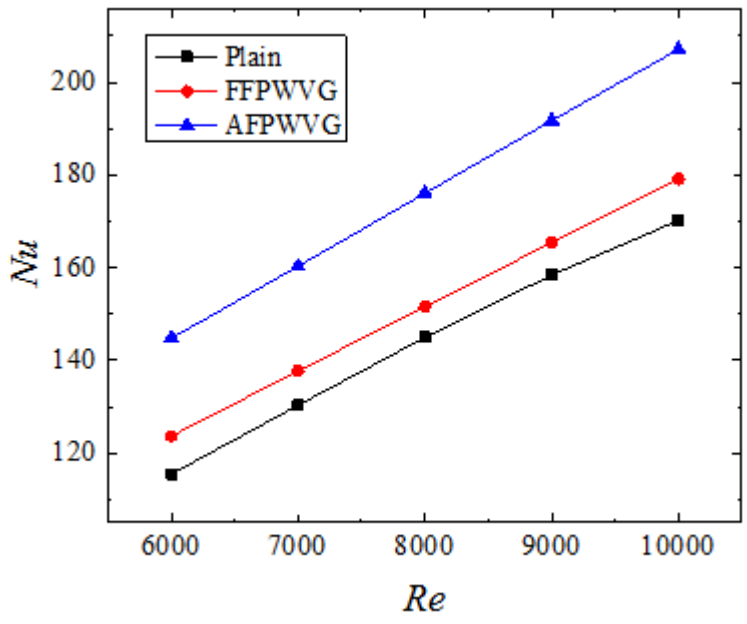

Figure 5. Reynolds number vs Nusselt number for Plain tube, leaned following the flow parallelogram winglet vortex generators arrangement and against the flow parallelogram winglet vortex generators arrangement

Volume 3, Issue 2, pages 215–224

p-ISSN 2655-8564, e-ISSN 2685-9432

Temperature gradient was also used in this study to understand the heat transfer phenomena occurred. Figure 6, Figure 7, and Figure 8 showed the thermal gradient of the plain tube, lean following the flow configuration, and lean against the flow configuration using Reynolds number 6000. The temperature gradient of Reynolds number 6000 was used to investigate the temperature distribution characteristic due to the highest increase of the Nusselt number. The plain case in Figure 6 showed that the working fluid temperature has a smooth pattern from the inlet to the outlet. It means that the working fluid has relatively low temperature distribution. The use of vortex generator increases the temperature distribution due to the increase of contact surface between the working fluid and tube wall [Liu et al., 2018]. The use of vortex generator in Figure 7 and Figure 8 showed the better temperature distribution compare with the plain case in Figure 6. The high temperature not only occurs in the middle stream but also near the tube wall. However, temperature distribution in the case of leaned against the flow configuration showed by Figure 8 is higher than the case of leaned following the flow configuration showed by Figure 7.

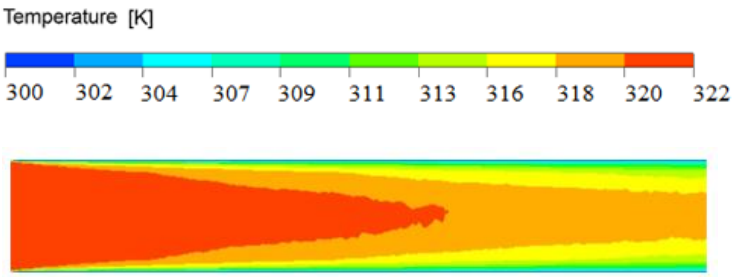

Figure 6. Temperature gradients of the plain case Re 6000

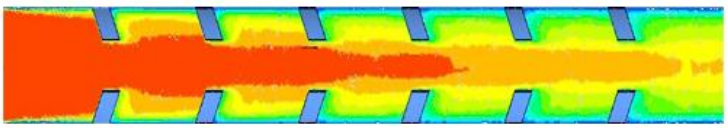

Figure 7. Temperature gradient of the leaned following the flow configuration Re 6000

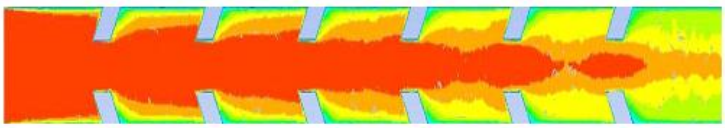

Figure 8. Temperature gradient of the leaned against the flow configuration Re 6000

4 Conclusion

This study investigates the effect of parallelogram winglet vortex generator inside circular tube heat exchanger. Plain circular tube heat exchanger was used in this study as the base case to be compared with the use of vortex generator deployed inside the tube with the configuration of leaned following the flow and leaned against the flow. The conclusion of the study based on the results acquired are:

a. The use of Parallelogram winglet vortex generator can increase heat transfer performance of plain tube heat exchanger using ammonia as the working fluid.
b. The use of against the flow configuration resulting in the increase of Nusselt number higher than the leaned following the flow configuration.
c. The use of leaned following the flow configuration can increase the Nusselt number ranging from 4.39% to 7.10% while the use of leaned against the flow configuration 21.04% to 25.36%.

References

[1] Y. Xu, M. D. Islam, and N. Kharoua, "Numerical study of winglets vortex generator effects on thermal performance in a circular pipe," *International Journal of Thermal Sciences*, 112, 304–317, 2017.

[2] P. W. Deshmukh and R. P. Vedula, "Heat Transfer and Friction Factor Characteristics of Turbulent Flow Through A Circular Tube Fitted with Vortex Generator Inserts," *International Journal of Heat and Mass Transfer*, 79, 551–560, 2014.

[3] Y. Xu, M.D. Islam, and N. Kharoua, Experimental study of thermal performance and flow behaviour with winglet vortex generators in a circular tube, *Applied Thermal Engineering*, 135, 257–268, 2018.

[4] H. Liu, H. Li, Y. He, and Z. Chen, "Heat transfer and flow characteristics in a circular tube fitted with rectangular winglet vortex generators," *International Journal of Heat and Mass Transfer*, 126, 989–1006, 2018.

[5] Y. Lei, F. Zheng, C. Song, and Y. Lyu, "Improving The Thermal Hydraulic Performance of A Circular Tube by using Punched Delta-Winglet Vortex

Volume 3, Issue 2, pages 215–224
p-ISSN 2655-8564, e-ISSN 2685-9432

Generators," *International Journal of Heat and Mass Transfer*, 111, 299–311, 2017.

[6] C. Zhai, M. D. Islam, R. Simmons, and I. Barsoum, "Heat Transfer Augmentation in A Circular Tube with Delta Winglet Vortex Generator Pairs," *International Journal of Thermal Sciences*, 140 , 480–490, 2019.

[7] Z. Sun, K. Zhang, W. Li, Q. Chen, and N. Zheng, "Investigations of the turbulent thermal-hydraulic performance in circular heat exchanger tubes with multiple rectangular winglet vortex generators," Applied Thermal Engineering, 168, 114838, 2020.

[8] S. Pourhedayat, S. M. Pesteei, H. E. Ghalinghie, M. Hashemian, and M. A. Ashraf, "Thermal-exergetic behavior of triangular vortex generators through the cylindrical tubes," International Journal of Heat and Mass Transfer, 151, 119406, 2020.

[9] J. F. Zhang, L. Jia, W. W. Yang, J. Taler, and P. Oclon, "Numerical analysis and parametric optimization on flow and heat transfer of a microchannel with longitudinal vortex generators," International Journal of Thermal Sciences, 141, 211–221, 2019.

[10] Y. Zhang, C. Kang, H. Zhao, and S. Teng, "Effects of in-line configuration of drag-type hydrokinetic rotors on inter-rotor flow pattern and rotor performance," Energy Conversion and Management, 196, 44–55, 2019.

International Journal of Applied Sciences and Smart Technologies

Volume 3, Issue 2, pages 225–240

p-ISSN 2655-8564, e-ISSN 2685-9432

Subgroup Graphs of Finite Groups

Ojonugwa Ejima[1,*], Abor Isa Garba[1], Kazeem Olalekan Aremu[1]

[1]*Department of Mathematics, Usmanu Danfodiyo University, Sokoto, Nigeria*

[*]*Corresponding Author: unusoj1@yahoo.com*

(Received 08-10-2021; Revised 29-12-2021; Accepted 29-12-2021)

Abstract

Let G be a finite group with the set of subgroups of G denoted by $S(G)$, then the subgroup graphs of G denoted by $\Gamma(G)$ is a graph which set of vertices is $S(G)$ such that two vertices $H, K \in S(G)$ $(H /= K)$ are adjacent if either H is a subgroup of K or K is a subgroup of H. In this paper, we introduce the Subgroup graphs Γ associated with G. We investigate some algebraic properties and combinatorial structures of Subgroup graph $\Gamma(G)$ and obtain that the subgroup graph $\Gamma(G)$ of G is never bipartite. Further, we show isomorphism and homomorphism of the Subgroup graphs of finite groups.

Keywords: subgroup, graph, finite group

1 Introduction

One of the mathematical tools for studying symmetries of object is group theory, hence, several structures in the field of algebra are depicted through groups. This mathematical concept has evolved rapidly since it discovery in the sixteenth century. According to [1], the rebirth of the axiomatic method and the view of mathematics as a human activity in the nineteenth century forms the major development that change the bearing on the evolution of group theory as a mathematical concept. [1], further noted that the evolution had caused the previous classical algebra polynomial equations

Volume 3, Issue 2, pages 225–240
p-ISSN 2655-8564, e-ISSN 2685-9432

transited to the modern algebra of axiomatic systems of the nineteenth century. Meanwhile, this concept has been applied in the field of physics, chemistry and biology, (see [2], [3], [4], [5]) for details.

In the same vein, in the last two decades, many studies have related graphs to group theory, providing a more easier way to visualize the concept of group; this relation brings together two important branches of mathematics, and has opened up a new wave of research with a better understanding of the fields. Many years after Euler's research work on the bridges of Konigsberg city, Cayley [6] used the generators of a finite group G to define a graphical structure called the Cayley graph of finite group G, he further showed that every group of order n can be represented by a strongly connected diagraph of n vertices [7]. Afterwards, in the last few decades, his view of diagraph has since been extended to different and modified graph of algebraic structures. Hence, more algebraic studies through the properties of these modified graphs have become topics of interest to many around the globe (See [8], [9], [10], [11], [12], [13], [14], [15]).

This study, the subgroup graph of finite groups $\Gamma(G)$ like [8], [9], [10], [11], [12], [13], [14], [15], will focus on finite groups G, however, the choice of it vertex set $V(\Gamma(G))$, is the subgroups $S(G)$ of G. In the literature, vertex set of graphs of finite groups are always the elements n G, a deviation from this norm is the motivation for this study.

1.1. **Preliminaries**. We state some known and useful results which will be needed in the proof of our main results and understanding of this paper. For the definitions of the basic terms and results given in this section ([16], [17], [18], [19], [20], [21], [22], [23]). A *graph* Γ is a combinatorial structure formed by finite non-empty set (V, E), where V is the set of vertices viewed as points and E is the set of edges viewed as line joining the points. The cardinality of $V(\Gamma)$ is called the *order* of Γ while the cardinality of $E(\Gamma)$ is called the *size* of Γ. The degree of a vertex x in a graph Γ denoted by $\delta(x)$ is the number of edges incident to it, that is the number of edges connecting x. A graph is said to have *parallel edges* if there are more than one edges which join the same pair of

Volume 3, Issue 2, pages 225–240
p-ISSN 2655-8564, e-ISSN 2685-9432

distinct vertices. A *loop* on the other hand is an edge that joins a vertex to itself while a *walk* of length $k \leq n$ in a graph Γ with vertex set $V(\Gamma)$ consist of an alternating sequence of vertices and edges consecutive elements of which are incident, that begins and ends with a vertex.

Definition 1.1. [20] A *complete graph* is a simple undirected graph in which has at least one vertex and every arbitrary pair of distinct vertices is joint by a unique edge. while a connected graph on the other hand is a graph where there is an edge between every pair of vertices.

Remark 1.2. Note that every complete graph is necessary connected but connected graphs are not necessary complete.

Definition 1.3. [20] A walk in a connected graph that visits every vertex of the graph exactly once without repeating the edges is called *Hamiltonian path*. If this walk starts and ends at the same vertex, the walk is called a Hamiltonian circuit or cycle.

Remark 1.4. A graph that contains a *Hamiltonian* cycle is said to be *Hamiltonian*.

Theorem 1.5. *(Sylow's First Theorem)* [21] *Let G be a finite group of order $p^r q$, where p is a prime, r and q are positive integers and $gcd(p,q) = 1$. Then G has a subgroup of order p^k for all k satisfying $0 \leq k \leq r$.*

Definition 1.6. [20] In graph theory, a *regular graph* is a graph where each vertex has the same number of neighbors, i.e. every vertex has the same degree or valency; a regular graph can be an x-regular graph where every vertex of the graph have the same degree x.

Definition 1.7. [20] The distance between two vertices $x, y\ V(\Gamma(G))$ is the *length* of the shortest path between x and y and it's denoted by $\delta(x,y)$. *Eccentricity* $\delta(x)$ of a vertex x in a graph is define as $\delta(x) = max\{\delta(x,y) : x, y\ V(G)\}$. The minimum and maximum eccentricity in a graph are called *radius*, rad(G) and *diameter*, diam(G) of the graph respectively.

Lemma 1.8. [20] *Let G and G' be any two finite groups. If $G \cong G'$, then $S'(G) \cong S'(G')$ and $S(G) \cong S(G')$. But the converse is not true.*

Definition 1.9. [21] A *group consists* of a set G with a binary operation * on G satisfying the following four conditions:

Volume 3, Issue 2, pages 225–240

p-ISSN 2655-8564, e-ISSN 2685-9432

1. Closure: $\forall a, b \in G$, we have $a * b \in G$.
2. Associativity: $\forall a, b, c \in G$, we have $a(b * c) = (a * b)c$.
3. Identity: There is an element $e \in G$ satisfying $e * a = a * e = a$ for all $a\ G$.
4. Inverse: For all $a \in G$, there is an element $a^{-1} \in G$ satisfying $a * a^{-1}\ a^{-1} * a = e$. (where e is as in the Identity Law)

Definition 1.10. [20] A finite group is a group containing finite number of elements. The order of a finite group G is the number of elements in G.

Definition 1.11. [21] A subset H of a group G is called a subgroup if it forms a group in its own right with respect to the same operation on G.

Definition 1.12. [21] Let G_1 and G_2 be groups. A homomorphism from G_1 to G_2 is a map θ which preserves the group operation.

Definition 1.13. [21] A subgroup H of G is said to be a normal subgroup if it is the kernel of a homomorphism. Equivalently, H is a normal subgroup if its left and right cosets coincide: $aH = Ha$ for all $a \in G$. We write "H is a normal subgroup of G" as $H \trianglelefteq G;\ if\ H \neq G$, we write $H \triangleleft G$. If H is a normal subgroup of G, we denote the set of (left or right) cosets by G/H. We define an operation on G/H by the rule $(Ha)(Hb) = Hab$ for all $a, b \in G$.

Definition 1.14. [24] Let a and b be elements of a group G such that $[a, b]$ yields an element of G and is defined by $[a, b] = a^{-1}.b^{-1}.a.b$, the collections of arbitrary $[a, b]$ in G forms the commutator subgroup of G.

Lemma 1.15. [16] Suppose $a, b, c \in G$ and e is a positive integer. Then

1. $[a, b] = [b, a]^{-1}$.
2. $[a, bc] = [a, c][a, b]^c$.
3. $[ab, c] = [a, c]^b[b, c]$.
4. $[a, b^e] = \prod_{i=0}^{e-1} [a, b]^{b^i}$.

Lemma 1.16. [25] Let G be a group with $P\ a\ p-$ subgroup of G and $T\ a\ p'-$ subgroup of $N_G(P)$. Set $R = [T, P]$, and the following holds

1. $[T, R] = R$, *and if* P *is abelian, then* $P = R * C_P\ (T)$.
2. *If* R *is abelian, then the minimal number of elements needed to generate* $R;\ d(R) \leq 2$ *and* $t \in T' - C_\tau\ (P)$, *then* $[t, R] = R$..

Volume 3, Issue 2, pages 225–240
p-ISSN 2655-8564, e-ISSN 2685-9432

3. *If R is abelian and the minimal number of elements needed to generate R; $d(R) \leq 2$, there exists $t \in T$ such that $[t, R] = R$.*
4. *If R is cyclic, then $T/C_\tau(P)$ is cyclic*

Lemma 1.17. [25] *Suppose $G = \langle x, y, A \rangle$ is a finite group with $A \geq G'$ abelian and $a = [x, y]$ of order n. If C is the commutator subgroup of G, then $\{a^e b \mid b \in [G, A], (e, n) = 1\} \subseteq C$.*

Theorem 1.18. [*25] Let G be a $p-$group with G' abelian and $d(G') \leq 2. Set\ C = CG(G'/\Phi(G'))$.*

1. *There exists $y \in G$ with $G' = [y, C]$. In particular, if $C < G$, then y can be taken to be any element of $G - C$.*
2. *Let $[y, C] = G'$. If either $p \neq 2$ or $[G', C] \leq \Omega^2 G'[y, G']$, then $G' = \Gamma_y(C)$.*
3. *G' is equal to the commutator subgroup of G.*

Lemma 1.19. [25] *Let P be a $p-$subgroup of G, t a $p'-$element of $N_G(P)$, and $s \in P$. If $[t, P]$ is abelian, then $\Gamma_{ts}(P) = [t, P]\Gamma_s(P)$.*

Theorem 1.20. [26] *Let G be a group and let H, K be two subgroups of G and define $= hk : h \in H, k \in K$, then*

1. *If both H and K are normal in G, then $H \cap K$ is also a normal subgroup of G.*
2. *If H alone is normal in G, then $H \cap K$ is a normal subgroup of K.*
3. *If H is normal in G, then $HK = KH$ and HK is a normal subgroup of G.*
4. *If both H and K are normal in G, then HK is a normal subgroup of G.*

Theorem 1.21. *(Sylow's theorems) Let G be a group of order $p^\alpha m$, where p is a prime, $m \geq 1$, and p does not divide m. Then:*

1. *$Sylp \neq \emptyset$, that is Sylow $p-$subgroups exist.*
2. *All Sylow $p-$subgroups are conjugate in G.*
3. *Any $p-$subgroup of G is contained in a Sylow $p-$subgroup.*
4. *$n_p(G) \equiv 1\ mod\ p$.*

Lemma 1.22. *(Lagrange's theorem) [22] Let H be a subgroup of a finite group G. Then the order of H divides the order of G.*

International Journal of Applied Sciences and Smart Technologies
Volume 3, Issue 2, pages 225–240
p-ISSN 2655-8564, e-ISSN 2685-9432

2 Research Methodology

This article is not a variable base research, however, well known algebraic definitions and results were used to investigate the algebraic and combinatorial properties of the subgroup graph of finite groups.

3 Results and Discussion

The Subgroup graphs of finite groups is introduce in this section. We begin with the definition and notion of the Subgroups graph of a finite group.

Definition 3.1. Let G be a finite group and $S(G)$ be the set of subgroups of G. Then the Subgroup graph of G is the graph $\Gamma(G)$ with vertex set $V(\Gamma(G) = S(G)$ and the edge set

$$E(\Gamma(G)) = \{\{H, K\} : H \neq K, H \leq K \text{ or } K \leq G\}.$$

Remark 3.2. Let G be a finite group of order n, some clear consequences of the definition of subgroup graphs of finite groups $\Gamma(G)$ are

1. The subgroup graph $\Gamma(G)$ is a simple graphs, thus, there are no loops nor multiple edges.
2. The trivial subgroups of G are adjacent to every other vertices on $\Gamma(G)$.
3. Since the trivial subgroups of G are adjacent to every other vertices on $\Gamma(G)$, then the graph is connected.
4. The $\Gamma(G)$ has a diameter and radius of 1 if $|G| > 2$.

Below, we give an example of Subgroups graph.

Example 3.3. Let G = the group of integer modulo 6 under addition $(\mathbb{Z}_6, +)$, then the following is the undirected Subgroups graph of $(\mathbb{Z}_6)$. See Figure 1.

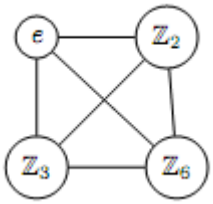

Figure 1. Subgroups graph of Z_6.

International Journal of Applied Sciences and Smart Technologies
Volume 3, Issue 2, pages 225–240
p-ISSN 2655-8564, e-ISSN 2685-9432

Theorem 3.4. [20] *A simple graph is bipartite if and only if it does not have any odd cycle.*

Remark 3.5. Let G be a finite group, the subgroup graph $\Gamma(G)$ of G is never bipartite.

Theorem 3.6. Let G be a finite group of prime order and let $S(G)$ be the set of subgroups of G, then the subgroups graph of G is a straight line with only two vertices.

Proof: Let G be a finite group of prime order and let $S(G)$ be the set of subgroups of G, then by Lemma 1.22, the order of every $H \in S(G)$ divides the order of G but the order of G is a prime which can only be divided by itself of 1. Thus the only subgroups of this group G are $H = \{\{e\} and\ G\ itself\}$; and they are adjacent.

Remark 3.7. Let G be a finite group and let $\Gamma(G)$ be the subgroups graph of G. Then the vertex set $V(\Gamma(G)) \geq 2$ and edge set $E(\Gamma(G)) \neq \emptyset$; therefore, the subgroups graph of a finite group G can never be empty.

Theorem 3.8. Let G be a group and let H, K be two subgroups of G and let $\Gamma(G)$ be the subgroup graph of G. Define $HK = \{hk: h \in H, k \in K\}$, then

1. If both H and K are normal in G, then $H \cap K$ is also a vertex on $\Gamma(G)$.
2. If H alone is normal in G, then $H \cap K$ is a adjacent to vertex K on $\Gamma(G)$.
3. If H is normal in G, then $HK = KH$ and HK is also a vertex on $\Gamma(G)$.
4. If both H and K are normal in G, then HK is also a vetex on $\Gamma(G)$.

Proof: From Theorem 1.20, the results follows.

Theorem 3.9. Let G be a finite group of non prime order $n > 2$, then the subgroup graph of G $(\Gamma(G))$ is never a star graph.

Proof: Suppose on the contrary, let the subgroup graph of a finite group of non prime order $n > 2$ be a star graph; then it implies that all other $H \in S(G)$ are subgroup to only an arbitrary subgroup $K \subseteq G$, but by Remark 3.2(2), every group has two trivial subgroups which are adjacent to all other $H \in S(G)$. So, the graph can not be a star graph, since, there is more than one vertex that is adjacent to all the vertices of $\Gamma(G)$.

Volume 3, Issue 2, pages 225–240
p-ISSN 2655-8564, e-ISSN 2685-9432

Theorem 3.10. Let G and G' be two isomorphic finite groups. Then the subgroup graph of G is isomorphic to subgroup graph of $G'(\Gamma(G) \cong \Gamma(G'))$.

Proof: Suppose G and G' are two isomorphic finite groups, then from Lemma 1.8, $S(G) \cong S(G')$. Thus, $(\Gamma(G) \cong \Gamma(G'))$.

Theorem 3.11. Let G be a group of order $p^{\alpha} m$, where p is a prime, $m \geq 1$ and p does not divide m. Suppose $\Gamma(G)$ is the subgroup graph of G, $V(\Gamma(G))$ and $E(\Gamma(G))$ are the vertex and edge sets of $\Gamma(G)$ respectively. Then:

1. There must exist Sylow p-subgroups of $G; H, K \in V(\Gamma(G))$ which are conjugate in G and are adjacent to each other on the subgroup graph of G.
2. There is a vertex H on the subgroup graph of G that is adjacent to a vertex K that is a Sylow p-subgroup of G.

Proof:

1. To show that there must exist Sylow p-subgroups of $G; H, K \in V(\Gamma(G))$ which are conjugate in G and are adjacent to each other on the subgroup graph of G, then it suffices if we can show $H, K \in V(\Gamma(G))$ to be conjugate and subsequently establish an edge between H and K. From Theorem 1.21, it is established that the group G has some Sylow p-subgroups. So, let H be a Sylow p-subgroup of G, and let S be the set of all distinct conjugates of H. Suppose k is the order S, we need to establish that p cannot divide $k = |S|$. Since each of the $K \in S$ is a conjugate to H, it implies every element of S is in the orbit of H. So using the formula for orbit size $|S| = |orbit\ of\ H| = (G: N_G(H))$ (where $N_G(H)$) is the normalizer of H). However, Lagrange's theorem established that $|G| = (G: N\_G(H))$ and clearly, H is a subgroup of $N_G(H)$ and it contains p^{α} as a factor and a maximum power p can assume. Thus, ($|G|$ $divides$ $|N_G(H)|$ and $|S|$ contains no factor of p and so p does not divide $|S|$.
2. Suppose H is any p-subgroup of G, it will suffice if we can show $H \leq K\_i, i = 1, \ldots, p$. Let H act on $K = \{K_i \ldots K_p\}$, by conjugation. Clearly, the the orbits of this action will partition K. Suppose the distinct orbits are the orbits of $\{K_{1i} \ldots K_{1p}\}$ then the orbit of $|K| = |orbit\ K_{1i}| + \cdots + |orbit\ K_{1p}|$. To compute the orbit for

Volume 3, Issue 2, pages 225–240
p-ISSN 2655-8564, e-ISSN 2685-9432

any $K_{1i} \in K$, $|orbit\ of\ K_{1i}| = (H: H \cap N_G(K_i)$, since $H \cap N_G(K_i)$ is the stabilizer of K_i under the action of H. Then the size of each orbit has to divide $|H|$, which is a power of p. Though p doesn't divide $|H|$ so there is no p dividing all the terms $|orbit\ of\ P_{1i}|, \ldots, |orbit\ of\ P_{1i}|$ and else p would divide their sum and also K. Assume $1 = |orbit\ of\ K_{1i}| = (H: H \cap N_G(K_i)$ which means $(H = H \cap N_G(K_i)$ and since H is a $p-$subgroup $H \cap N_G(K_i) = H \cap K_i$. This implies $H = H \cap K_i$ so every element of H is also in K_i then $H \leq K$, therefore, the $p-$subgroup H is a subgroup of the arbitrary Sylow $p-$subgroup of G. So, H and K are adjacent of the subgroup graph $\Gamma(G)$ of G.

Theorem 3.12. Let G and G' be two finite groups and $\phi: G \to G'$ be a group homomorphism. Suppose there is an N, a normal subgroup of G and an N', a normal subgroup of G' such that N is adjacent to G on $\Gamma(G)$ the subgroup graph of G and N' is adjacent to G' on $\Gamma(G')$ the subgroup graph of G'. Then

1. $\phi(N)$ is adjacent to $\phi(G)$ on $\Gamma(\phi(G))$ the subgroup graph of $\phi(G)$.
2. $\phi^{-1}(N)$ is adjacent to G on $\Gamma(G)$ the subgroup graph of G.

Proof: Suppose G and G' are two finite groups and $\phi: G \to G'$ is a group homomorphism, if there is an N , a normal subgroup of G and an N', a normal subgroup of G' such that N is adjacent to G on $\Gamma(G)$ and N' is adjacent to G' on $\Gamma(G')$ then to show that $\phi(N)$ is also adjacent to $\phi(G)$ on $\Gamma(\phi(G))$ and $\phi^{-1}(N)$ is adjacent to G on $\Gamma(G)$; it will suffice if we can show $\phi(N)$ to be a normal subgroup of $\phi(G)$ and $\phi^{-1}(N)$ to be a normal subgroup of G respectively.

1. Let $\phi(g) \in \phi(G)$, since ϕ is a group homomorphism and N is normal in G. $\phi(g)\phi(N)\phi(g)^{-1} = \phi(gNg^{-1}) = \phi(N)$. Thus, $\phi(N)$ is normal in $\phi(G)$.
2. Let a be an arbitrary element of G, then the set $a\phi^{-1}(N')a^{-1}$ satisfies that $\phi(a\phi^{-1}(N')a^{-1}) = \phi(a)\phi(\phi^{-1}(N')\phi(a^{-1}) \subseteq \phi(a)N'\phi(a)^{-1} \subseteq N'$ since N' is normal in G'. Thus, $a\phi^{-1}(N')a \subseteq \phi^{-1}(N')$ for every $a \in G$. This shows that $\phi^{-1}(N')$ is a normal subgroup of G.

Volume 3, Issue 2, pages 225–240
p-ISSN 2655-8564, e-ISSN 2685-9432

Corollary 3.13. [27],[28] The alternating group A_n is a subgroup of the symmetric group S_n.

Theorem 3.14. Let $\Gamma(S_n)$, $\Gamma(D_n)$ and $\Gamma(A_n)$ be the subgroups graphs of symmetric groups, S_n, dihedral groups D_n and the alternating groups A_n, $n \geq 3$. Suppose K and M are vertices on $\Gamma(D_n)$ and $\Gamma(A_n)$ respectively, then both K and M are also vertices on $\Gamma(S_n)$ and are adjacent to S_n if and only if K is adjacent to D_n on $\Gamma(D_n)$ and M is adjacent to A_n on $\Gamma(A_n)$.

Proof: Let $\Gamma(S_n)$, $\Gamma(D_n)$ and $\Gamma(A_n)$ be the subgroups graphs of symmetric groups, S_n, dihedral groups D_n and the alternating groups A_n, $n \geq 3$. To show that K and M which are vertices on $\Gamma(D_n)$ and $\Gamma(A_n)$ respectively are also vertices on $\Gamma(S_n)$ and are adjacent to S_n if and only if K is adjacent to D_n on $\Gamma(D_n)$ and M is adjacent to A_n on $\Gamma(A_n)$, then it suffices, if we can show both K and M to be subgroups of S_n.

Assume that K is a subgroup of D_n and M is a subgroup of A_n. Then observe the structure of the group of symmetries of a regular $n-$gon in a plane (dihedral group (D_n)), it is isomorphic to a subgroup of S_n then it is a proper subgroup of S_n. Also, by Corollary 3.13, A_n is a subgroup of S_n. Moreover, since $K \leq D_n$and $M \leq A_n$ by implication, they are also subgroups of S_n and hence are vertices on $\Gamma(S_n)$.

Conversely, assume that K is adjacent to D_n on $\Gamma(D_n)$ and M is adjacent to A_n on $\Gamma(A_n)$, then by Definition 3.1, $K \leq D_n$ and $M \leq A_n$. But both D_n and A_n are subgroups of S_n, also, by implication, they are adjacent to S_n.

Theorem 3.15. [29] If $n \geq 3$, then the number of subgroups of the dihederal group D_n is $\tau\,(n) + \sigma(n)$. Where $\tau\,(n)$ is the number of divisors of n and $\sigma(n)$ is the sum of divisors of n.

Remark 3.16. Let D_n be a dihedral group of order $n \geq 3$, then the number of vertices on the subgroups graphs $\Gamma(D_n)$ of the dihederal group D_n is $\tau(n) + \sigma(n)$, where $\tau(n)$ is the number of divisors of n and $\sigma(n)$ is the sum of divisors of n.

Volume 3, Issue 2, pages 225–240
p-ISSN 2655-8564, e-ISSN 2685-9432

Theorem 3.17. Let C be a commutator subgroup of a finite group G of order n, suppose there exist a normal subgroup N of G such that G/N is Abelian, then C and N are adjacent on the subgroup graphs of G.

Proof: Let G be a finite group of order n and C the commutator subgroup of G. If there exist a normal subgroup N of G such that G/N is Abelian, then to show that C and N are adjacent on $\Gamma(G)$ (the subgroup graph of G), we must show that either $C \leq N$ or $N \leq C$. Note that N is normal in G and G/N is Abelian, then for $x, y \in G$, we have $(xN)(yN) = (yN)(xN)$ and using the definition of Coset multiplication $xyN = yxN$. Which implies $xy(yx)^{-1} \in N$, where $xy(yx)^{-1} = xyx^{-1}y^{-1}$. Similarly, $xyx^{-1}y^{-1} \in N$ and since x and y are arbitrary then any commutator in G is an element of N and since N is a subgroup of G then any finite product of commutators in G is an element of N and thus $C \leq N$.

Theorem 3.18. Let C be a commutator subgroup of a finite group G of order n and let H be a subgroup of G. If there exist an $x \in G$ such that $[x, H] \subseteq C_G(H)$, then $[x, H]$ and C are adjacent on the subgroup graphs of G.

Proof: By Lemma 1.15(2) and using the method of [25], the map sending $h \in H$ to $[x, H^{-1}]$ is a homomorphism. Thus, the image map of H is the subgroup $[x, H]$.

Theorem 3.19. (Schur Zassenhaus) [16] Let G be a finite group and write $|G| = ab$ where $(a, b) = 1$. If G has a normal subgroup of order a then it has a subgroup of order b.

Remark 3.20. Let G be a finite group and write $|G| = ab$ where $(a, b) = 1$. Then the vertex set $V(\Gamma(G))$ of the subgroup graph of G contains at least two vertices $H, K \leq G$ which orders are a and b respectively.

International Journal of Applied Sciences and Smart Technologies
Volume 3, Issue 2, pages 225–240
p-ISSN 2655-8564, e-ISSN 2685-9432

Theorem 3.21. Let G be a finite nilpotent group, such that G' is an abelian p-group with the minimal number of elements needed to generate G'; $d(G') \leq 3$, then G' is a vertex on the subgroup graph $\Gamma(G)$ and it is adjacent to G.

Proof: Suppose G is a finite nilpotent group, such that G' is an abelian p-group with $d(G') \leq 3$, then to show that G' is a vertex adjacent to G on the subgroup graph $\Gamma(G)$ of G, it will suffice if we can show G' to be equal to C, the commutator subgroup of G. Now, since G is finite, we assume an arbitrary $P \in Syl_P(G)$ such that $G' \leq P$ and obviously, P is normal in G and by Theorem 3.19 (Schur Zassenhaus theorem) and the methods in [25], $G = PQ$ where $P \cap Q = \{e\}$. Also, by Lemma 1.16(3), and Lemma 1.17, we set $R = [T, P]$ and if $G' = R$ there exist $t_1, t_2 \in T$ such that $R = [t_1, R][t_2, R]$ and $G' = \{[t_1 a, t_2 b] \mid a, b \in R\} = C$. Thus, we can assume $d(R) \leq 2$, and they also exists $t \in T$ with $R = [t, P]$. Since G/R is nilpotent, by Theorem 1.18 and Lemma 1.19,

$$G' = R(C) = R\left(\bigcup_{s \in P} \Gamma_s(P)\right) = \bigcup_{s \in P} \Gamma_{ts}(P) = C$$

Lemma 3.22. Let G and H be two non nilpotent finite groups, such that there is an isomorphism ϕ of G' and H', if the commutator subgroup C of G is adjacent to G on the subgroups graph $\Gamma(G)$ of G, then the commutator subgroup C of H is also adjacent to H on the subgroups graph $\Gamma(H)$ of H.

Proof: Suppose G and H are non nilpotent finite groups such that there is an isomorphic map between G' and H', then we can safely say there is also isomorphic map between the commutator subgroups of G' and H', which shows the isomorphic relationship between G and H. Also, since the commutator subgroup of G is adjacent to G on $\Gamma(G)$ then the commutator subgroup of H is also adjacent to H on $\Gamma(H)$.

Example 3.23. Let Q_8 be a quaternion group generated by the following matrices

$$1 = \begin{pmatrix} 1 & 0 \\ 0 & 1 \end{pmatrix}, i = \begin{pmatrix} i & 0 \\ 0 & -i \end{pmatrix}, j = \begin{pmatrix} 0 & 1 \\ -1 & 0 \end{pmatrix}, k = \begin{pmatrix} 0 & i \\ i & 0 \end{pmatrix}$$

Volume 3, Issue 2, pages 225–240

p-ISSN 2655-8564, e-ISSN 2685-9432

[30], using the matrix multiplication obtained $Q_8 = \{\pm 1, \pm i, \pm j, \pm k\}$, observe that the subgroups of Q_8 consists of Q_8 itself and of the cyclic subgroups $\langle 1\rangle = \{e\}, \langle -1\rangle = \{1, -1\}, \langle i\rangle = \{1, i, -1, -i\}, \langle j\rangle = \{1, j, -1, -j\}, \langle k\rangle = \{1, k, -1, -k\}$ and the following is the subgroups graph of Q_8. See Figure 2.

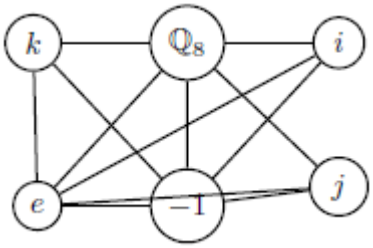

Figure 2. Subgroups graph of Q8.

4 Conclusion

This study has highlighted some algebraic properties and combinatorial structures of Subgroups graph $\Gamma(G)$ of finite groups. The connections between the Subgroups graphs of finite groups upto homomorphism and isomorphism were also studied and further looked at the relationships between the subgroups graphs of symmetric groups, S_n, dihedral groups D_n and the alternating groups An, when $n \geq 3$.

Acknowledgements

The authors wish to thank the reviewers for their helpful comments and recommendations on this article.

References

[1] I. Kleiner, "History of Group theory," *History of Abstract Algebra*, Birkhauser Boston, 17–39, 2007.

[2] J. Zhang, F. Xiong and J. Kang, "The application of Group theory in communication operation pipeline system," *Mathematical problems in Engineering*, 2018.

Volume 3, Issue 2, pages 225–240

p-ISSN 2655-8564, e-ISSN 2685-9432

[3] J. Laane and E. J. Ocola, "Application of symmetry and group theory for the investigation of molecular vibrations," *Acta Applicandae Mathematicae*, **118**(1), 3–24, 2012.

[4] E. A. Rietman, R. L. Karp and J. A. Tuszynski, "Review and application of group theory to molecular system biology," *Theoretical Biology and medical modeling*, **8**(21), 2011.

[5] H. Osborn, "Symmetry relationships between Crystal Structures: application of crystallographic group theory in crystal chem- istry," *Contemporary Physics*, **6**(1), 97–98, 2015.

[6] A. Cayley, "Desiderata and suggestions: The theory of groups: graphical representation," *American Journal of Mathematics*, **1** (2), 403–405, 1878.

[7] W. B. Vasantha Kandasamy and F. Samarandache, "Groups as Graphs," *Editura cuart and authors*, 2009.

[8] P. H. Zieschang, "Cayley graph of finite groups," *Journal of Algebra*, **118**, 447–454, 1988.

[9] P. J. Cameron and S. Ghosh, "The power graph of finite groups," *Discrete Mathematics*, **311**, 1220–1222, 2011.

[10] S. U. Rehman, A. Q. Baig, M. Imran and Z. U. Khan, "Order divisor graphs of finite groups," *An. St. Ovidus Constanta*, **26**(3), 29–40, 2018.

[11] J. S. Williams, "Prime graph components of finite groups," *Journal of Algebra*, **69**(2), 487–513, 1981.

[12] X. L. Ma, H. Q. Wei and G. Zhong, "The cyclic graph of a finite groups," *Algebra*, 2013.

[13] A. Erfanian and B. Tolue, "Conjugate graphs of finite groups," *Discrete Mathematics, Algorithm and Applications*, **4**(2), 2012.

[14] B. Akbari, "Hall graph of a finite group," *Note Mat*., **39**(2), 25–37, 2019.

[15] A. Lucchini, "The independence graph of a finite group," *Monatsheft Fur Mathematik*, **193**, 845–856, 2020.

[16] D. Gorenstein, "Finite Groups," *Harper & Row*, New York, 1968.

[17] D. J. S. Robinson, "A course in the theory of Groups," *2nd edition, Springer-Verlag, New York*, 1996.

Volume 3, Issue 2, pages 225–240

p-ISSN 2655-8564, e-ISSN 2685-9432

[18] S. D. David and M. F. Richard, "Abstract algebra, 3rd Edition," *John Wiley and Son Inc.*, 2004.

[19] C. Godsil and G. Boyle, "Algebraic graph theory, 5th edition," *Springer, Boston New York*, 2001.

[20] A. Gupta, "Discrete mathematics," *S.K. Kataria & Sons*, 258–310, 2008.

[21] P. J. Cameron, Notes on finite group theory, www.maths.qmul.ac.uk, 2013.

[22] H. E. Rose, "A Course on Finite Groups," *Springer Science & Business Media*, 2009.

[23] A. E. Clement, S. Majewicz and M. Zyman, "Introduction to Nilpotent Groups," *The Theory of Nilpotent Group Birkhauser, Cham*, (2017).

[24] W. A. Trybulec, "Commutator and Center of a Group, Formalized Mathematics," *Universite Catholique de Louvain*, **2**(4), 1991.

[25] R. M. Guralnick, Commutators and Commutator Subgroups, *Advances in Mathematics*, **45**, 319–330, 1982.

[26] people.math.binghamton.edu (Accessed on 2nd October, 2020).

[27] www.math.columbia.edu (Accessed 6th November, 2020).

[28] K. Conrad Simplicity of An; *kconrad.math.uconn.edu* (Accessed on 7th November, 2020).

[29] S. R. Cavior, "The Subgroups of the Dihedral groups," *Mathematics Magazine*, **48**, 107, 1975.

[30] M. Tarnauceanu, "A characterization of the quaternion group," *An. St. Univ. Ovidius Constanta*, **21**(1), 209–214, 2013.

International Journal of Applied Sciences and Smart Technologies

Volume 3, Issue 2, pages 225–240

p-ISSN 2655-8564, e-ISSN 2685-9432

This page intentionally left blank

International Journal of Applied Sciences and Smart Technologies

Volume 3, Issue 2, pages 241–256

p-ISSN 2655-8564, e-ISSN 2685-9432

Independence Test and Plots in Correspondence Analysis to Explore Tracer Study Data

Endang Sri Kresnawati[1], Irmeilyana[1,*], Ali Amran[1],

Danny Matthew Saputra[2]

[1]*Department of Mathematics, Faculty of Mathematics and Natural Science, University of Sriwijaya, Indralaya, South-Sumatra, Indonesia*

[2]*Department of Informatics Engineering, Faculty of Computer Science, University of Sriwijaya, South-Sumatra, Indonesia*

[*]*Corresponding Author: irmeilyana@unsri.ac.id*

(Received 17-11-2021; Revised 30-12-2021; Accepted 31-12-2021)

Abstract

The results of the exploration of tracer study data can be used as information about the career of graduates and the relevance of work to the field of study as well as the competencies obtained before graduation. The question items discussed were a description of the time and process of looking for a job, the length of time to get the first job, the relationship between length of study, gender, field of work, total income, alumni's perception of the closeness of the field of study to work, the suitability of the level of education on the job, and average level of competence. The aim of this study was to analyze the relationship between these variables in the 2020 tracer study data from graduates of all faculties at Sriwijaya University. Respondents studied were 2,669 people. The method used is descriptive statistics, biplot analysis, independence test and plots by simple correspondence analysis. Respondents' perceptions of the suitability of the level of education in employment are related to gender and also with respondents' perceptions of the closeness of the field of study to the field of work. Meanwhile,

Volume 3, Issue 2, pages 241–256
p-ISSN 2655-8564, e-ISSN 2685-9432

respondents' perceptions of the closeness of the field of study with work are related to the field of work. The average length of study, the average number of job applications, the number of companies or agencies that responded to applications, and invited interviews for female respondents were lower than male respondents.

Keywords: Alumni perception, to explore, field of work, field of study, tracer study data.

1 Introduction

Data from alumni resulting from tracer studies is useful for obtaining information that can be used for higher education development, to evaluate the relevance of hard skills, soft skills, and internal / external factors obtained by alumni when they become students and work [1]. The Career Development Center (CDC) is a character and career development center in Unsri, where the CDC was formed in 2013 to respond to the low achievement of tracking points for graduates who are blocked by AIPT forms. CDC has tracked alumni from 10 faculties at Sriwijaya University starting from the alumni in 2013 to 2020. The tracer study report can be seen at [2], [3], [4], [5], [6], [7].

CDC of Sriwijaya University (Unsri) conducted a tracer study to study alumni early careers, as well as obtaining alumni feedback for improving the learning system in Unsri and evaluating / developing a curriculum that meets stakeholder expectations and market needs. Apart from tracer studies, CDC also provides other services, including: Unsri Career Expo, soft skills training, online assessment, career training, and career counseling [6]. Reference to learn various things related to career center and its services, also to study the solution to the problems of graduates and employment faced such as problems of alignment of the world of education with the world of work can be seen in [8], [9], [10].

Interpretation of the questionnaire results in the form of descriptive statistics from the data, both in the form of numbers (percentages), graphics, and the interpretation is very helpful in providing information for further analysis. The results of the analysis are very useful for the successful implementation of the tracer study. Tracer study data can

Volume 3, Issue 2, pages 241–256
p-ISSN 2655-8564, e-ISSN 2685-9432

be big data which consists of many objects and many variables, so to extract as much information as possible from the data, it is necessary to use other analysis techniques, including multivariate analysis.

In [11], it was obtained a lot of information regarding the comparison between FKIP respondents (alumni) and FMIPA respondents (alumni) in each of the 4 departments/study programs, based on data from the 2013 to 2016 tracer study. Information obtained includes: the relationship between GPA, duration thesis, and length of study; profiles of alumni who received scholarships and those who did not during college were reviewed from the GPA, length of thesis, and length of study; field of work of each alumni; the relationship between the GPA and the length of time getting the first job and the relationship between the GPA and the suitability of the level of education in the job; the relationship between the closeness of the field of study and the suitability of the level of education with the job; alumni perceptions about the contribution of Higher Education (Unsri) to all competency items owned by alumni; the relationship between competency groups and GPA, level of education, and length of time to get a job.

Information on the relationship between the factors studied in [12] obtained after studying the descriptive statistics of the data obtained from the results of the tracer study. The description of the alumni of each faculty and the comparison of alumni between faculties in Unsri will provide a lot of input not only regarding the competencies of alumni needed by the world of work but also regarding the steps of all academicians to work together to prepare higher quality graduates in accordance with the vision and mission of the university which of course must be supported by vision and mission of the faculty and departments / study programs.

In [13], it was analyzed the relationship between GPA and the suitability of education level with the field of work of Sriwijaya University alumni from 5 faculties, namely FISIP, FMIPA, FE, FH, and FT based on 2019 tracer study data. The perception of the majority of respondents to the level of education and also the closeness of the field of study required in their work is not related to the GPA. Only in FT respondents, there is a relationship between GPA and the closeness of the field of study on the job. Based on [14], in 5 faculties data, both in the form of graduates and respondent data,

Volume 3, Issue 2, pages 241–256
p-ISSN 2655-8564, e-ISSN 2685-9432

women's GPA is higher than men. On the other hand, the length of study and income of women is lower than that of men. The average GPA of FH alumni is the highest compared to other faculties. The average length of study of FISIP alumni is the highest compared to other faculties. The average income and total income of FT respondents were the highest compared to respondents in other faculties.

Meanwhile in [15], based on the results of the analysis in the boxplot form, it was found that GPA did not affect the income and field of work of the 2010 ITB alumni. In [16], it was analyzed the comparison of 4 majors (study programs) at the Faculty of Mathematics and Natural Sciences (FMIPA) and the Faculty of Teacher Training and Education (FKIP) in terms of the relationship between gender variables, the average alumni perception of the competencies possessed and needed in the field of work, length of time study, length of time to get a first job, income, field of work, alumni's perception of the suitability of education level with the field of work, and respondents' perceptions of the closeness of the field of study to the field of work. This research is based on tracer study data from 2020 on each FKIP and FMIPA respondents, as many as 216 and 239 respondents.

In [17], it was examined the relationship between alumni perceptions of competencies mastered with competencies needed by the world of work for Unsri graduates in 2018. There are 8 out of 29 competencies that should be further improved. In addition, the types of competencies that are further enhanced between female graduates and male graduates are different.

This study aims to analyze the relationship between several variables from the question items of the tracer study questionnaire simultaneously and explore further the data using the objects of all 2020 tracer study respondents from 10 faculties at Unsri. Quantitative variable data were analyzed descriptively and exploratory using biplot analysis. Variable data of qualitative type, nominal and ordinal scale were analyzed using independence test and plots in correspondence analysis. Independence test used chi squares (□2) test. The output of correspondence analysis include symmetric and asymmetric plot. Because this study uses data from all respondents from all faculties, the results of the analysis can describe in general the characteristics of Unsri graduates

Volume 3, Issue 2, pages 241–256
p-ISSN 2655-8564, e-ISSN 2685-9432

in 2018 in their careers and the relevance between the competencies obtained from college and their work.

2 Research Methodology

This research is a case study, using secondary data from questionnaires in the 2020 tracer study conducted by CDC Unsri. Respondents in the 2020 tracer study are alumni who graduated in 2018. The data used includes the results of tracer studies in 10 faculties at Unsri.

This study only uses answers to several questionnaire questions used for descriptive analysis and exploratory analysis, namely gender, length of study, length of time looking for a job, number of job applications, number of responses to job applications, number of interview calls, length of time getting the first job, field of work, main income, total income, respondent's perception of the most appropriate level of education for alumni's work, closeness of field of study to alumni's job, average respondent's perception of competency level. Alumni (graduates) who filled out the tracer study questionnaire were declared as respondents. The analytical technique used is descriptive statistics, biplot analysis (including correlation between variables), chi square test (χ^2), and simple correspondence analysis.

The steps taken in the combined data of all faculties are:

1. Select the required questionnaire questions as variables.
2. Compile a data matrix from the answers to the questionnaire questions in Step 1 with the objects being all respondents from 10 faculties. The data matrix variables include: length of time looking for a job, both before graduation and after graduation (f3), length of time getting the first job (f5), number of job applications (f6), number of companies responding (f7), number of job interview calls (f7a), field of work (f11), income (f13), alumni's perception of the closeness of the field of study to alumni's work (f14), the suitability of the most appropriate level of education for alumni's work (f15), and the average alumni perception of the level of competencies that are mastered and needed in the field of work (f17).

Volume 3, Issue 2, pages 241–256
p-ISSN 2655-8564, e-ISSN 2685-9432

3. Develop a new data matrix by removing data on respondents who did not fill in questions about income.
4. Add gender and length of study variables.
5. Do descriptive statistics.
6. Perform a biplot analysis as a graphical representation of a data matrix whose variables are quantitative.
7. Perform the chi square test
    a. Arrange column and row categories in the contingency table.
    b. Calculate the frequency of cross-relation between column and row categories.
    c. Perform the chi square test on the contingency table.
    d. If the cell frequency from the contingency table is less than 5, then the categories can be merged, or if not, skip to Step 8.
8. Perform a correspondence analysis on the relationship between two interrelated variables based on the results of Step 7.
9. Interpretation of results.

Data processing is done with the help of Minitab 19 software.

3 Results and Discussion

The tracer study data for 2020 came from 3,850 respondents, consisting of 2018 graduates in 10 faculties at Unsri. The data is compiled in the form of a new data matrix, which consists of 2,669 respondents with variables as in Step 2. This new data matrix is formed with the assumption that respondents did not fill in their income (either because they have not found a job, are not working, or are graduates who are continuing their studies) not included in the data matrix. So, there are only 2,669 respondents who are all working. Furthermore, the length of study and gender variables were added to the data matrix.

Table 1 displays descriptive statistics from the answers to several questionnaire questions. The majority of respondents looked for work 1.63 months after graduation and got their first job 5.94 months after graduation. There are only 46 respondents who are looking for work, but did not fill in the question about the length of time they got their first job.

Volume 3, Issue 2, pages 241–256

p-ISSN 2655-8564, e-ISSN 2685-9432

Table 1. Descriptive statistics of variables regarding the process of respondents looking for and getting a job

Variable	*n*[e]	%age	Mean	StDev	Median
f302[a]	561	21.4	6.992	13.671	2
f303[b]	2061	78.6	1.625	2.8753	1
Bgrad[c]	290	11.3	11.14	17.52	3
Agrad[d]	2286	88.7	5.936	4.887	5

Note: [a]length of time to find a job before graduating (in months)
[b]length of time looking for a job after graduation (in months)
[c]length of time to get first job before graduating (in months)
[d]length of time to get first job after graduation (in months)
[e]number of respondents

Comparison of the length of study, the status of the job search process, income, and the average perception of alumni on the level of competence can be seen in Table 2. Male respondents had the number of job applications (f6), the number of companies that responded (f7), the number of interviews (f7a), which is more than female respondents. From the number of job applications that are made, only about a third are responded to by companies (or users). From the number of users (companies/agencies) who responded, only about half called respondents for job interviews.

Table 2. Descriptive statistics of study duration, status of the job search process, income, and perception of competence

Variable	Gender	*n*	Mean	StDev	Median
Length of study (in years)		2669	4.58	1.08	4
	0	1510	4.42	0.95	4
	1	1159	4.79	1.19	5
f6		2601	24.19	62.34	10
	0	1484	19.68	37.94	10
	1	1117	30.20	84.12	10
f7		2596	7.86	11.92	5
	0	1484	6.95	8.58	4
	1	1112	9.06	15.20	5
f7a		2586	4.67	6.00	3
	0	1480	4.20	5.00	3
	1	1106	5.30	7.09	3
Income		2669	4007294	4399354	3100000
	0	1510	3269989	3244314	3000000
	1	1159	4967890	5407720	4000000

Volume 3, Issue 2, pages 241–256

p-ISSN 2655-8564, e-ISSN 2685-9432

Total Income		2669	4546057	4781143	3700000
	0	1510	3703070	3514537	3000000
	1	1159	5644341	5868338	4500000
S-KK		2669	3.84	0.48	3.83
	0	1510	3.83	0.47	3.83
	1	1159	3.84	0.49	3.83
S-PT		2669	3.79	0.59	3.79
	0	1510	3.81	0.58	3.83
	1	1159	3.76	0.59	3.79

Based on Table 2, there are 1,510 (57%) female respondents and 1,159 (43%) male respondents. The length of study for male respondents (average 4.79 years) is higher than the length of study for female respondents (average 4.42 years). Male respondents also have higher average income and total income than female respondents. The average respondent's perception of the level of competency mastered (with notation S-KK) and the competencies required by the world of work (notation S-PT) are more likely to be the same. The correlation between the variables in Table 2 can be seen in Table 3 and the biplot graph in Figure 1.

Table 3. Correlation between length of study, status of job search process, income, and perception of competence

	Length of study (in years)	**f6**	**f7**	**f7a**	**Income**	**Total Income**	**S-KK**
f6	0.042						
f7	-0.016	**0.722**					
f7a	-0.024	0.383	**0.721**				
Income	0.007	0.058	0.080	0.088			
Total Income	0.007	0.051	0.077	0.089	**0.945**		
S-KK	-0.023	0.019	0.018	0.039	0.046	0.042	
S-PT	-0.023	-0.018	-0.024	-0.003	0.034	0.027	**0.773**

Based on Table 3, income is only correlated (very high) with total income. The number of job applications, the number of users who responded to the application, and the number of interview calls were highly correlated with each other. Likewise, a high correlation occurs between the average respondent's perception of the level of competence mastered with the competencies needed by the world of work. The same interpretation can be seen in Figure 1a.

International Journal of Applied Sciences and Smart Technologies

Volume 3, Issue 2, pages 241–256

p-ISSN 2655-8564, e-ISSN 2685-9432

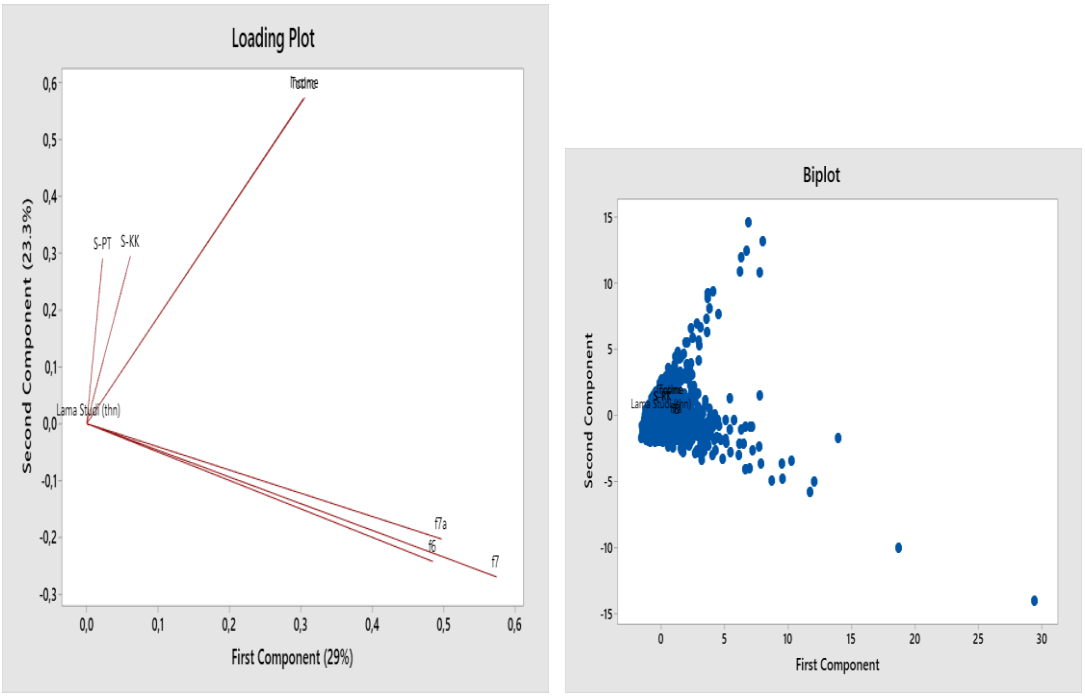

1a. Correlation between variables 1b. Biplot

Figure 1. Biplot of length of study, status of job search process, income, and perception of competence

Based on Figure 1a, the biplot can represent a data variation of 52.3%. The first component is dominant represented by the respondent's process status variable in looking for work (f6, f7, and f7a). While the second component is dominant represented by income and total income variables. Based on the distribution of respondents' positions tend to spread in the direction of the variable vectors. Only a small proportion of respondents have a high income, their number of job applications are responded and get the opportunity to be interviewed.

Furthermore, the relationship between several variables of the data matrix is explored using the independence test, i. e. by using chi squares test. If the test results state that there is a relationship between the two variables, the process is continued with a simple correspondence analysis. The cells in the contingency table represent the frequency of the number of respondents from the cross-relationship between the row variable category and the column variable category. Figure 2 is the partial output of the chi square test on the relationship between length of study and gender.

International Journal of Applied Sciences and Smart Technologies

Volume 3, Issue 2, pages 241–256

p-ISSN 2655-8564, e-ISSN 2685-9432

Chi-Square Test for Association: Length of study (in years); Gender

Rows: Length of study (in years) Columns: Gender

	0	1	All
2	41	22	63
3	33	34	67
4	931	522	1453
5	349	350	699
6	67	78	145
7	86	122	208
8	3	31	34
All	1510	1159	2669

Cell Contents
Count

Chi-Square Test

	Chi-Square	DF	P-Value
Pearson	106,684	6	0,000
Likelihood Ratio	110,179	6	0,000

Figure 2. The output of the chi squares test on the relationship between length of study and gender

Based on Figure 2, the majority of respondents graduated in 4 years and were female respondents (931 people or around 35%). The value of □2 count (106.684) > □2 table (0.05; 6) (12.592); namely the relationship between the length of study with gender. The same thing can be seen from the p-value < 0.05.

Chi-Square Test for Association: Level of education; Gender

Rows: Level of education Columns: Gender

	0	1	All
1	28	35	63
2	1475	1113	2588
4	7	11	18
All	1510	1159	2669

Cell Contents
Count

Chi-Square Test

	Chi-Square	DF	P-Value
Pearson	6,250	2	0,044
Likelihood Ratio	6,183	2	0,045

Figure 3. The output of the chi squares test on the relationship between respondents' perceptions of education level and gender

Based on Figure 3, the majority of female respondents have the perception that the level of education that is most suitable for their job is at “the same level” (there are

Volume 3, Issue 2, pages 241–256

p-ISSN 2655-8564, e-ISSN 2685-9432

1,475 people or 55%). The value of □2 count (6.25) > □2 table (0.05; 2) (5.99); namely the existence of a relationship between perceptions of the suitability of the level of education on the job with gender. The same thing can be seen from the p-value < 0.05. Furthermore, the same way is also carried out to analyze the close relationship between the categories on the two variables, so that the recapitulation is obtained as in Table 4.

Table 4. Recapitulation of chi square test on correspondence analysis results

No	Row Variable	Column Variable	Majority category (%)	χ^2_{count} Value	χ^2_{table} value	χ^2 Test results	Conclusion
1	Length of study	Gender	4 years for female respondents (35)	106.68	$\chi^2_{0,05;\ 6}$ (= 12.59)	Reject H_0	There is a relationship
2	f15[a]	Gender	The same level for female respondents (55)	6.25	$\chi^2_{0,05;\ 2}$ (= 5.99)	Reject H_0	There is a relationship
3	f14[b]	Gender	Very Close to female respondents (21.5)	2.484	$\chi^2_{0,05;\ 4}$ (= 9.49)	Accept H_0	No relationship
4	f14	f15	Very Close and Same Level (36)	39.809	$\chi^2_{0,05;\ 8}$ (= 1551)	Reject H_0	There is a relationship
5	f11[c]	f15	Same rate in private companies (54)	6.256	$\chi^2_{0,05;\ 8}$ (=15.51)	Accept H_0	No relationship *)
6	f14	f11	Very close to private companies (21) and government agencies (16)	212.95	$\chi^2_{0,05;\ 16}$ (=26.3)	Reject H_0	There is a relationship

Note: [a]The most appropriate level of education for the respondent's job
[b]Close relationship between the field of study and work
[c]Field of work
*) the test results of both categories of variables are invalid

Based on Table 4, only 2 forms of relationship from the chi squares test whose □2value < □2 table; namely the relationship between gender and the respondent's perception of the closeness of the field of study on the job, and also the relationship between the field of work and the respondent's perception of the suitability of the level of education on the job. Furthermore, the existence of a relationship between row variables and column variables whose categories are more than 2 can be described

Volume 3, Issue 2, pages 241–256

p-ISSN 2655-8564, e-ISSN 2685-9432

through the output of correspondence analysis. The output of the correspondence analysis includes the distance of chi squares and the total inertia of the two axes on the graph. The output plot of this simple correspondence analysis has a total inertia of 100% (Figure 4a) and 95.7% (Figure 4b), so it is very representative in presenting data diversity.

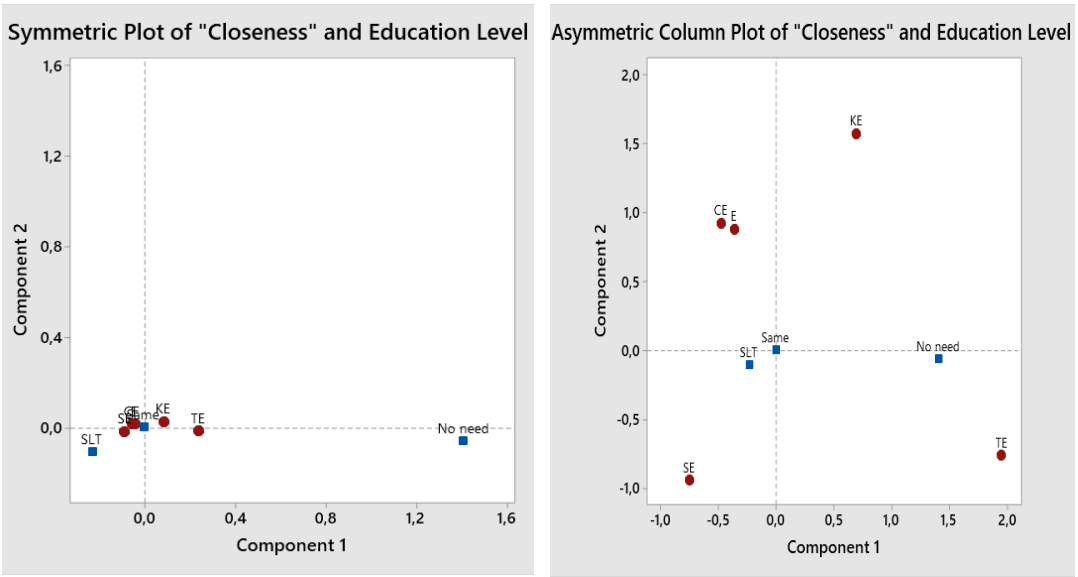

a. The Relationship of respondents' perceptions on closeness of fields of study and suitability of education level with employment

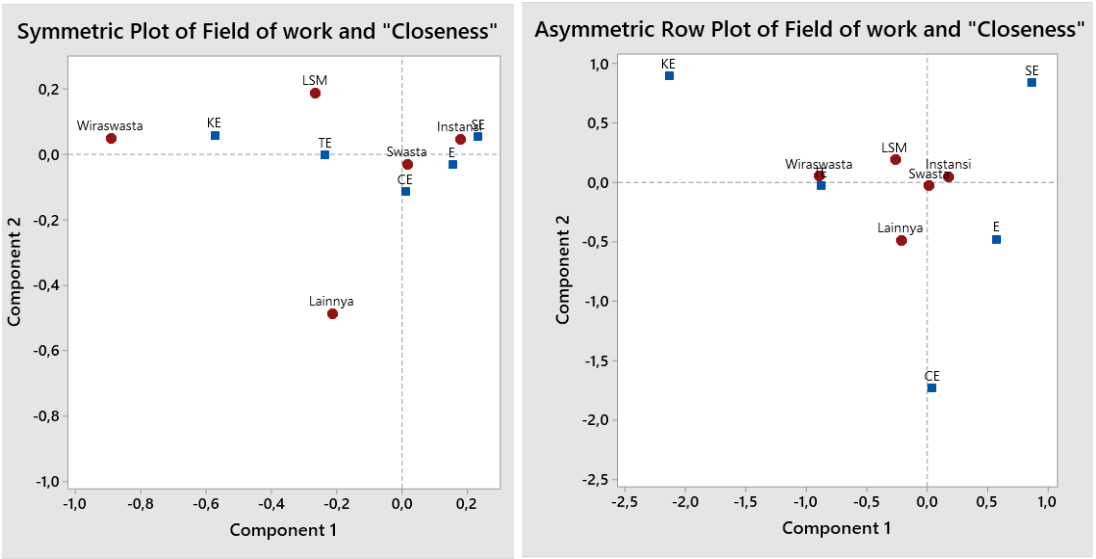

b. The relationship between the field of work and respondents' perceptions of the closeness between the field of study and work

Figure 4. Plot of the relationship between two variables of correspondence analysis results

Volume 3, Issue 2, pages 241–256
p-ISSN 2655-8564, e-ISSN 2685-9432

Based on Figure 4a, respondents who have the perception that their field of study is “not closely” related to their work, tend to have the perception that their work does “not need higher education”. Meanwhile, respondents who have the perception that their field of study is related "quite closely" to "very closely" with their work, tend to have the perception that their work is "the same" with their level of education.

Based on Figure 4b, respondents who work in government agencies (including BUMN) and the private sector have the perception that the field of study is “very closely” related to work. Meanwhile, respondents who work as entrepreneurs have the perception that the field of study is not closely related to work.

4 Conclusion

Based on the results and discussion, it is concluded that the majority of respondents are looking for and getting their first job after graduation. The number of job applications, the number of users who responded to the application, and the number of interview calls were highly correlated with each other. Likewise, a high correlation occurs between the average respondent's perception of the level of competence mastered with the competencies needed by the world of work. Male respondents have a higher length of study, average income, and total income than female respondents. The average respondent's perception of the level of competence mastered and the competencies needed by the world of work are more likely to be the same.

Based on the independence test, gender is related to the length of study and respondents' perceptions of the suitability of the level of education on the job. There is a relationship between respondents' perceptions of the closeness of the field of study and the suitability of the level of education with the field of work. The results of the correspondence analysis show that respondents who have the perception that the field of study is not closely related to their work, tend to have the perception that their work "does not need higher education", and work as entrepreneurs. Respondents who work in government agencies (including BUMN) and the private sector have the perception that the field of study is “very closely” related to work.

The study describes the general characteristics of all respondents from 10 faculties at Unsri based on 10 question items on the tracer study questionnaire. For further research, it is better to examine the comparison of these characteristics in each faculty at Unsri.

Acknowledgements

Authors wishing to acknowledge assistance or encouragement from our discussion group and also special thanks for the staff of CDC (Career Development Center) University of Sriwijaya that had provided tracer study data.

References

[1] Divisi Riset ITB Career Center. Tracer Study ITB Tahun 2017. ITB, Bandung, 2017.
[2] CDC Unsri. Tracer study Universitas Sriwijaya Tahun 2016 (Lulusan Tahun 2014). Universitas Sriwijaya, Indralaya, 2016.
[3] CDC Unsri. Tracer study Universitas Sriwijaya Tahun 2017 (Lulusan Tahun 2015) Universitas Sriwijaya, Indralaya, 2017.
[4] CDC Unsri. Tracer study Universitas Sriwijaya Tahun 2018 (Lulusan Tahun 2016) Universitas Sriwijaya, Indralaya, 2018.
[5] CDC Unsri. Tracer study Universitas Sriwijaya Tahun 2019 (Lulusan Tahun 2017) Universitas Sriwijaya, Indralaya, 2019.
[6] CDC Unsri. Tracer study Universitas Sriwijaya Tahun 2020 (Lulusan Tahun 2018) Universitas Sriwijaya, Indralaya, 2020.
[7] CDC Universitas Sriwijaya. http://cdc.unsri.ac.id
[8] Proceedings of the Indonesian Career Center Network (ICCN) 2019. Universitas Mulawarman, Samarinda, 2019.
[9] Proceedings of the Indonesian Career Center Network (ICCN) Summit 3. Surabaya, 2018.
[10] Proceedings of the Indonesian Career Center Network (ICCN) Summit 2. Bogor, 2017.

Volume 3, Issue 2, pages 241–256

p-ISSN 2655-8564, e-ISSN 2685-9432

[11] A. Amran, Irmeilyana, A. Desiani, and R. Zulfahmi, "Characteristics comparison on FMIPA and FKIP alumni of Sriwijaya University based on relationship between GPA, field of work, and length time to get first job," *International Conference 15th ICMSA, Bogor: IPB*, 2019.

[12] A. Amran, Irmeilyana, A. Desiani, R. P. Oktarian, "Relationship between GPA, length of study, and competency with the length of time to get a job at the alumni of the Faculty of Mathematics and Natural Sciences, University of Sriwijaya Proceedings of 3rd Forum in Research, Science, and Technology (FIRST)," *Part of Series: Advances in Social Science, Education and Humanities Research*, 20–28, 2020.

[13] A. Amran, Irmeilyana, Ngudiantoro. "Hubungan antara IPK dengan kesesuaian tingkat pendidikan dan bidang studi pada pekerjaan alumni," *Jurnal Penelitian Sains*, **23**(2), 67–77, 2021.

[14] A. Amran, Irmeilyana, and Ngudiantoro, "Relationship among Gender, GPA, Length of Study, and Alumni Income of Sriwijaya University Paper was presented," *The Virtual Conference of the 10th International Seminar on New Paradigm and Innovation of Natural Sciences and Its Application (ISNPINSA)*, 2020.

[15] I. I. Sari and A. D. Adrianto, "Pengaruh Nilai Indeks Prestasi (IP) terhadap Pekerjaan Alumni ITB (Studi Kasus Alumni ITB Angkatan 2010)," *Indonesia Career Center Network Summit 3*, 89–93, 2018.

[16] E. S. Kresnawati, Irmeilyana, A. Amran, D. M. Saputra, "Profil alumni FMIPA dan FKIP Universitas Sriwijaya ditinjau dari variabel dan persepsi pada pekerjaan," *Aksioma*, **12**(2), 213–224, 2021.

[17] A. Amran, Irmeilyana, E. S. Kresnawati, D. M. Saputra, "Eksplorasi Data Persepsi Alumni pada Tingkat Item-Item Kompetensi dari Hasil Tracer Study Unsri Tahun 2020," *Infomedia*, **6**(1), 1–8, 2021.

International Journal of Applied Sciences and Smart Technologies

Volume 3, Issue 2, pages 241–256

p-ISSN 2655-8564, e-ISSN 2685-9432

This page intentionally left blank

International Journal of Applied Sciences and Smart Technologies

Volume 3, Issue 2, pages 257–264

p-ISSN 2655-8564, e-ISSN 2685-9432

Writer Identification Based on Hand Writing using Artificial Neural Network

Rosalia Arum Kumalasanti[1,*]

[1]*Department of Informatics, Faculty of Science and Technology, Sanata Dharma University, Yogyakarta, Indonesia*
[*]*Corresponding Author: rosaliasanti@usd.ac.id*

(Received 26-11-2021; Revised 30-12-2021; Accepted 31-12-2021)

Abstract

Humans are social beings who depend on social interaction. Social interaction that is often used is communication. Communication is one of the bridges to connect social relations between humans. Communication can be delivered in two ways, namely verbal or nonverbal. Handwriting is an example of nonverbal communication using paper and writing utensils. Each individual's writing has its own uniqueness so that handwriting often becomes the character or characteristic of the author. The handwriting pattern usually becomes a character for the writer so that people who recognize the writing will easily guess the ownership of the related handwriting. However, handwriting is often used by irresponsible people in the form of handwriting falsification. The acts of writing falcification often occur in the workplace or even in the field of education. This is one of the driving factors for creating a reliable system in tracking someone's handwriting based on their ownership.

In this study, we will discuss the identification of a person's handwriting based on their ownership. The output of this research is in the form of ID from the author and accuracy in the form of percentage of system reliability in identifying. The results of this study are expected to have a good impact

Volume 3, Issue 2, pages 257–264
p-ISSN 2655-8564, e-ISSN 2685-9432

on all parties, in order to minimize plagiarism. Identification of handwriting to be built consists of two main processes, namely the training phase and the testing phase. At the training stage, the handwritten image is subjected to several processes, namely threshold, wavelet conversion, and then will be trained using the Backpropagation Artificial Neural Network. In the testing phase, the process is the same as in the training phase, but at the end of the process, a comparison will be made between the image data that has been stored during training with a comparison image.

Backpropagation ANN can work optimally if it is trained using input data that has determined the size, learning rate, parameters, and the number of nodes on the network. It is expected that the offered method can work optimally so that it produces an accurate percentage in order to minimize handwriting falcification.

Keywords: Handwriting, Artificial Neural Networks, backpropagation

1 Introduction

The use of communication in the digital era is growing and becomes an important need in various aspects of life. Communication is the essence of humans as social beings in interacting with each other. In general, communication is defined as the process of delivering and receiving messages between two or more people directly or indirectly. In short, it can be concluded that the purpose of communication is to create understanding between two or more parties. One example of how to communicate nonverbally is by writing. Handwriting is still often used for various purposes, such as writing documents or forms, writing letters, and also for signatures. Everyone's handwriting has different characteristics and patterns so that handwriting is considered a unique attribute that is owned by each person or also known as a biometric attribute. The uniqueness of handwriting allows people to be able to distinguish one writing from another according to the characteristics of the pattern.

Handwriting is often considered a trivial thing so many people think that the validity of handwriting is not too important. This causes an increasing number of plagiarism that

Volume 3, Issue 2, pages 257–264
p-ISSN 2655-8564, e-ISSN 2685-9432

occurs, especially in the work environment and even in the educational environment. Visually or with the naked eye, humans cannot directly distinguish and identify the owner of the handwriting. Even if humans know that there are differences in the handwriting, they have difficulty in identifying the owner of the handwriting. This is an example of a person's lack of concern for handwriting ownership.

This study aims to protect handwriting as a biometric attribute that is protected by ownership. The handwriting identification system will be built using Backpropagation ANN and supporting parameters. A reliable system is expected to be a solution in minimizing handwriting forgery and providing awareness to all people about the importance of handwritten characters. ANN works like the human brain in identifying an object by studying patterns and storing characteristics for comparison with other objects. The more characteristics that are stored for study, the smarter the ANN will be in identifying.

2 Research Methodology

Writing is one of the ways humans communicate with the aim of conveying information using written media. Although the digital era has developed, handwriting is still often used for formal and non-formal activities. Handwriting has become one of the biometric attributes that offers several methods that can be developed in research. Most handwriting identification uses ANN and several other supporting algorithms ANN is used to perform initial analysis and categorize handwritten input images [1]. Each individual's writing has its own characteristics that can make a difference.

2.1. Biometrics and Character of a Person. Biometrics is a science and innovation to describe information from the human body naturally [2]. Biometrics refers to individual differences based on physiological or social attributes. The biometric value itself can be an individual's physiological or social attributes of completeness. A person's handwriting has its own characteristics related to a person's character. Graphology is the science of analyzing handwriting and the characteristics of a person's personality through the extraction of features based on shape [3]. The identification of the four

Volume 3, Issue 2, pages 257–264
p-ISSN 2655-8564, e-ISSN 2685-9432

dominant forms of handwriting is divided into several attributes, as shown in table 1 below.

2.2. JST Backpropagation. Artificial Neural Networks (ANN) refers to the paradigm of information processing or computing systems inspired by biological neural networks in the human brain. The system is not biologically identical to the nervous system, but is designed to process information in the same way that the human brain processes information. The network consists of many neurons that are interconnected and work simultaneously to achieve certain goals. Just like the human brain, ANN learns from the object examples presented, so ANN can be configured for an application. The application in question is like data classification or character recognition through the learning process. Figure 1 shows the architecture of ANN

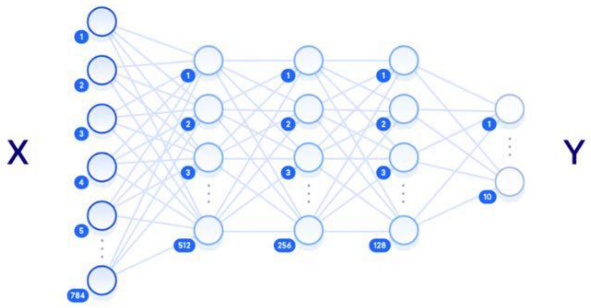

Figure 1. Artificial Neural Network Architecture [4]

Backpropagation is one of the ANN models that has the ability to get a balance between the network's ability to recognize the patterns used during training and the ability to provide the correct response to input patterns that are similar to the patterns used during training. Backporpagation algorithm is an algorithm that can find the minimum error or error in the weights by using gradient descent. The combination of weights that can minimize errors is considered capable of providing solutions to the learning process. Backpropagation has several neurons at each network layer.

Wavelet Transform Preprocessing in this study utilizes wavelet switching to represent the time and shape frequency signal. Wavelet transform is the basis of mathematical tools on several transfer layer functions and produces coefficients that

Volume 3, Issue 2, pages 257–264
p-ISSN 2655-8564, e-ISSN 2685-9432

represent signal characteristics [5]. Wavelets provide accuracy and analysis of signals of more than one resolution, which is known as multi-resolution capability. The advantage of this multi-resolution analysis is that features that may not be detected at one resolution can be detected using another resolution [6]. Discrete Wavelet Transform is the choice as an efficient way to be used on images in the form of discrete data. Wavelet has a decomposition level that is useful for obtaining optimal information on an image. Figure 2 below is a level 2 decomposition image.

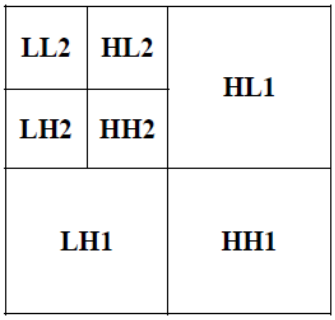

Figure 2. Decomposition level 2 [7]

3 Results and Discussion

Identification of handwritten images consists of two phases, namely training and testing. A number of samples in the form of handwritten images are used as input data. The greater the amount of input data, the better for ANN in studying patterns, but it is also necessary to consider the amount of time needed for ANN to study it. This identification aims to build an effective and efficient system for users to obtain the identity of the author. Image samples with a certain size also need to be uniform so that the system can easily get the characters in each image with optimal size and results. Figure 3 below is a handwriting identification flow using Backpropagation ANN.

International Journal of Applied Sciences and Smart Technologies
Volume 3, Issue 2, pages 257–264
p-ISSN 2655-8564, e-ISSN 2685-9432

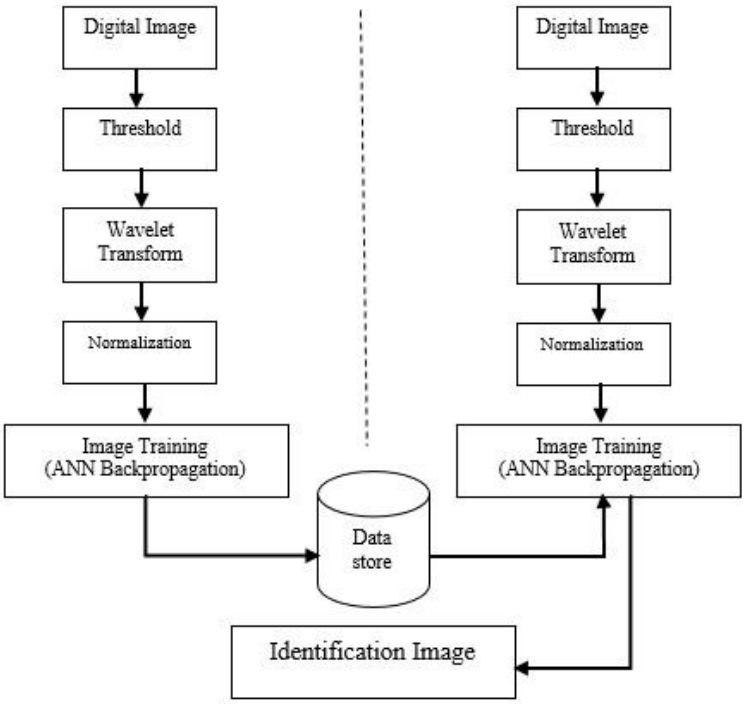

Figure 3. Handwriting Identification Flowchart

The handwritten image that will be sampled must first be converted into a digital image with the help of a scanner so that a digital image is obtained that is ready to be processed. Preprocessing is the initial step that will be given to the image, including the threshold and then it will be subjected to a wavelet transform to get important information in the image. After that the image will be normalized before entering the training phase. The image training phase is carried out on each ID / author in order to get the character and pattern of the handwritten image. The results of the signature character in the form of weights generated by Backpropagation ANN are then stored in the data store to then be compared with the test image. The test image can be taken from the same author with different raw images, so the test image will also go through the same preprocessing. The system is considered successful if the system can provide appropriate results. Figure 4 below represents the training phase on each ID/author.

International Journal of Applied Sciences and Smart Technologies
Volume 3, Issue 2, pages 257–264
p-ISSN 2655-8564, e-ISSN 2685-9432

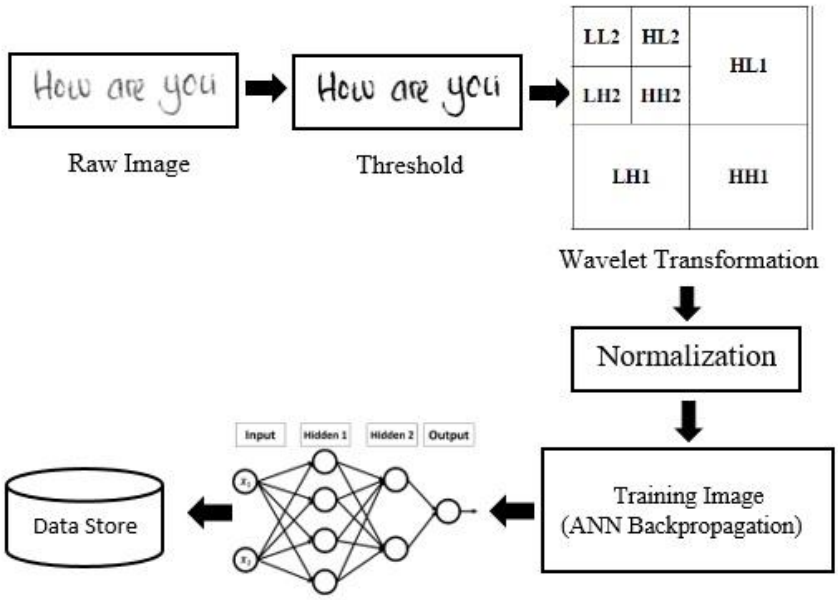

Figure 4. Training Phase

The system is considered reliable and successful if it can learn the character of each handwriting pattern so as to be able to distinguish the author's handwritten characters from one another. The indicator of the success of the system will be seen from the percentage of identification ability in all the IDs studied. Of course, here it is possible for errors to occur, so handwriting identification needs to be simulated using several parameters to get the optimal percentage. The consistency of a person's handwriting is also one of the influential factors so that the identification of this handwriting can also be added to several attributes to get more optimal results.

4 Conclusion

This study presents a method to identify handwriting using a Backpropagation Neural Network. ANN can be used in high complexity and is able to provide a progressive approach that is verified by various error rates. Utilization of the Backpropagation algorithm can minimize errors because there is a reverse/backward checking phase to correct errors. It is hoped that the design of this handwriting identification system can help minimize plagiarism among the public in all aspects. As

for things that can be added from this research in the form of real-time identification that can provide direct results so that it is more effective and efficient.

References

[1] M. Sutajha, M. Sandeep, C. Aiswarya and B. Mounika, "Hand Writing Recognition System Based on Neural Network," *International Journal on Innovative Technology and Exploring Engineering (IJITEE)*, **9** (1), 4977–4980, 2019.

[2] R. Ahuja and L. Duhan, "Optimized Multi Model Biometric Based Human Authentication Using Deep Neural Network," *International Journal of Recent Technology and Engineering (IJRTE)*, **8** (3), 280–290, 2019.

[3] P. B. Nair, A. M. Johnson, A. M. Alex and A. Sebastian, "Android App for Handwriting Analysis Using Deep Learning," *Journal of Communication Engineering and Its Innovations*, **5** (3), 16–21, 2019.

[4] S. Aqab and M. U. Tariq, "Handwriting Recognition using Artificial Intelligence Neural Network and Image Processing," *International Journal of Advanced Computer and Application (IJACSA)*, **11** (7), 137–146, 2020.

[5] P. G. Patil and R. S. Hegadi, "Offline Handwritten Signature Classification Using Wavelet and SUpport Vector Machines," *International Journal of Engineering Science and Innovative Technology (IJEAT)*, **2** (3), 573–589, 2013.

[6] P. Divyasri, K. Depti and D. S. Rao, "Signature Analysis of Centrifugal Fan Response Due to Unbalance Using Wavelet Analysis," *International Journal of Advance Research in Science and Engineering*, **3** (7), 205–213, 2014.

[7] Suma'inna, "Detection of Cardiac Abnormalities Based on ECG Pattern Recognition Using Wavelet and Artificial Neural Network," *Far East Journal of Mathematical Sciences*, **76** (1), 111–122, 2013.

International Journal of Applied Sciences and Smart Technologies

Volume 3, Issue 2, pages 265–266

p-ISSN 2655-8564, e-ISSN 2685-9432

AUTHOR GUIDELINES

Author guidelines are available at the journal website:
http://e-journal.usd.ac.id/index.php/IJASST/about/submissions#authorGuidelines

International Journal of Applied Sciences and Smart Technologies

Volume 3, Issue 2, pages 265–266

p-ISSN 2655-8564, e-ISSN 2685-9432

This page intentionally left blank